A NEUROMOTOR MODEL OF HANDWRITING GENERATION: HIGHLIGHTING THE ROLE OF BASAL GANGLIA

A THESIS
submitted by

G.GANGADHAR

For the award of the degree

Of

MASTER OF SCIENCE

DEPARTMENT OF ELECTRICAL ENGINEERING
INDIAN INSTITUTE OF TECHNOLOGY - MADRAS
APRIL 2006

THESIS CERTIFICATE

This is to certify that the thesis entitled **A NEUROMOTOR MODEL OF HANDWRITING GENERATION: Highlighting the Role of Basal Ganglia** submitted by **Garipelli Gangadhar** to Indian Institute of Technology, Madras for the award of Master of Science by Research is a bonafide record of research work carried out by him under my supervision. The contents in this thesis, in full or in parts, have not been submitted to any other Institute of University for the award of any degree or diploma.

Madras 600036 Research Guide

Date:

ACKNOWLEDGEMENTS

I express my sincere gratitude to my research guide **Dr. V. Srinivasa Chakravarthy**, for his constant support, guidance and encouragement throughout the project and without whose help the completion of this thesis would have been difficult. His enthusiasm for the subject has been a great of source of inspiration for me.

I thank My GTC Members, **Dr. Hema A. Murthy** and **Dr. A. N. Rajagopalan** for their valuable reviews.

I thank **Dr. Bapiraju, University of Hyderabad** for healthy criticism and stimulating conversation in the middle of the thesis work.

I thank **Dr. Rohith Manchanda, IIT Bombay** for his encouragement in doing research in computational neuroscience.

I am greatly indebted to **Dr. Suresh Devasahayam, CMC Vellore**, for his valuable suggestions and reviews of my work.

I thank **Dr. K. Sridharan** for his kind help and valuable suggestions during my research work.

I acknowledge **Karthikeyan** and **Arun Kumar** for their continuous discussions and encouragement. I thank **P.S. Prashanth**, **Dinesh**, **Gunjan**, **Anchal** and **J. Srinivas** for their assistance during the research work. I thank **K. Umender, Rajiv Ranjan Sahay** and **N. Rajeev Lochan** who made my stay at IIT-M memorable. My gratitude to my lab members, particularly **Krishnan** and **Ranjan Kumar Pradhan** for their valuable assistance during the work.

I am grateful to my parents, brother and my sister for their support and encouragement.

Gangadhar Garipelli

ABSTRACT

Keywords: Handwriting; Handwriting generation; Motor preparation; Basal ganglia; Reinforcement learning; Parkinson's disease; Computational neuroscience; Motor control; Oscillatory neural networks.

Handwriting (HW), unlike reaching or walking, is a high-level motor activity, engaging large parts of cortical and sub-cortical regions that include supplementary motor area (SMA), premotor area (PM), primary motor area (M1), basal ganglia (BG), cerebellum, spinal cord etc. Since each of these regions contributes to HW output in its own unique fashion, pathology of any of these regions is manifest as characteristic features in HW. For example, in Parkinson's disease, a disorder of BG, HW is marked by diminutive letter size or *micrographia*. Recognition of rich diagnostic value of HW had prompted a systematic study of HW and the extensive neuromotor organization that generates it. Computational modeling offers an integrative framework in which results of such studies – which come from several domains, like behavioral, imaging, etc – are brought together and given a concrete shape. An integrative computational model of human motor system and BG is proposed. Dopamine deficient conditions as in PD patients are simulated in the model to reproduce PD-like handwriting features like micrographia, fluctuating velocities, jagged contour etc.

The model primarily consists of a neuromotor model which is capable of learning and generating strokes, and a timing model which coordinates events in the neuromotor model. In the neuromotor model of handwritten stroke generation, stroke velocities are expressed as a Fourier-style decomposition of oscillatory neural activities. The timing network, which resembles the timing action of BG, controls the events in the neuromotor model. The model gives a precise description of what is loosely termed as "motor preparation," involving a dynamic interaction between BG and SMA. The model is further extended for multiple stroke production. The special emphasis given to BG in the models qualifies it as a candidate model for Parkinsonian handwriting. It is shown that model "pathologies" can capture several features of Parkinsonian handwriting like micrographia, irregular velocity profiles etc.

TABLE OF CONTENETS

Table of contents (continued) **Page**

Table of contents (continued) **Page**

LIST OF TABLES

LIST OF FIGURES

ABBREVIATIONS

ARP	Associative Reward Penalty
AVITEWRITE	Vector Integration to Endpoint WRITE
BG	Basal Ganglia
BP momentum	Backpropagation algorithm with momentum
BP	Bereitschafts Potential
GP	Gate Pulse
GPe	Globus Pallidus external
GPi	Globus Pallidus internal
HW	Handwriting
ICSS	Intra Cranial Self Stimulation
IGP	Input Gate Pulse
M1	Primary Motor area
OGP	Output Gate Pulse
PD	Parkinson's Disease
Plain BP	Plain Backpropagation algorithm
PM	Pre Motor Area
PMd	dorsolateral Premotor Area
PP	Preparatory Pulse
PPD	Post Preparatory Delay
RL	Reinforcement Learning
SMA	Supplementary Motor Area
SNc	Substantia Nigra pars compcta
SNr	Substantia Nigra pars reticula
SOM	Self Organizing Map
STN	Subthalamic nucleus
STR	Striatum
TD	Temporal Difference
VTA	Ventral Tegmental Area

CHAPTER 1

INTRODUCTION

1.1 HANDWRITING AS A DIAGNOSTIC TOOL

Handwriting is a learned, highly practiced human motor skill that involves the control and coordination of complex movement sequences. In the past decade (Cobbah, M.C. and Fairhrust, 2000; Kuenstler et al, 1999; van Gemmert et al, 1999), handwriting has been gaining attention as a source of diagnostic information, which carries precise signatures of a variety of neurological disorders including Parkinson's disease (van Gemmert et al; 1999; Teulings et al, 2002), Schizophrenia (Gallucci et al, 1997), Obsessive Compulsive Disorder (Marvogiorgou et al, 2001) etc. Since handwriting, unlike reaching or walking, is a high-level motor activity, it engages large parts of cortical and subcortical regions that include Supplementary motor area (SMA), Premotor area (PM), Primary motor area (M1), Basal ganglia (BG), Cerebellum, Spinal cord etc. Since each of these regions contributes to handwriting output in its own unique fashion, pathology of any of these regions is manifest as characteristic features in handwriting. For example, in Parkinson's disease, a disorder of BG, handwriting is marked by diminutive letter size or *micrographia* (fig.1.a). Similarly handwriting in patients with cerebellar damage is often characterized by omissions and unnecessary repetition of strokes (fig.1.b). Recognition of rich diagnostic value of handwriting had prompted a systematic study of handwriting and the extensive neuromotor organization that generates it. Computational modeling offers an integrative framework in which results of such studies – which come from several domains, like behavioral, imaging, etc – are brought together and given a concrete shape. Several computational models of handwriting

production have been developed to investigate the complex interaction among these structures.

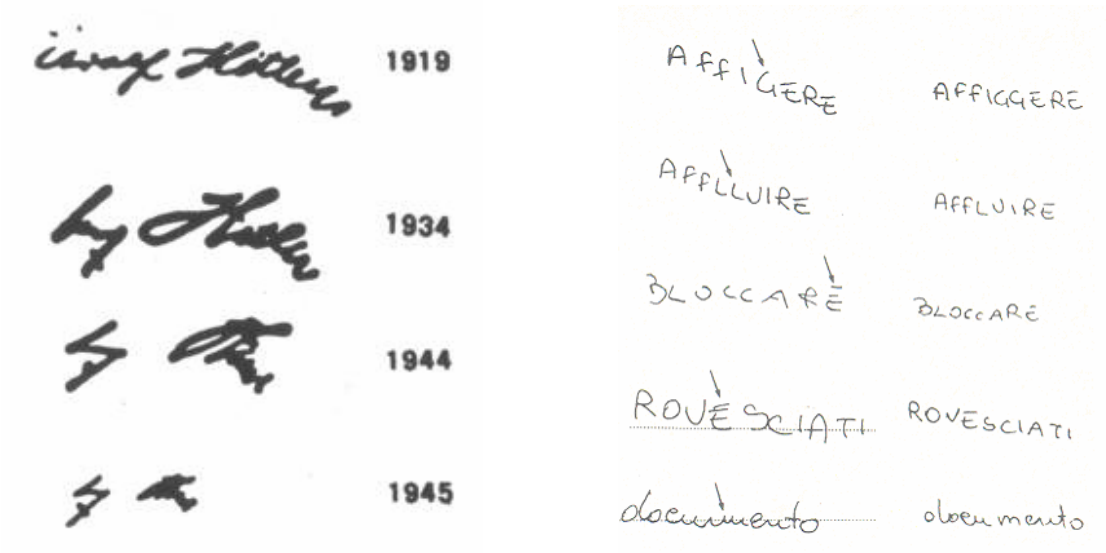

(a) (b)

Fig.1.1Handwriting in neurological diseases (a) Micrographia in PD: The signature of Adolf Hitler, who suffered from PD. The signatures start in 1919, when he did not have PD, and end in 1945, the day before he committed suicide. Note how the letters become smaller and more crowded together: micrographia[1]. (b) Samples of handwriting from a patient with cerebellar lesion (Silveri et al, 1999) (Spatial Dysgraphia). Errors in handwriting like, downward sloping strokes, stroke repetition, and stroke omission are shown with arrows[2].

1.2 COMPUTATIONAL MODELS OF HANDWRITING GENERATION

One of the earliest ideas of handwriting models is to resolve handwritten stroke data into oscillatory components (Hollerbach, 1981; Schomaker, 1991; Kalveram, 1996). Hollerbach proposed a model of hand-pen system, represented by two orthogonal pairs of opposing springs acting on an inertial load. It was pointed out that the oscillatory natural motions of this system resemble real handwriting segment (Hollerbach, 1981). Several authors attempted to fit such family of solutions to handwritten strokes or components (Plamondon, 1989; Schomaker, 1991). Schomaker proposed a neural network model in

[1] The signatures are adapted from url: www.liebermanparkinsonclinic.com/content/view/197/25/
[2] Handwriting samples taken from Silveri et al, 1999.

which a network of oscillators outputs horizontal and vertical pen motion (Schomaker, 1991). Network training, performed using a variation of delta-rule, led to uncertain results. More recently Kalveram proposed a model in which stroke data is resolved to its Fourier components (Kalveram, 1996). An oscillatory neural model of handwriting, for it to be biologically viable, has to address certain fundamental issues. The first key issue, one of preparing the initial state of the oscillatory network, does not seem to have received adequate attention (Schomaker, 1991; Kalveram, 1996). Essentially there is a need for auxiliary mechanisms that 1) initiate/prepare (a rhythm in the oscillatory network's state), 2) that align (that rhythm with respect to the time of onset of the stroke), and 3) terminate (the rhythm at the appropriate time).

The neuromotor model of handwritten stroke generation presented in this thesis addresses the issues discussed above. In line with oscillatory theories of handwriting, the present model consists of a network of neural oscillators, which learns to resolve a handwritten stroke into its oscillatory components. A key component of the model is a timing network which coordinates the events occurring in various parts of the network like stroke initiation, output gating etc. The action of this timing network has close resemblances to that of BG in human motor function. Specifically, its role in preparing the state of appropriate motor cortical areas prior to initiation of motor act is highlighted by the model. The special emphasis given to BG in our models qualifies it as a candidate model for Parkinsonian handwriting. It will be shown that model "pathologies" can capture several features of Parkinsonian handwriting like micrographia, irregular velocity profiles etc.

1.3 PARKINSON'S DISEASE AND BASAL GANGLIA

Parkinson's disease is a progressive neurodegenerative disorder that occurs in 1% of the population over 55; the mean age at which the disease is first diagnosed (Prunier, 2003; Singhala et al 2003). PD symptoms include tremor, rigidity, postural abnormalities, micrographia and bradykinesia. The principal pathological characteristics of PD are the loss of dopaminergic neurons in the substantia nigra pars compacta (SNc) in BG. Handwriting in PD has characteristic changes like reduced handwriting size and jagged handwriting. Handwriting-based diagnostics of PD takes a "black box" approach to patients, wherein the PD handwriting is compared empirically with that of normal controls (Fairhrust, 2000). But unless there is a clear understanding of what aspects of handwriting are controlled by what modules of motor system, such diagnostic methods can only have limited value.

Enormous progress has been made in characterizing the structure and functionality of the BG, and yet comprehensive understanding of the contribution of these nuclei to behavioral control remains elusive. Functional models of BG are thus in great need for comprehensive theory of BG operations. Functional models should be able both to assimilate the constraints imposed by the neurobiological data and to simulate various candidate behavioral functions in which these structures (nuclei) are believed to participate (Alexander, 1999).

BG consists of five extensively connected subcortical nuclei: the caudate nucleus, putamen, globus pallidus (externus and internus), subthalamic nucleus(STN), and substantia nigra. Caudate and Putamen together named as Striatum(STR) which serves as

the input to BG. The neurons of STR project to GPi constituting direct pathway. The indirect pathway is STR – GPe – STN – Gpi. Experimental studies reveal that BG are involved in 6 diverse functions:

i. Regulation of the degree of action gating,
ii. Selection between competing actions,
iii. Sustaining working memory representations,
iv. Storing and enhancing sequences of behavior,
v. Actor critic models(Reinforcement learning),
vi. Representation of timing or Coincidence detection or (recent view on cortico-striatal circuits) (Buhusi and Meck, 2005).

Existing computational models of BG highlight only one or two of the above functions. The present model accommodates few of the above functions, and probably is well on its way to incorporate the remaining features also in an integrated model of BG.

1.4 COMPUTATIONAL NEUROSCIENCE AND DISEASE MODELS

Computational neuroscience offers a firm foundation on which experimental data from diverse sources can be integrated; it provides a convenient language by which the function of nervous system may be studied at multiple levels, and described at a chosen level at a given time while momentarily de-emphasizing other levels (Jennings and Aamodt, 2000; Abbot and Dayan, 2001). Computer simulation of neurons and neural networks are complementary to traditional techniques in neuroscience (Churchland and Sejnowski, 1994). Computational neuroscientists are fundamentally interested in the rich interplay of highly nonlinear intrinsic properties of individual neurons, and in the

coupling properties between cells that determine the dynamical activity of neuronal networks (Abbot and Dayan, 2001). These models describe neural organization and dynamics at many levels of abstraction of the physical processes and anatomical units, at a range of spatial and temporal scales – short-term to long-term changes (Jennings and Aamodt, 2000).

Computational modeling of neurological disease represents a new research paradigm, competing with traditional methods such as clinical studies and animal models (Reggia, et al 1996). Computational models for neurological diseases like, Epilepsy (Silva and Pijn, 1995), Alzheimer's disease (Ruppin et al, 1996), Parkinson's disease (Vidal et al, 1996; Terman et al, 2002; Teulings et al, 2003), Schizophrenia(Horn and Ruppin, 1995; Grossberg, 1999), Autism(Bjorne, 2005; Grossberg, 2006), Dyslexia (Harm and Seidenberg 1999), etc[3] are developed to get insight into these diseases. "Pathologies" are simulated with virtual neural models to study various brain and cognitive disorders. The goals of such research is to construct computational models that can explain how specific neuroanatomical and pathological changes can result in various clinical manifestations, and to investigate the functional organization of symptoms that result from specific brain pathologies(Reggia et al, 1996).

1.5 A MODEL OF PARKINSONIAN HANDWRITING

The neuromotor model and the model of BG mentioned above in (Sections 1.2 and 1.3 respectively) are combined to realize a model of Parkinsonian handwriting. Further, it is shown that under dopamine-deficient conditions, simulating Parkinson's disease, the

[3] Refer http://www.cnbc.cmu.edu/Resources/disordermodels/index.html for other disorders to which computational approaches are attempted.

model produces PD-like handwriting with micrographia, irregular velocity profile etc. With the help of the present model it is possible to link signaling inside BG (e.g., dopamine signal, activity of STN-GPe etc.) to observable behavior, namely, handwriting. The model is a "systems level," neural network model of BG consisting of abstract "neurons." However, even this simple model provides tremendous insight into the nature of BG, complete understanding of which eludes us to this day. For example the proposed model suggests that complex activity of STN-GPe loop is essential for reinforcement learning. Loss of this complexity is manifest as PD handwriting symptoms according to the model. More detailed extensions of the present model might find applications in several aspects of PD treatment: 1) in drug dosage determination, 2) in designing of Deep Brain Stimulation protocols etc.

1.6 ORGANIZATION OF THE REPORT

The rest of the report is organized as follows: In chapter 2, a neuromotor model of handwriting generation in which stroke velocities are expressed as a Fourier – style decomposition of oscillatory neural activities is presented along with a review of the existing handwriting models in the literature. Issues involved in the preparation of oscillator network which are neglected the literature, were discussed and a solution is attempted. Difficulties in multiple stroke generation were discussed and a solution is proposed. Studies on preparatory delay, origins of motor variability and isochrony were discussed. A possible mapping of the model on to neuroanatomy is attempted.

In Chapter 3, a model of reaching, involving BG is presented along with the literature reviews of existing models of BG. A possible functional role of direct pathway and indirect pathway were suggested.

Chapter 4 reviews PD models of handwriting. The proposed combined model of neuromotor model of handwriting generation and BG model is presented along with review of existing models of PD handwriting.

In Chapter 5 the results of neuromotor model of handwriting generation, model of reaching involving BG and a model of PD handwriting were discussed. Finally the report concludes with discussion of findings in the present work in Chapter 6.

CHAPTER 2

AN OSCILLATORY NEUROMOTOR MODEL OF HANDWRITING GENERATION

To the theoretical question, can you design a machine to do whatever a brain can do?
The answer is this: If you will specify in a finite and unambiguous way what you think a brain does ... then we can design a machine to do it...
But can you say what you think brain do?

– W. S .McCulloch

2.1 HANDWRITING AND HANDWRITING GENERATION

Handwriting (HW) is a learned, highly practiced human motor skill that involves the control and coordination of several subsystems in our motor system. The production of handwriting requires a hierarchically organized flow of information through various transformations (Ellis 1998; Teulings et al 1986). The writer starts with the intention to write a message (semantic level), which is transformed into words (lexical and syntactical level). When the individual letters (graphemes) are known, the writer selects specific letter shape variants (allographs). The selection is done with respect to the formal allograph selection syntax, according to individual preference or just random choice (Schomaker, 1991). Below this level, the allographs are transformed into movement patterns, which is the object of focus of the present work.

2.2 MODELS OF HANDWRITING

Two general methodologies of handwriting modeling become apparent from the literature. The first one, dubbed the “bottom-up” approach, refers to computational models which attempt to empirically reproduce features of human writing such as velocity and acceleration profiles etc; they do not claim any fidelity to neuromotor processes underlying handwriting processes (Plamondon, 1989; Grossberg and Paine,

2000; Hollerbach, 1981; Kalveram, 1996). The second methodology of handwriting modeling focuses on psychologically descriptive models (van Galen and Weber 1991, Grossberg and Paine 2000). These "top-down" models usually summarize many issues such as, motor learning, movement memory, planning and sequencing, coarticulatory and task complexity of strokes, etc.

2.2.1 Hollerbach's Oscillation Theory of Handwriting

An important class of handwriting models is centered on the philosophy that stroke data can be resolved into certain oscillatory components by Fourier-style decomposition. The approach was pioneered by Hollerbach (1981) who proposed an insightful model of handwriting generation where the hand-pen system is represented by two orthogonal pairs of opposing springs acting on an inertial load. It was pointed out that the oscillatory natural motions of this system resemble real handwriting segments. Anatomical justification of such a simple system has also been explored (Hollerbach, 1981).

2.2.2 Schomaker's Model

Schomaker (1991) proposed a neural network model in which a network of oscillators outputs horizontal and vertical pen motion. Network training, performed using a variation of delta-rule, led to uncertain results: performance depended critically on network parameters. In spite of the shortcomings of the performance of the model, Schomaker's work clearly elucidates certain issues related to any possible handwriting model. Accordingly, the handwriting process – and hence its model – must have four basic events or phases both in chaining and shaping of handwriting:

1. *System configuration*: This stage is known as motor programming, coordinative structure gearing, preparation, planning, schema build-up etc.
2. *Start of pattern*: After configuring the system for the task at hand, there must be a signal releasing the pattern.
3. *Execution of pattern*: The duration of this phase and actions that are performed depend on pieces of information such as the amount of time that has passed, the distance from a spatial target position or force target value, or even the number of motor segments produced.
4. *End of pattern*: this stage deals with the termination of the movement.

Though the network includes important episodes during handwriting execution, the network training, performed using a variation of delta-rule, led to uncertain results.

2.2.3 Kalveram's Model

More recently Kalveram (1996) proposed a model in which stroke data is resolved into its Fourier components. This simple mathematical operation is described using the metaphor of 'central target pattern generator'. The model in our view has several drawbacks. Since a handwritten stroke – for that matter any real motor sequence – lives for a finite duration, the dynamics of a system that produces it must be appropriately initiated and terminated. Fourier decomposition assumes a set of oscillators with precise initialization and phase-relationships. A network that performs such decomposition, and produces a stroke by re-synthesis, has to be appropriately *prepared*. Accurate preparation of the initial state may be crucial for successful stroke generation. Further, in a large network of oscillators this preparation of the initial state can be a challenge in itself, in addition to

accurate stroke learning/acquisition and production. Another drawback is that in (Kalveram, 1996) a separate network has to be trained for every stroke.

2.2.4 Plamondon's Model

Plamondon and Guefali (1998) presented a bottom-up model using "delay-lognormal synergies". The name refers to author's definition of the velocity of a muscle synergy as a Gaussian function of the movement parameters that vary logarithmically with time. The model therefore produces bell-shaped velocity profiles similar to human bell shaped velocities. They also demonstrated the "Two-Thirds Power Law" relation between angular velocity and curvature for a limited range of elliptical movements for which the law accurately describes human writing.

2.2.5 AVITEWRITE Model

Adaptive VITEWRITE (AVITE) model (Grossberg and Paine, 2000) is a neural network handwriting learning and generation system that joins together the mechanisms from Bullock's (Bullock and Grossberg 1988a) cortical VITE (Vector Integration to Endpoint) and VITEWRITE trajectory generation models and cerebellar spectral timing model of Fiala et al (1996). This synthesis creates a single system capable of both reactive movements as well as memory based movements based on previous cerebellar movement learning and subsequent read out from long-term memory. AVITEWRITE model successfully explained the psychophysical and neurobiological data about how synchronous multi-joint reaching trajectories could be generated at variable speeds. The AVITEWRITE model is used to simulate the key psychophysical and neural data about learning to make curved movements, including decrease in writing time as learning

progresses; generation of unimodal, bell shaped velocity profiles for each movement synergy; size and scaling with preservation of the letter shape and shapes of velocity profiles; an inverse relation between curvature and tangential velocity; and Two –Thirds Power Law relation between angular velocity and curvature. Though the model successfully explains several features of handwriting, it may be noted that it does not belong to the family of "oscillatory" models of handwriting. We will argue in this paper that investigating handwriting in terms of its oscillatory components throws up certain important aspects of handwriting – or perhaps all voluntary control – like preparation, motor delay etc. These issues are addressed by the present model.

In the present work an oscillatory neural network model for handwritten stroke generation is proposed. Particularly, the issues involved in preparing the initial state of the network are highlighted. In the next section, features of the present model and a mechanism for preparing the initial state of the network are described.

2.3 PRESENT MODEL

The essence of the proposed approach is to produce a stable rhythm in a network of oscillators and resolve the stroke output in a Fourier-style in terms of the oscillatory activities of network oscillators. The architecture of our network that learns strokes has 3 layers – 1) input layer, 2) oscillatory layer, and 3) output layer (fig.2.1). Each node in the input layer represents a separate stroke. In resting condition all the inputs are in a 'low' (0) state. To produce a stroke the corresponding input line is taken to a 'high' (1) state and held in that state for a fixed duration. The oscillatory layer has several sublayers. All the neurons in a sublayer have the same oscillation frequency. In each sublayer, neurons

are connected in a ring topology. Our model differs from the model of Schomaker (1991) in this respect: lateral connections were absent in Schomaker's model[4]. Output layer has two outputs representing horizontal and vertical velocities (U_x and U_y) of the pen tip. Each of the outputs is connected to all the oscillators in the oscillator layer. Events in the above 3-layered network are controlled by a timing network (see fig.2.1). Aspects of the network are described in greater detail below.

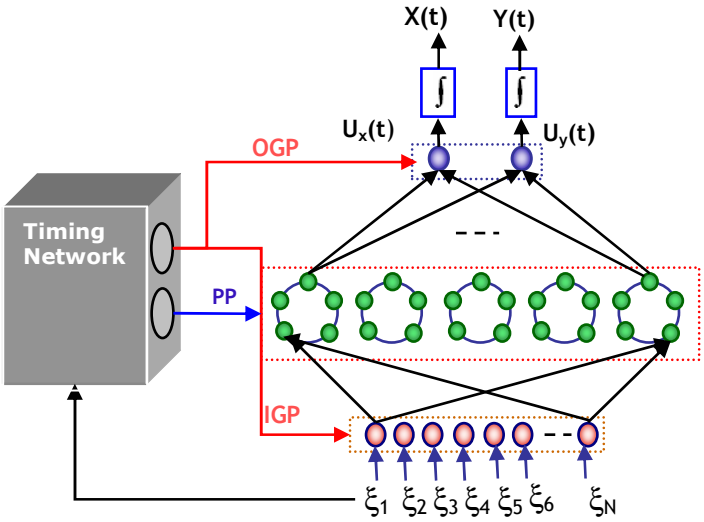

Fig.2.1. Architecture of Oscillatory network

2.3.1 Single Oscillator Model

Dynamics of a single neural oscillator used in the hidden layer of our network are given as,

$$\frac{dx}{dt} = -x + V - s + I \tag{2.1}$$

$$V = \tanh(\lambda x) \tag{2.2}$$

$$\frac{ds}{dt} = -s + V \tag{2.3}$$

[4] This might be a reason behind uncertain results of this model, since lateral connections are essential to stabilize the rhythm in the oscillatory layer.

where ‘V’ denotes the oscillatory output, and ‘x’ and ‘s’ are auxiliary, internal variables of the neuron. Note that while ‘x’ has excitatory influence on ‘s’ and ‘s’ in turn inhibits ‘x’. Such excitatory-inhibitory pair is a standard recipe for producing oscillations.

Analysis of eqn. (2.1) shows that, for I=0, s = 0, and $\lambda > 1$, ‘*V*’ in (2.1) has 2 stable states, $V \approx \pm 1$. Moreover, if *V* is at negative (positive) stable state, a sufficiently large negative (positive) ‘s’ in eqn. (2.1) flips ‘*V*’ to its positive (negative) stable state. In eqn. (2.3), ‘s’ simply follows ‘*V*’ with a delay. Therefore, a persistent value of *V* induces a change in ‘s’ such that ‘*V*’ is toggled periodically. Oscillations are produced by the above system, but only within certain limits of the external input I (fig.2.2). Beyond those limits the neuron has fixed point behavior. The average output of the neuron as a function of I has a sigmoidal form (fig.2.2). The proof for the existence of limit cycle in the above system described by eqns.(2,1, 2.2 and 2.3) is discussed in Appendix A.

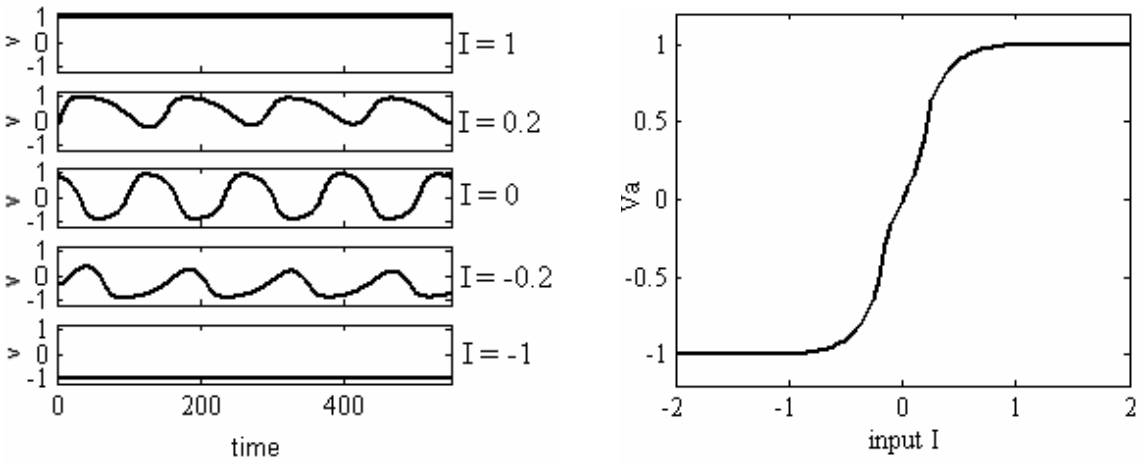

(a) (b)

Fig.2.2 (a) Output of a single neuron for various values of external input, I. (λ=3). (b) Average output value (Va) of a single neuron as a function of I.

2.3.2 Sublayer Model: Ring of Oscillators

Each sublayer consists of a network of oscillators (of eqns. (2.1, 2.2, 2.3)) connected in a ring topology with one side connections as shown in fig.2.3. By a proper choice of parameters, such a network of oscillators can produce a limit cycle, with specific phase relationships among individual oscillators.

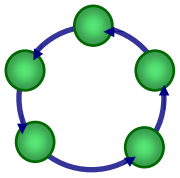

Fig.2.3. Oscillators in a ring topology with unidirectional connections

Odd number of oscillators in ring (sublayer) is preferred for mode locking as even number of oscillators may lead to loss of rhythm stability i.e., "oscillator death" (Chirikov, 1979). A sublayer with ring topology, odd number of oscillators and with sufficient coupling strength (negative weight) exhibits mode locking, where each oscillator produces a periodic output and adjacent oscillators differ by a phase difference of $\Delta\phi = \pi + 2\pi/m$ (m is the number of oscillators) (Bressloff, 2000; Bressloff, 2002).

2.3.3 Preparing The Network State

This important stage is referred to by varied expressions as motor programming, coordinative structure gearing, preparation, planning, schema build-up etc (Schomaker, 1991). Although the problem of motor programming has several dimensions, in the context of our network we give it a specific meaning. Since the network is a dynamic system, it must be brought to a "standard" state, if possible, from a random, unspecified state, before it can produce a stroke. This standard state is the one in which individual

oscillators of a sublayer are brought to target phases (ϕ_1, …, ϕ_i,…, ϕ_n) by the time the network is ready for stroke execution. This preparation is achieved by giving a Preparatory Pulse (PP) to a specific neuron (chosen to be the 1st neuron in every sublayer without loss of generality) and waiting for a specific delay interval. *The delay must be long enough to allow the oscillatory layer to approach the limit cycle sufficiently closely; beyond this minimum value the delay must be precisely chosen such that the oscillatory layer state is at a predetermined phase in the limit cycle.* We refer to this state as the "standard state" henceforth. Thus, by proper choice of pulse (its duration, τ, and amplitude, A) and the delay, Δ, (elapsed after the PP and before the stroke execution begins) the network can be brought to the desired state ($V=[V_1, \ldots, V_i, \ldots, V_n]$) with sufficient accuracy.

2.3.4 The Timing Network

The timing network controls the timing of various events in the network (see fig.2.4). The command to execute a stroke corresponding to the j^{th} neuron in the input layer, is received by the timing network at t = 0. At the same time the j^{th} input line in the input layer is set to a 'high' value. Immediately (at t=0+) the timing network sends PPs (of duration τ) to all the sublayers in the oscillatory layer. After a delay, Δ, (i.e. $t = \tau+\Delta$) the timing network sends an Input Gating Pulse (IGP) to the input layer so that the input signal, transformed by a weight stage, reaches the oscillator layer. An Output Gate Pulse (OGP) is also sent to the output layer enabling the output. That is, during this interval ($t = [0, \tau+\Delta]$) the oscillator layer does not know about the change in the state of the input lines. Immediately after ($t > \tau+\Delta$), the OGP is given to the output layer, and the stroke velocity information begins streaming out of the output layer. The gating duration, T_i, is

specific to the stroke that is being produced and is presently equal to the time period, T_f, of the slowest oscillators (those of first sublayer) in the oscillatory layer. We will relax this condition in future section and study its consequences. A summary of events in fig. 2.4 are shown in table 2.1:

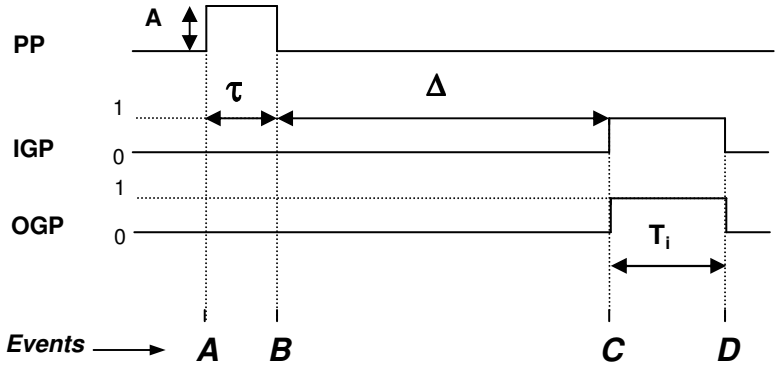

Fig.2.4.The timing signals (PP: Preparatory Pulse, IGP: Input Gate Pulse, OGP: Output Gate Pulse), **A** is the amplitude of preparatory pulse, 'τ' is the duration of PP, T_i is the duration of OGP for i^{th} stroke and 'Δ' is the delay. The Post preparatory delay is given by (PPD) the sum τ+Δ time units.

Table.2.1. Summary of events in handwriting generation

Events	Event Summary
A	*The input is fed to the network (also to timing network). The timing network injects PP for the duration (τ), to the 1st oscillator in every sublayer. Input to the oscillatory network is disabled during this interval since the IGP is low.*
B	*This event is the end of PP and start of delay for duration Δ. IGP and OGP continues to be low.*
C	*Start of IGP and OGP with duration T_i, which enable the input and output. The network starts generating velocity information.*
D	*The end of IGP and OGP, the network is again disabled, velocities become zero, and the pen tip stops.*

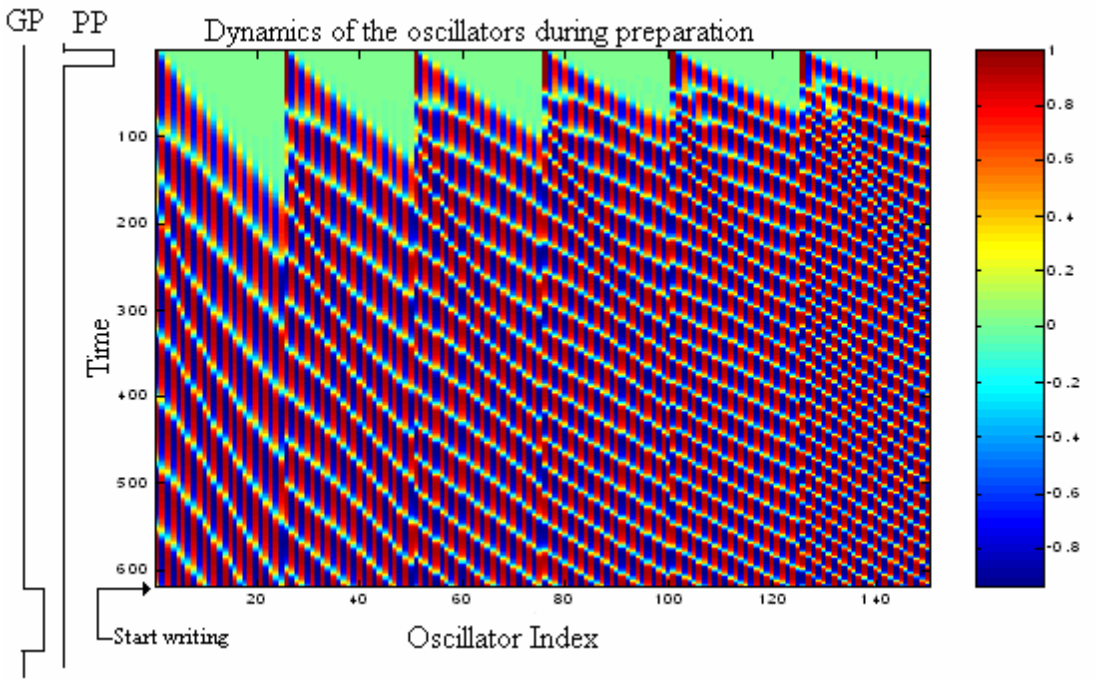

Fig.2.5. Dynamics of the oscillators network during preparation. The oscillator layer has 6 sublayers with 25 oscillators for each sublayer. GP represents both IGP and OGP. The PP is given from zero time units to 20 time units. The GP is brought up from 620 time units onwards.

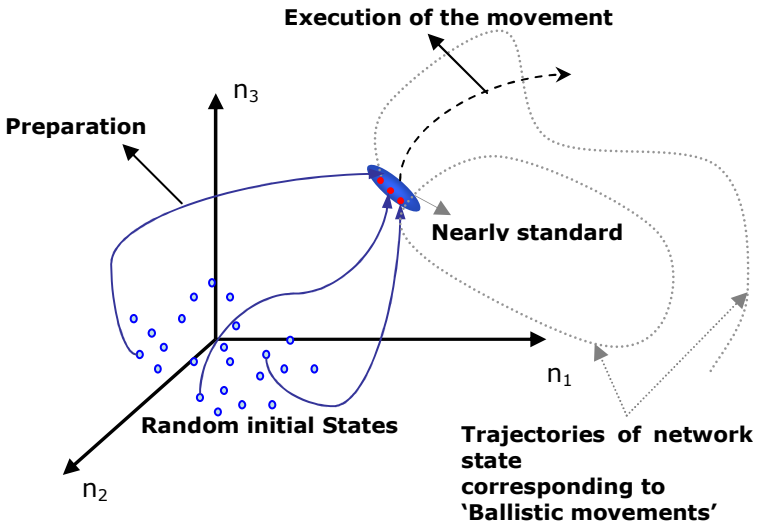

Fig.2.6. Cartoon of state space illustrating trajectories in preparation and execution of a movement. Average firing rates of neurons n1, n2 and n3 are shown along the axes. The initial activity of the neurons is near the origin (shown as one small circle per trial). Following target onset, activity of neurons settles (through curved paths) to a subspace of states appropriate for the desired movement (volume inside the shaded region). The standard state is part of this subspace.

The dynamics of the network along with Gate Pulse, GP (is shown considering IGP = OGP) and PP during preparation are shown in fig.2.4. A PP signal is given at the beginning of the session. The onset of handwriting movement starts at GP. Note that there is 'mode locking' in each sublayer towards end of preparation delay. The onset of GP or handwriting movement occurs at the registry of standard state (at time units 620 in fig.2.5). The more details on 'time unit' are discussed in section 5.1 of chapter 5.

The fig.2.6 explains the events of the network in terms of network's state and trajectory followed by the state. The trajectory from the initially variable state (near the base line; shown as one dot per trial) to standard state (states in shaded volume shape in fig.2.6) corresponds to preparation of the network. Different trajectories emanating from the standard state leads to various movements. Note that all trajectories corresponding to variable initial states go through the standard state, which is the essence of preparation.

2.3.5 Network Response

Pen-tip velocities (U_x and U_y) estimated by the network are expressed as weighted sum of the outputs of the oscillator layer:

$$U_x(t) = \sum_{k=1}^{Ns} \sum_{i=1}^{Nk} W_{ik}^{x} V_{ik}(t) \tag{2.4}$$

$$U_y(t) = \sum_{k=1}^{Ns} \sum_{i=1}^{Nk} W_{ik}^{y} V_{ik}(t) \tag{2.5}$$

where, N_s is the number of sublayers in the oscillatory layer and N_k is the number of oscillator in k^{th} sublayer, W^{x}_{ik} and W^{y}_{ik} are connections from i'th oscillator in k'th sublayer to output nodes U_x and U_y respectively. Output, V_{ik}, of the i'th oscillator in the k'th sublayer is given by:

$$\frac{dx_{ik}}{dt} = -x_{ik} + \sum W_{irk}^{lat} V_{rk} - s_{ik} + I_{ik}^{net} \tag{2.6}$$

$$V_{ik} = \tanh(\lambda x_{ik}) \tag{2.7}$$

$$\frac{ds_{ik}}{dt} = -s_{ik} + V_{ik} \tag{2.8}$$

where, x_{ik} is the state of i'th neuron in k'th sublayer, s_{ik} is the auxiliary internal variable of the i'th oscillator in the k'th sublayer, W^{lat}_{irk} is the lateral connection from r'th oscillator to i'th oscillator in k'th sublayer. I_{ik}^{net} is the net input to i'th oscillator in the k'th sublayer is given by,

$$I_{ik}^{net} = \sum_{l} W_{lik}^{1} \xi_l \tag{2.9}$$

where, ξ_l is l'th input in input vector ξ = { ξ_1, ξ_2, ξ_3 ... ξ_l ... ξn ,-1}and W^{l}_{lik} is the weight connecting l'th input node and i'th oscillator in k'th sublayer. Finally, the movement of pen tip along x – direction and y – direction are calculated by integrating the velocity signals U_x and U_y respectively.

2.3.6 Training

Three kinds of learning algorithms are formulated for training, namely, 1) Backpropagation with momentum (Similar to backpropagation for MLP with static neurons discussed in standard texts like Haykin (2001)) 2) Plain Backpropagation and 3) Reinforcement learning. As the network has to learn a temporal signal, a temporal error measure has to be constructed; the reconstruction error in the velocity domain is constructed. The error is formulated in the velocity domain due to the reason that the error can be easily propagated back for the update of weights with backpropagation

algorithm. If the error is constructed in spatial domain the error needs to be differentiated and hence formulation of backpropagation algorithm becomes tedious.

Back propagation with momentum and batch-mode update (BP momentum): Since the average value of output of the oscillatory neuron varies in a sigmoid form as a function of external input (see fig.2.2), backpropagation (BP) algorithm may be used for training. Weight update equations of this algorithm for the 2nd stage weights are given as,

$$\Delta W_{ik}^{y}(t+1) = \alpha_2 \Delta W_{ik}^{y}(t) + \eta_2 \delta_y^2(t) V_{ik}(t) \tag{2.10}$$

$$\Delta W_{ik}^{x}(t+1) = \alpha_2 \Delta W_{ik}^{x}(t) + \eta_2 \delta_x^2(t) V_{ik}(t) \tag{2.11}$$

where, $\delta_x^2(t) = V_x(t) - U_x(t)$ and $\delta_y^2(t) = V_y(t) - U_y(t)$, are the instantaneous error signals along x – direction and y – direction respectively where, V_x, *and* V_y are temporal signals of desired velocities along x – direction and y – direction respectively and actual velocities emanating from network, U_x and U_y are defined in equations (2.4, 2.5)

For 1st stage weights,

$$\Delta W_{lik}^{1}(t+1) = \alpha_1 \Delta W_{lik}^{1}(t) + \eta_1 \delta_{ik}^{1}(t) \xi_l \tag{2.12}$$

where, $\delta_{ik}^{1}(t) = W_{ik}^{x}(t)\delta_x^2(t) + W_{ik}^{y}(t)\delta_y^2(t)$, η_2 and η_1 are learning rates and α_2 and $\alpha_1$are the momentum constants. Instantaneous 'Δw' s are accumulated and the weights are updated once for every stroke presentation.

Plain Backpropagation (PainBP): Weights are updated instantaneously and the learning equations are same as that of section (2.6.1) except the momentum constants $\alpha_2$and α_1 are equal to zero.

Reinforcement learning(RL): The network is also tested with reinforcement learning (Barto, 1999; Hertz, 1991) for the 1st stage weights, and is given as,

$$\Delta w^1_{lik}(t+1) = \eta_+ V_{ik}(t)\xi_l \qquad \text{if } e \le \varepsilon \tag{2.13}$$

$$\Delta w^1_{lik}(t+1) = \eta_- V_{ik}(t)\xi_l \qquad \text{if } e > \varepsilon \tag{2.14}$$

where, η_+ (η_-)is small positive(negative) constant, 'e' is the output error, and ε is the error threshold for reward-based learning. The second layer update equations are formulated using gradient descent method similar to backpropagation algorithm. The equation for weight update 2nd stage is the same as that of back propagation of error given as in eqn (2.10 and 2.11) with $\alpha_2$and α_1 being equal to zero.

Calculation of mean reconstruction error: The reconstruction error of pth stroke is given by the formula as,

$$E^p = \sum_q^{Nl} \left\{ (Vx_q^p(t) - Ux_q^p(t))^2 + (Vy_q^p(t) - Uy_q^p(t))^2 \right\} \tag{2.15}$$

And the mean error of all strokes is given by,

$$E = \frac{\sum_p^{Ns} E^p}{Ns} \tag{2.16}.$$

Where, *Ns* is the number of strokes and *Nl* is the number of points in velocity profile of pth stroke. And $V_x^p(t)$ and $V_y^p(t)$ are the desired velocity profiles of the pen tip which are collected using a stylus connected to computer. More details about the data collection are discussed in chapter 5. The mean reconstruction error defined in eqn.2.16 is compared over several trials for the training algorithms discussed above (see fig2.7). BP with

momentum found to be faster and efficient compared to the other two algorithms (see fig.2.7). The samples reconstructed strokes are shown in fig2.8.

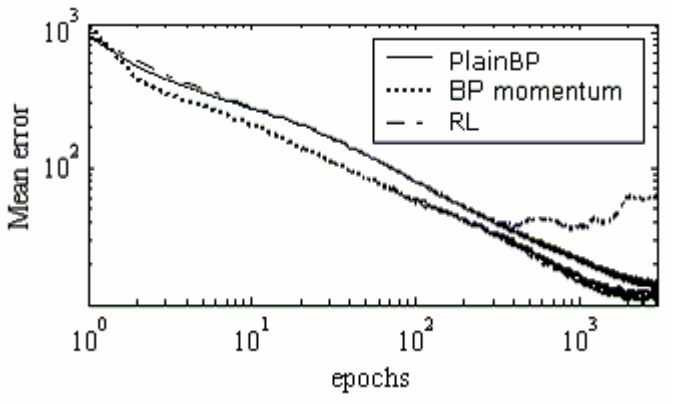

Fig.2.7. Comparison of three kinds of learning algorithms (Plain BP, BP with momentum, Reinforcement learning (RL)). The mean error for "BP with momentum and batch-mode update" converges faster than other two learning mechanisms.

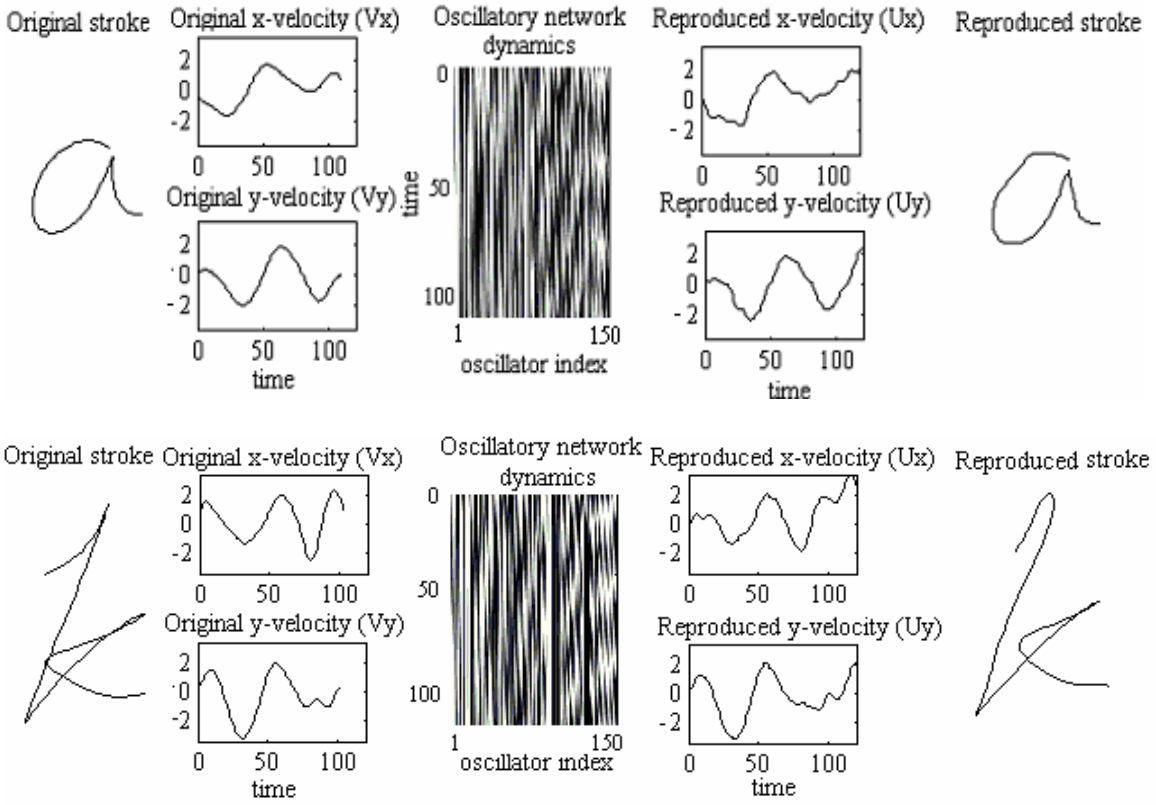

Fig. 2.8. Reconstructed strokes 'a' and 'k'. The dynamics of oscillatory layer along with the stroke velocity profiles are shown. On left side original stroke and corresponding velocity profiles and to right side velocities generated and strokes reconstructed are shown.

2.4 SUMMARY

In the present chapter a model of handwriting generation based on Fourier style reconstruction is discussed. The model is further investigated to optimize several aspects of the network like assignment of frequencies of oscillator sublayers, size of the oscillator layer, multiple stroke production etc. These experiments along with results are discussed in detail in chapter 5. The current model can be mapped on to neuroanatomy; the 'timing network' which controls the events in the main network, resembles BG. BG is known to have a role in timing and preparation of SMA and PM activity in executing a motor activity. More details of mapping of the current model onto neuroanatomy are discussed in chapter 6. Next chapter discusses about the BG and its functional roles along with a model. It is shown in the next chapter that apart from functional roles like timing and preparation, BG has a role in reinforcement learning.

CHAPTER 3

BASAL GANGLIA AS A SOURCE OF EXPLORATORY DRIVE: A MODEL FOR REACHING

Any act which in a given situation produces satisfaction becomes associated with that situation so that when the situation recurs the act is more likely than before to recur also.
– E.L. Thorndike (1911)

3.1 BASAL GANGLIA

3.1.1 Neuroanatomy of Basal Ganglia

BG receive inputs from most of the sensory motor areas of the cerebral cortex, including primary and secondary somatosensory areas, primary motor cortex (M1) and a variety of premotor areas, including supplementary area, the dorsal and ventral premotor areas. The anatomical basis of motor functions of BG is illustrated in fig. 3.1. The portions of cortex which are responsible for movement SMA, PM, M1, somatosensory cortex, and the superior parietal lobule make dense, topographically organized projections to the motor portion of Putamen (input nuclei of BG). The output of this pathway, termed the motor circuit of the BG, is directed primarily back to the SMA and PM cortex. These areas are reciprocally interconnected with each other and with motor cortex and all have direct descending projections to brain stem motor centers and spinal cord.

BG consists of five extensively connected subcortical nuclei: the caudate nucleus, putamen, globus pallidus, subthalamic nucleus (STN), and substantia nigra (pars Compacta SNc, and pars reticula SNr). Caudate and Putamen are together named as STR which is the input nuclei of the BG. Most striatal neurons are medium spiny and have GABAergic projections. Globus Pallidus can be divided into two parts namely Globus

Pallidus external (GPe) and Globus pallidus internal (GPi). SNc projects axons of Dopaminergic neurons onto STR. The neurons of STR project to GPi and GPe. Also there exist excitatory and inhibitory connections between STN and GPe. The STN neurons project onto GPi. The nuclei GPi and SNr constitute output nuclei of BG, which send Gabaergic projections to Thalamus.

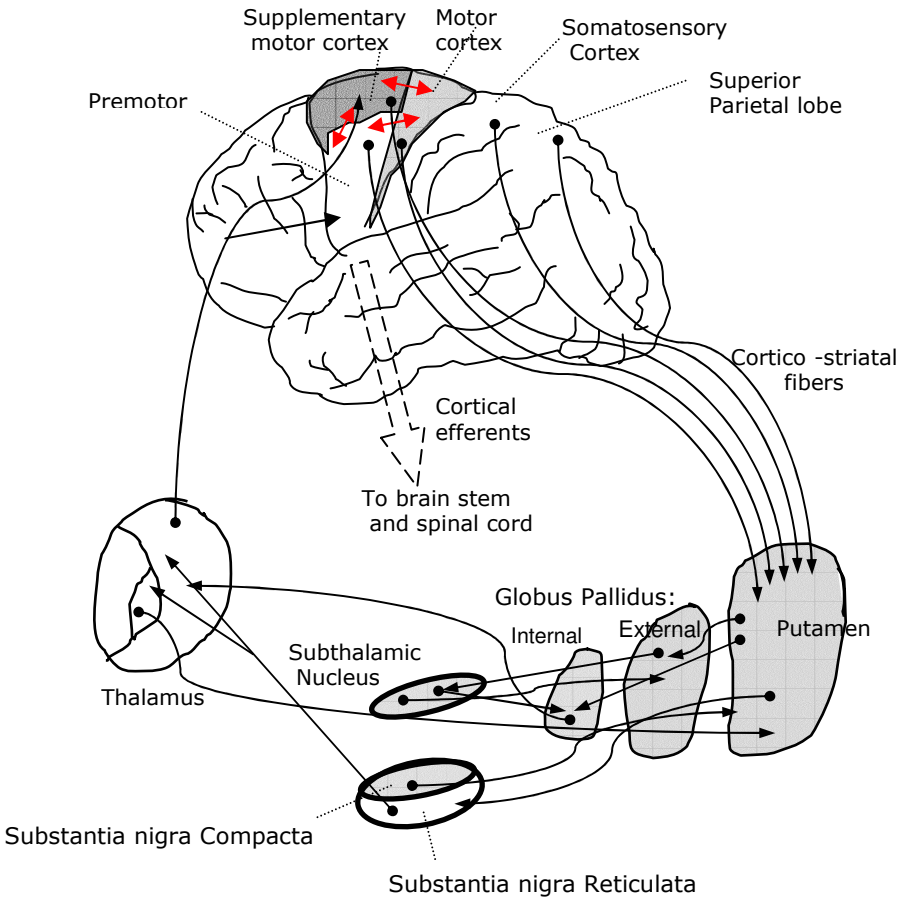

Fig.3.1: Anatomical basis for motor functions of basal ganglia

There are two important alternate pathways between the input port STR and output port GPi. One, the *direct pathway*, represents the direct connection between STR and GPi. The other, the *indirect pathway*, connects STR, GPe, STN and GPi in that order. Gabaergic neurons of GPe project mainly to the STN, whose excitatory, glutamergic

neurons send feed forward connections to GPi/SNr, completing the arm of indirect pathway. STN neurons also send glutamatergic connections back to GPe and the putamen. The GPe also sends projections to the output nuclei themselves, thereby completing second arm of the indirect pathway. Activation of striatal neurons associated with indirect pathway tend to increase BG output by increasing neuronal activity at the level of output nuclei – in one case by disinhibiting the STN with its excitatory projections to GPi/SNr, and the other by disinhibiting GPi/SNr.

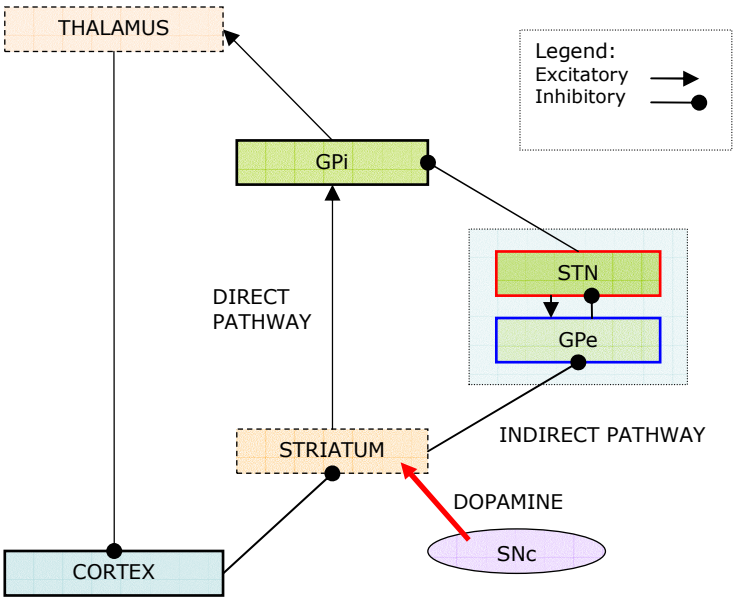

Fig: 3.2. The direct and indirect pathways in Basal ganglia

Recent anatomical, physiological and computer modeling studies by Terman et al (2002) have revealed that oscillatory process at the level of single neurons and neural networks in STN and GPe are associated with the operation of the BG in health and in Parkinson's disease(PD) (Bevan, 2002). An autonomous oscillation of STN and GPe neuron underlies tonic activity and is important for synaptic integration, whereas abnormal low

frequency rhythmic bursting in the STN and GPe is characteristic of PD. Normal information processing is characterized by complex spatiotemporal patterns of firing, whereas in PD, STN and GPe neurons display more correlated synchronous and rhythmic activity (Bevan, 2002; Bergman, 1998). The obvious question that arises is, "what is the functional significance of these complex oscillations?" In this chapter an attempt is made based on a computational model of BG. It is argued that the complex activity of BG acts as a source of exploratory drive. The subsequent sections emphasize reward signaling in BG and realization of reinforcement signal.

3.1.2 Reward Signaling in Basal Ganglia: How does Reward Lead to Learning?

Dopaminergic inputs to the putamen consist of nigrostriatal projections that originate in the SNc. At the network level dopamine appears to have different role in the direct and indirect pathway. Given the reciprocal reentrant effects associated with differential activations of the direct versus the indirect pathways, the differential effects of dopamine on these two pathways would be viewed as resulting in the enhancement of positive feedback, and suppression of negative feedback, returned to the various cortical areas that receive BG influences (Alexander, 1998).

Dopamine has also been shown to have a role in synaptic plasticity within the STR, being implemented in both Long term Potentiation (LTP) and Long term Depression (LDP). Dopamine neurons may play an important role in determining when striatal neurons should be strengthened or weakened. In this respect Dopamine might be seen as playing a role in striatal information processing, analogous to "adaptive critic" in connectionist networks.

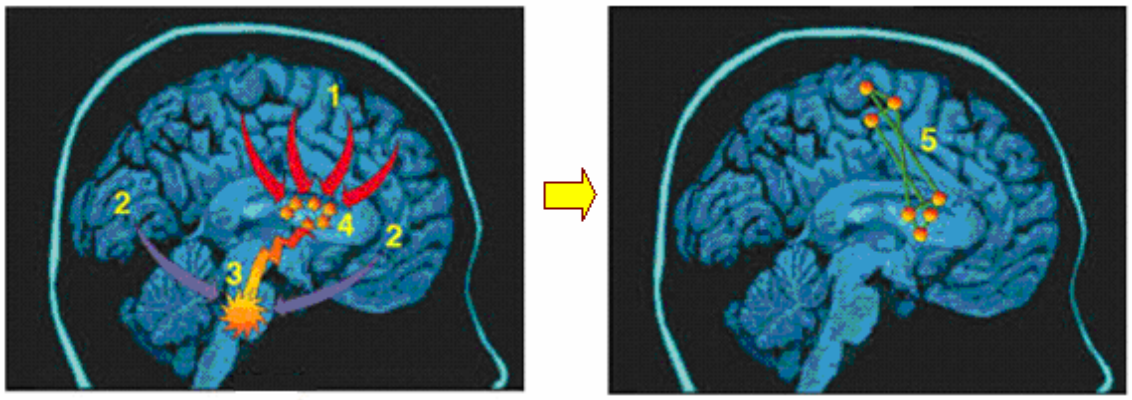

Fig. 3.3 How rewards lead to learning? Steps involved in reward based learning[5]. See text for the explanation of these steps.

Currently a widely accepted view is that the input from dopaminergic neurons to the STR provides the reinforcement signal required for adjusting the probabilities of subsequent action selection. Positive reinforcement helps to control the acquisition of learned behaviors (Reynolds et al, 2001). Reynolds et al (2001) report a cellular mechanism in the brain that may underlie the behavioral effects of positive reinforcement. They have used intracranial self-stimulation (ICSS) as a model of reinforcement learning, in which each rat learns to press a lever that applies reinforcing electrical stimulation to its own substantia nigra. With experiments on Intra Cranial Self Stimulation (ICSS) model of reinforcement learning, they explain how rewards could lead to learning (see fig.3.3).

[5] Figure taken from url: http://anatomy.otago.ac.nz/research/basal-ganglia/publications/abstracts/2001_nature.html

[7] This part of the discussion is heavily drawn from the excellent review article on Computational Approaches to Neurological Diseases by Crystal and Finkel in the book, Reggia, Ruppin and Berndt, Neural Modeling of Brain and Cognitive disorders, World Scientific, 1996.

Steps involved in reward based learning in BG:

1. *Cells within the brain involved in generating movement are activated and send their output to STR.*
2. *Other brain areas decide if the movement produced an outcome that was rewarding and send the result to the dopamine cells.*
3. *If the result is interpreted as "good," the dopamine cells are activated and release a pulse of dopamine into the STR.*
4. *The released dopamine causes connections within those circuits which were active in the production of the movement to be strengthened.*
5. *The reinforcement of the connections between neurons induced by dopamine is long – lasting. Next time, the same situation is much more likely to produce the same movement response (Reynolds, 2001).*

The current model of BG is based on RL, draws the above mentioned steps to some extent. Any realization of reinforcement learning requires, in addition to a reward signal, a noise source that can exhaustively explore the output (or action space). It is proposed in this chapter that the complex activity of STN – GPe loop accounts for the noise signal.

3.2 COMPUTATIONAL MODELS OF BASAL GANGLIA

Enormous progress has been made in characterizing the structure and functionality of the BG, and yet comprehensive understanding of the contribution of these nuclei to behavioral control remains elusive. Functional models of BG are thus in great need for a comprehensive theory of BG operations. Functional models should be able to both assimilate the constraints imposed by the neurobiological data and to simulate various candidate behavioral functions in which these structures (nuclei) are believed to participate (Alexander, 1998). Computational modeling of neurons and neural networks is complementary to traditional techniques in neuroscience (Houk et al, 1998). Thus computational modeling of BG based on neurobiological data is significant for comprehensive understanding. In this section a brief review of computational models of BG highlighting its functional roles is presented. This effort has drawn heavily from the excellent reviews presented by Prescott et al (2003) and Houk et al (1998).

Most of the effort so far directed at BG modeling has been concerned with simulating interactions between the various BG structures, and between the BG and other key brain regions such as cortex, thalamus, and brain stem (Prescott et al 2003). The chief computational hypotheses governing the BG model investigate the following functions:

i. Regulation of the degree of action gating
ii. Selection between competing actions
iii. Sustaining working memory representations
iv. Storing and enhancing sequences of behavior
v. Reinforcement learning
vi. Timing and coincidence detection

Action Gating

A key function of the STR is to provide intermittent, focused inhibition (via the 'direct pathway') within output structures which otherwise maintain inhibitory control over motor/cognitive systems throughout the brain. This architecture strongly suggests that a core function of BG is to gate the activity of target system via the mechanism of disinhibiting. Many BG models employ selective gating, however that of Vidal and Stelmach (1995) is interesting as it explores gating operations in both normal and dysfunctional model variants. These authors coupled a simulation of BG intrinsic circuitry to a neural network (Bullock's VITE model) that computed arm movements. Excitatory striatal input resulted in a smoothly varying signal to thalamic targets that provided 'GO' signal for the motor command, and also sets its overall velocity. The time taken to execute movements decreased with increasing BG input thereby matching the

results of striatal micro stimulation studies. A 'dopamine depleted' version of the model exhibited akinesia and bradykinesia similar to that observed in Parkinson's disease.

Selecting Between Competing Actions

The proposal that the BG acts to resolve action selection competition is based on a growing consensus that a key function of these structures to arbitrate between sensory motor systems competing for access to the final common motor path. A computational hypothesis developed from this idea relies on the premise that afferent signals to the STR encode the salience of 'requests for the action' to the motor system (Redgrave et al, 1999). Multiple selection mechanisms embedded in BG could resolve conflict between competitors and provide clean rapid switching between winners. First, the up/down states of the striatal neurons may act as a first pass filter to exclude weakly supported 'requests'. Second, local inhibition within the STR could selectively enhance the activity of the most salient channel. Third, the combination of focused inhibition from STR with diffused excitation from STN could operate as a feed forward, off-center/on surround network across the BG as a whole (Mink, 1996). Lastly, local reciprocal inhibition within the output nuclei could sharpen up the final selection. An earlier model of Berns and Sejnowski (1996) shared the 'action selection' premise of Gurney et al (2001), but emphasized possible timing differences between the direct and indirect pathways in a model that included just the feed-forward intrinsic BG connections. An interesting feature of this model is that it incorporated a version of the dopamine hypothesis for reinforcement learning as a means for adaptively tuning the selection mechanism.

Sustaining Working Memory

The relationship between BG and cortex is characterized by segregated parallel loops, in which cortical projections to the STR are channeled through BG outputs to the thalamus and then back to their cortical areas of origin. The thalamic nuclei in this circuit have reciprocal, net excitatory, connections to their cortical targets. This architecture suggests a pattern of cortical thalamic activity which, once initiated by disinhibitory signals from BG, could be sustained indefinitely. Several authors proposed that this circuit would act as a working memory store (e.g.: Houk et al., 1995)

Sequence Learning

A plausible use for the working memory mechanism outlined in the previous section would be to link successful selection during the development of behavioral / cognitive sequences. This idea has therefore become a central theme in a number of BG models. For example, Berns and Sejnowski (1998) propose a systems level computational model of the BG based closely on known anatomy and physiology. They assume that the thalamic targets, which relay ascending information to cortical action and planning areas, are tonically inhibited by the BG. Another assumption is that the output stage of the BG, GPi, selects a single action from several competing actions via lateral interactions. Finally they propose that a form of local working memory exists in the form of reciprocal connections between the external GPe and STN, with the STN-GPe connections learning by an associative learning rule. Thus the STR, which was assumed to be a conjunction of cortical states directly, selects an action from GPe during training which, after training is complete, acts as a cue for the production of the complete sequence of actions, thereby

providing a mechanism for encoding action sequences. Sequence learning is another important issue in BG modeling. For instance Dominey (1995) have extended their model of delayed saccade control to include a mechanism for associative and sequence learning based, again, on the hypothesis that dopamine provides a reinforcement learning signal.

Reinforcement Learning

The term "Reinforcement Learning(RL)" comes from the studies of animal learning in experimental psychology, where it refers to the occurrence of an event, in a proper relation to a response, that tends to increase the probability the response will occur again in the same situation (Barto, 1998). The term RL is widely adopted by theorists in engineering and artificial intelligence. It is usually formulated as an optimization problem with the objective of finding an action or strategy for producing an action that is optimal or best in some well-defined way. Most of the models of reinforcement learning are based on actor–critic architecture wherein critic sends reinforcement to actor in response to an action made by it. There exists non – associative and associative reinforcement learning in the literature. In non – associative learning, the only input to the learning system is reinforcement signal, whereas in associative case the learning system also receives stimulus process that provides information about the process and possibly other information as well. In both the cases following are the key observations suggested by Barto (1998).

1. *Uncertainty* plays a key role in the RL.
2. The critic is an abstract model that evaluates the learning system's actions.
3. The reinforcement signal can be any signal evaluating the learning system's actions.

4. The critic's signal does not does not directly tell the leaning system what action is the best; it only evaluates the action taken.
5. RL algorithms are *selection* processes.
6. RL involves a conflict between exploitation and exploration.

The increased interest in RL is due to its applicability to learning by autonomous robotic agents, and hence a number of models and learning algorithms have evolved. Some of these are listed below.

1. Classical conditioning

   a. Roscorla Wagner rule: It is based on "theory of Pavlovian conditioning" (Roscorla and Wagner, 1972) for the prediction of reward.
   b. Predicting future reward by Temporal Difference Learning Rule (TDRL).

The prediction error (δ) plays an important role in both of the above learning rules. Schultz et al (1998) and Montague et al (1996) recognized that dopaminergic neurons in SNc and ventral tegmental area (VTA) carry a (dopamine) signal that encodes prediction error.

2. Associative RL rules
   a. Associative search rule (Klopf, 1982): It is basically hebbian correlation rule with the reinforcement signal acting as a modulatory factor.
   b. Selective bootstrap (Widrow et al, 1973): It is an extension of LMS rule.
   c. Associative reward penalty (A_{RP}) (Barto and Anandan, 1985): This can be realized with essential ingredients as stochastic output units. In terms of cost function as there is no gradient information, it is important to have randomness in the learning system, so that possible outputs can be explored until a correct (rewarding) output is found.

3. Sequential action choice

Sequential reinforcement requires improving the long – term consequences of action, or of a strategy for performing actions, in addition to short-term consequences. An important special case of this problem occurs when there is no immediate reinforcement until a goal state is reached. Samuels checkers player, Sutton's temporal difference TD methods(1988), Tesauro's backgammon(1992), Watkin's Q- learning(1989) comes under this category.

There is considerable evidence that the dopaminergic neurons which project from the midbrain to the neostriatum mediate an internal reinforcement signal. A major target of this signal is the synapses that connect the cerebral cortex to neostriatum. However the effect of dopamine on these synapses is not completely understood (Wickens, 1998; Barto, 1998). Is has been shown that dopamine has positive reinforcement on striatal neurons. A model based on corticostriatal interactions, in which modifiable synapses located in the corticostriatal pathway, promises to be a useful way of integrating cellular mechanisms of reinforcement into intelligent behavior.

Timing and Coincidence Detection

Coordinating the relative timing of multiple streams of processing is crucial in both motor performance and sensory perception. Temporal processing in biological systems occurs over a range of time scales and is broadly classified into 3 categories: 1) circadian timing, which corresponds durations of the order of days, and handled by brain structures like suprachiasmatic nuclei, 2) interval timing, which corresponds to durations in the range of seconds to minutes, and coordinated primarily by corticostriatal interactions, and

3) millisecond timing, which obviously corresponds to millisecond durations, controlled by the cerebellum (Buhusi and Meck, 2005).

The role of BG in 'interval timing' appears to emerge from the dynamics of thalamo-cortico-striatal loops. In the Striatal Beat Frequency (SBF) model (Buhusi and Meck, 2005), a model that highlights the timing function of BG, the cortical oscillators are assumed to increase synchrony just before movement onset and maintain the rhythm throughout the performance. The dopaminergic burst at trial onset could trigger the synchronization of cortical oscillators according to SBF model(Buhusi and Meck, 2005) and the striatal neurons are tuned to respond to specific patterns of cortical oscillations (Buhusi and Meck, 2005).

Apart from the above conceptual additions to knowledge on BG's functional significance, it is known to have a role in cognitive and memory operations (Houk et al, 1998). BG model is still in the stage of exploring the space of alternative hypothesis, seeking to rationalize theoretical proposals whilst trying to match known neurological constraints (Prescott et al, 1999). We hence propose a model of BG in the next section with specific neurobiological analogs.

3.3 PRESENT MODEL

The present model is based on the hypothesis that the dopamine signal that encodes reward for an action, selects the pathways in BG to coerce the animal into exploration or exploitation for a given situation. For the purpose of simulating the above hypothesis, a task based model is assumed wherein the BG learns to persuade a 2-joint model of arm to reach a target.

3.3.1 Architecture of Proposed Model

The neural model proposed is having two parts, namely 1) Model of BG, 2) A 2 link model of 2D arm. The architecture of the model is shown in fig. 3.4.

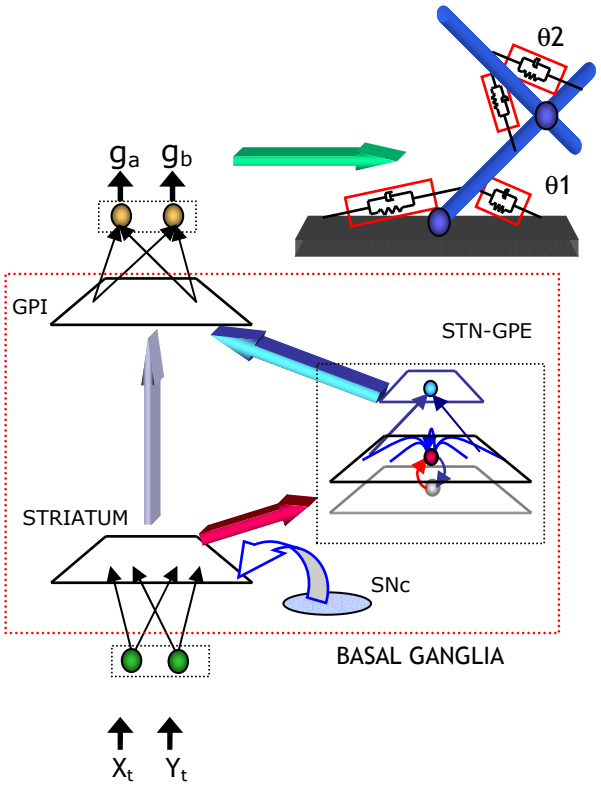

Fig.3.4: Architecture of a model of basal ganglia

Model of Basal Ganglia

Each of the nuclei of BG is realized with neural networks such as self organizing maps and oscillator neural networks. Realization of each of these nuclei is discussed below.

Striatum (STR): This nucleus is realized with a self organizing map (SOM) which is trained on randomly chosen target points from the workspace (see fig.3.9.b) of the arm. This map can also be interpreted as Sensory Map (sensory MAP). The output of this nucleus is given by Y_{direct}.

Globus Pallidus internal (GPi): An inverted SOM is considered for the realization of GPi. Firstly a SOM is trained on a subset of possible for muscles of activations (g_a, g_b) which can set the arm into various configurations. The trained SOM is inverted to realize a motor map or GPi. A Gaussian like input activation to inverted SOM can set the arm to an equilibrium configuration where its end-effector reaches a point (x_e, y_e).

Subthalamic nucleus (STN) and Globus Pallidus external (GPe): A pair of neuron layers, connected in excitatory-inhibitory fashion represent the STN-GPe system. A single STN – GPe neuron pair with glutamergic and Gabaergic connections are shown as excitatory and inhibitory connections in fig.3.5. The neuron model in each of these networks is given by a pair of first order nonlinear differential equations as shown below. The dynamics of GPe neuron given by,

$$\frac{dx}{dt} = -x + V + s + I \tag{3.1}$$

$$V = \tanh(\lambda x) \tag{3.2}$$

Where 'x', denotes the state of the GPe neuron, 'I' is the external input to the neuron, 's' is the state of STN neuron and '*V*' denotes output of GPe neuron and $\lambda(>>1)$ controls the slope of 'tanh' function. The dynamics of STN neuron is given by

$$\frac{ds}{dt} = -s - V \tag{3.3}$$

Where's' is the output of STN neuron. Note that while 'x' has inhibitory influence on 's', 's' in turn excites 'x'. Such excitatory-inhibitory pair is a standard recipe for producing oscillations. Analysis of eqns. (3.1, 3.2, and 3.3) shows that, for I=0, s = 0, and $\lambda >>1$, *V* in (3.1) has 2 stable states, $V \approx \pm 1$. Moreover, if *V* is at negative (positive) stable state, a sufficiently large positive (negative) 's' in eqn. (3.3) flips '*V*' to its positive (negative)

stable state. In eqn. (3.3),'s' simply follows '-*V*' with a delay. Therefore, a persistent value of '*V*' induces a change in 's' such that '*V*' is toggled periodically. Oscillations are produced by the above system, but only within certain limits of the external input I. Existence of limit cycle is proved in Appendix A.

Pair of neurons discussed above is replicated and connected in a 2D grid fashion for realizing STN-GPe nuclei as shown in fig. 3.5 (a) and fig. 3.7 (b). The connections between these inter nuclei are assumed to be one to one with inclusion of lateral connections in the GPe layer and no lateral connections in STN layer. There exists one-to-one connection from STN to GPe and vice versa. The GPe network also has lateral connections in it, these connections strengths are calculated using the eq.3.7 (see fig.3.5 (b)).

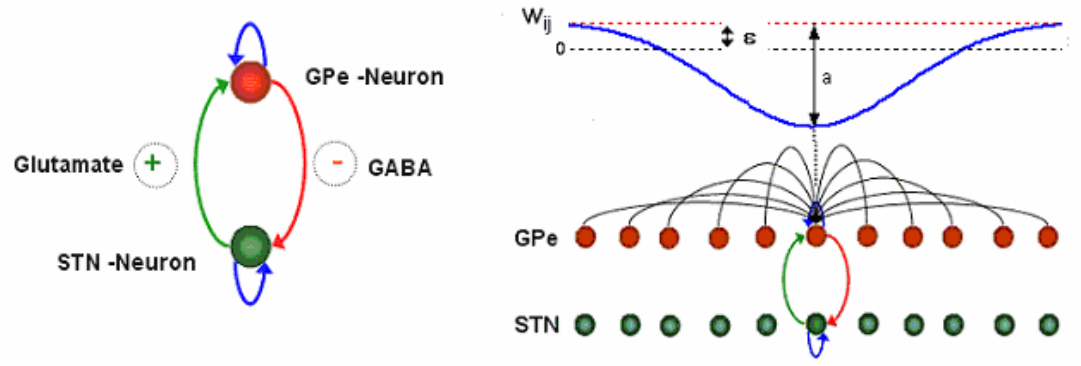

(a) (b)

Fig.3.5. (a) STN – GPe neuron pair illustrating the excitatory and inhibitory connections, (b) Network model of STN – GPe loop with lateral connections

Dynamics of network model of STN – GPe loop are given by,

$$\frac{dx_{ij}}{dt} = -x_{ij} + \sum_{q=1}^{n}\sum_{p=1}^{n} w_{ij,pq} V_{pq} + s_{ij} + I_{ij} \tag{3.4}$$

$$V_{ij} = \tanh(\lambda x_{ij}) \tag{3.5}$$

$$\frac{ds_{ij}}{dt} = -s_{ji} - V_{ij} \tag{3.6}$$

where (i, j) and (p, q) denote the neurons position on the 2D grid, n is the size of the 2D grid, x_{ij} is the state of (i, j) th neurons on the GPe grid, s_{ij} is $_{the}$ state of (i, j) th neurons on the STN grid, V_{ij} is the output of (i, j) th neuron on the GPe network, S_{ij} is the output of (i, j) th neuron on the STN network. The lateral connections, within GPe layer are assumed to be translation invariant and are given by,

$$W_{ij,pq}^{GPe} = \varepsilon - a\exp(-r_{lat}^2 / \sigma_{lat}^2) \qquad \text{for } r < R$$

$$= 0, \text{ otherwise.} \tag{3.7}$$

where $r_{lat} = [(i-p)^2 + (j-q)^2]^{1/2}$, squared distance of the neurons on 2D grid; 'a' controls the depth of the Gaussian bell function and 'σ_{lat}' its width, and 'R' is the neighborhood size. Thus each unit has a negative center and a positive surround; the relative sizes of center and surround are determined by ε. Smaller ε implies, more negative lateral GPe connections.

In the absence of input from the input layer (i.e., $I_{ij} = 0$), as ε is varied from 0 to 'a', the activity of STN-GPe system exhibits three different regimes: 1) chaos, 2) traveling waves, and 3) clusters (see fig.3.6.). Similar dynamic behavior has also been observed in more detailed electrophysiological models of STN-GPe system by Terman et al, 2002. Operation of the network in the first regime – chaos – is most crucial since it is the chaotic dynamics in the STN-GPe layer that makes the network extensively explore the output space.

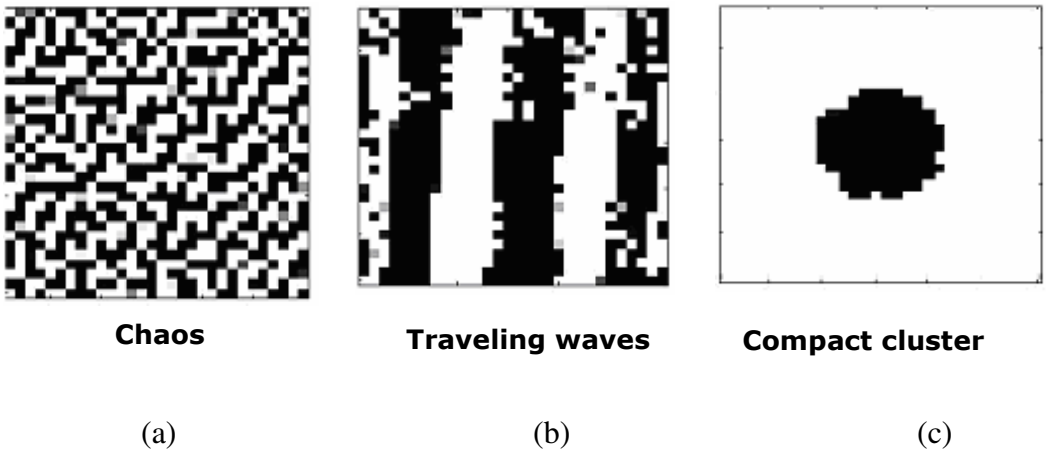

Fig.3.6: Dynamics of STN - GPe Loop: Three characteristic patterns of activity of the STN-GPe layer – (a) chaotic, (b) traveling waves and (c) compact center. The three activity regimes (from left to right) are obtained by progressively increasing ε from 0 to 2. Increasing ε increases the percentage of positive lateral connections in STN. I n regime (c), "compact center," the array splits into a center and a surround, with neurons is either region forming a synchronized cluster.

As the STN - GPe loop has a relatively large state space, the exploration becomes a time consuming process. To avoid this problem a convergence layer is assumed as shown in fig3.7. The connections from STN output are connected to GPi. These connections are trained offline with SOM algorithm.

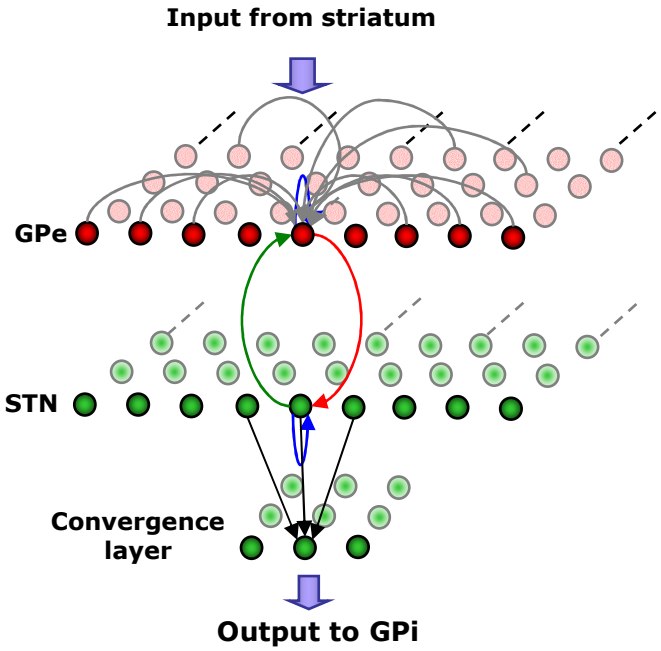

Fig. 3.7 The convergence layer for STN – GPe network

Substantia nigra pars compcta and Dopamine

The output nuclei, GPi, receive inputs from both direct and indirect pathways. Hence the net input to GPi is given by,

$$Y = rY_{direct} + (1-r)Y_{indirect} \tag{3.8}$$

where, 'r' assumes '1' for 'reward' and '0' for 'punishment', Y_{direct} is the output of STR, whereas $Y_{indirect}$ is the output of convergence layer of STN nuclei. The reward signal, 'r' can be interpreted as a form of dopamine signal. If the reward is low, indirect path way is selected and if reward is high, direct pathway is selected.

Model of 2D Arm

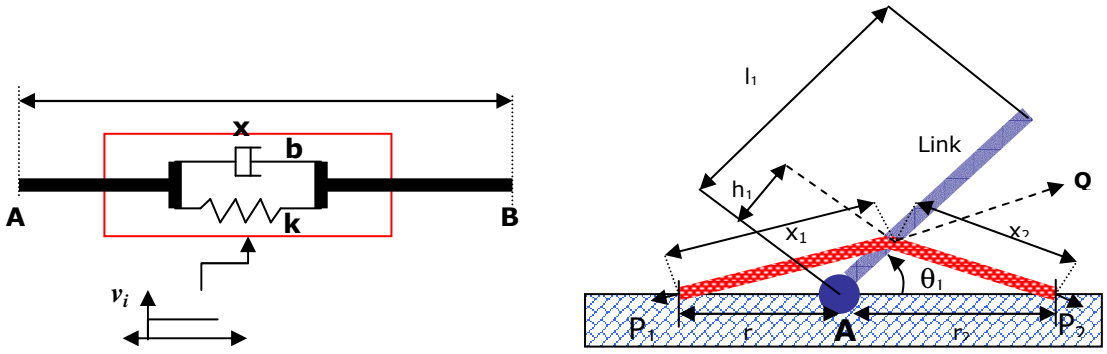

(a) (b)

Fig.3.8 (a) A simple muscle model based on spring damper system (b) a single link configuration with agonist and antagonist muscles

The arm model consists of two links with four muscles as shown in the fig. 3.9(a). For the realization of reaching task, it is assumed that the muscles of the arm model are driven by the neural activation from the model of BG. A simple muscle model which consists of a spring and damper system as shown in fig.3.8, with eqns. 3.9 and 3.10 is used for simulating muscle. The resting length (L_i) and tension (T_i) of simple muscle model (lumped) can be controlled by the neural activation as,

$$L_i(v_i) = \alpha(V_0 - v_i) \tag{3.9}$$

$$T_i = k_i(x_i - L_i(v_i)) + b_i\dot{x}_i \tag{3.10}$$

where, α is a constant, v_i is the neural input to i^{th} muscle , k_i is spring constant , x is the actual length of the muscle, and b_i is damper coefficient.

The effect of a given set of neural activations to agonist and antagonist muscles is to place the arm in a configuration. Note that the mapping from neural activations to arm configurations is many-to-one. Activations of agonist and antagonist pair of a given joint can be increased in such a way that joint angle remain the same. Therefore, to avoid multiple solutions for a single joint angle an assumption is made on the neural activations to agonist and antagonist muscles on their resting lengths,

$$L_1 + L_2 = L_3 + L_4 = C \tag{3.11}$$

where C is a constant, L_1 and L_2 resting lengths muscles corresponding to shoulder joint '***A***' where as L_3 and L_4 are that of elbow joint '***B***'(see fig.3.9). The neural activations (v_1 and v_3) are calculated using the GPi signals g_a and g_b as $v_1 = g_a$, $v_3 = g_b$ (see fig. 3.10). For the given neural inputs, the resting lengths of all the muscles can be calculated using eqn.3.9 and 3.11. The joint angle corresponding to these neural activations (valid for both the joint angles θ_1 and θ_2) is solved using the equation,

$$\frac{d\theta}{dt} = -\frac{(h_1 r_1 x_1)(k_2(x_2 - L_2)) - k_1(x_1 - L_1)(h_1 r_1 x_2)}{2h_1^2 r_1^2 (\frac{x_2}{x_1}) b_1 \sin(\theta) + 2h_1^2 r_1^2 (\frac{x_1}{x_2}) b_2 \sin(\theta)} \tag{3.12}$$

where, the r_1, r_2, are the pivot lengths (at points P_1, and P_2), h_1, is the heights at which the pivots on the link – 1(at Point Q_1) to the joint '**A**' (see fig3.8 (a)). And x_1 and x_2 is calculated using the cosine rule as, $x_1^2 = h_1^2 + r_1^2 + 2h_1 r_1 \cos\theta$ and $x_2^2 = h_2^2 + r_2^2 - 2h_2 r_2 \cos\theta$.

The above equation is derived by equating the momentums due to tensions in agonist and antagonist muscle at joints . The position of the end effector's due to these joint angles is calculated as,

$$x_e = l_1 \cos(\theta_1) + l_2 \cos(\theta_1 + \theta_2) \quad (3.13)$$

$$y_e = l_1 \cos(\theta_1) + l_2 \sin(\theta_1 + \theta_2) \quad (3.14)$$

where l_1, l_2 being the lengths of link 1 and 2 respectively. The reachable region by the 2-link arm model is called as 'workspace' of the arm. The workspace of the current model with $r_1 = r_2 = r_3 = r_4$, $h_1 = h_2$, $l_1 = l_2$ is shown in the fig.3.9 (b).

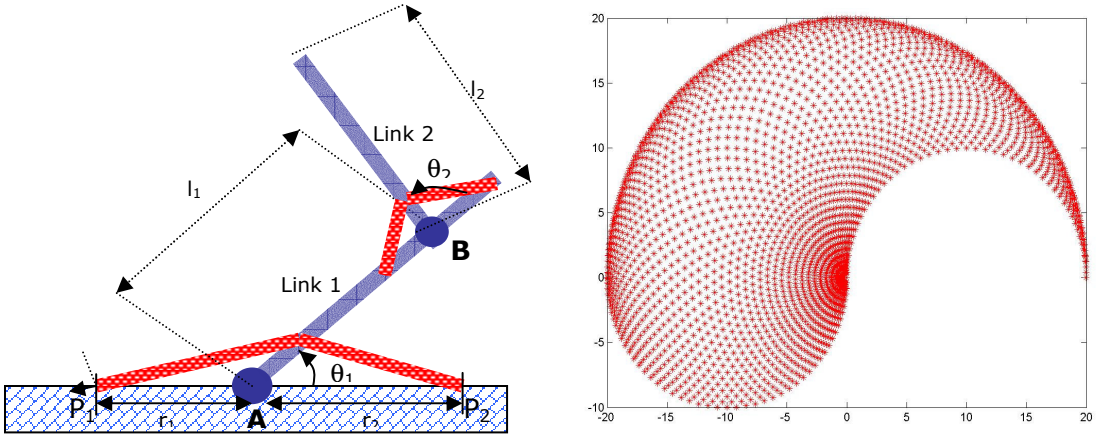

(a) (b)

Fig: 3.9 (a) The 2-link arm model, (b) The workspace (shaded region; the origin corresponds to elbow joint) of the 2-link arm with $r_1 = r_2 = r_3 = r_4$, $h_1 = h_2$, $l_1 = l_2$.

3.3.2 Training Phase: Exploration and Consolidation

The target point (x_t, y_t) is fed to STR (sensory SOM). The output of the STR is propagated to the output nuclei GPi map in the direct pathway for the first time. The output motor map (GPi) will generate (motor SOM) for the first time. The output of this nucleus further generates neural activations, which stimulate the muscles of the arm model. Due to the activations to the arm, its configuration changes from initial

configuration to a final configuration due to which the 'end effector' of the arm reaches a point (x_e, y_e) in its workspace. A reward (dopamine) signal that is generated due to the current action is given by,

$$\begin{aligned} r &= 1 \quad \text{if } d \le d_{thresh} \\ &= 0 \quad \text{else} \end{aligned} \tag{3.13}$$

where, 'd' is the Euclidean distance between the target point to end effector's location is given by $d = \sqrt{(x_t - x_e)^2 + (y_t - y_e)^2}$, and d_{thresh} is a threshold distance. That is, no reward is received until the end effector is sufficiently close to the end effector. The reward signal assumed as a modulator (multiplicative) signal to the synaptic strengths of STR to GPi and STR to GPe as shown in the fig.3.10. The low reward, r = 0, is interpreted as failure to reach. In effect the net input from the direct pathway to GPi is 'zero'. The indirect pathway is activated due to the reason that the inhibitory action onto GPe is also 'zero'. This lead to sustained complex (chaotic) activity in STN-GPe loop. The chaotic activity which drives the output nuclei, GPi, makes the arm to explore the workspace. Due to the exploration, the arm model hits the target by chance. This leads to a positive reward signal (r = 1) that activates the direct pathway and the activity of indirect pathway gets suppressed due the high inhibitory inputs to GPe network (a huge negative input can freeze the activity of STN-GPe loop). Due to the positive reward (dopamine) signal on to the STR, the connections ($w_{STR-GPi}$) of STR and GPi are reinforced using the rule given by,

$$\Delta w_{STR-GPi} = \eta (y_{Gpi}^{r=1} - y_{Gpi}^{r=0}) y_{STR} \tag{3.14}$$

Where $y_{Gpi}^{r=1}$, is the activity of GPi corresponding to reward r= 1 due to exploration, $y_{Gpi}^{r=0}$ is the activity of GPi due to the direct pathway, that corresponds to reward r = 0, η is the learning rate.

Interpretation of pathways in BG as 'consolidation' and 'exploration' pathways

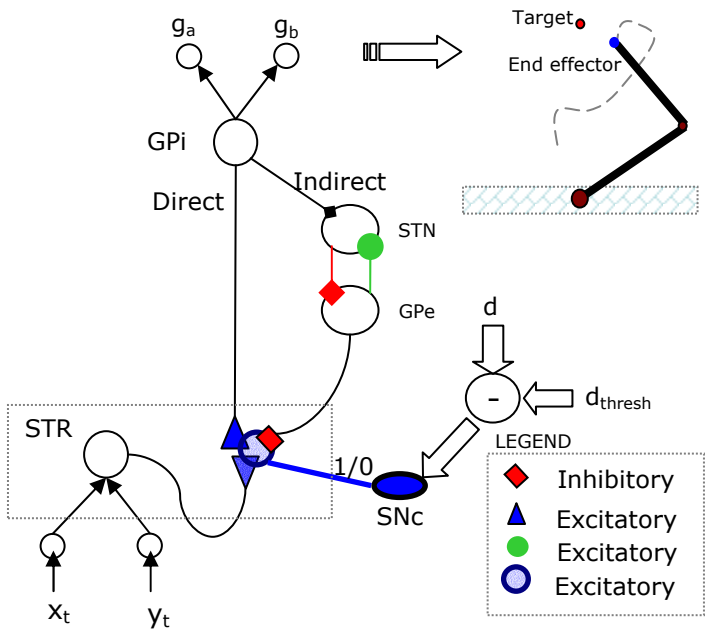

Fig.3.10. Microcircuit illustrating selection of pathways based on dopamine signal

The proposed model is a neural network architecture consisting of two parallel pathways (fig.3.10). The pathways in BG, traditionally called "direct" and "indirect" pathways, can be renamed as "consolidation" and "exploration" pathways based on their functional roles. The consolidation pathway from STR to GPi consists of learnable connections that represent the sensory-motor map involved in reaching task. The exploratory pathway consisting of the STN-GPe loop is a network of oscillatory neurons; internal connections among the oscillators are designed such that the STN-GPe loop produces chaotic activity (similar to the model of STN-GPe in [13]). Output of the STN – GPe loop to GPi provides a "noisy" or exploratory signal that is necessary for the realization of reward. The reward signal, representing dopamine, from SNc is fed to STR which selects between the consolidation pathway and the exploratory pathway depending on the reward level. When the reward is low, the exploratory pathway is selected. Complex activity of

STN-GPe loop, then, explores the output space, resulting in exploratory movement of the arm. When the exploring arm chances upon the target, the system receives a strong reward signal, the consolidation pathway is selected (the exploratory drive is suppressed) and the connections between STR and GPi are reinforced in a Hebb-like fashion.

3.4 SUMMARY

In the current chapter, a computational model of BG is presented. The computational model explains how BG can act as a source of exploratory drive. Particularly an answer to the question of the functional significance of complex activity in STN-GPe loop is suggested. It is also hypothesized that dopamine signal selects the direct pathway and indirect pathway which act as consolidation and exploration pathways, depending on the action generated. The training and testing results are discussed in chapter 5.

In the previous chapter the functional significance of BG is presented highlighting a point that it is involved in timing. Whereas in the present chapter it is shown that BG has a role in exploratory drive. The next chapter deals with an integrated model of handwriting generation and BG model. The dopamine deficient conditions in BG are simulated to understand the Parkinsonian handwriting.

CHAPTER 4

UNDERSTANDING PARKINSONIAN HANDWRITING THROUGH A COMPUTATIONAL MODEL

4.1 INTRODUCTION

Handwriting (HW) is a learned, highly practiced human motor skill that involves the control and coordination of complex movement sequences. In the past decade, handwriting has been gaining attention as a source of diagnostic information, in a variety of neurological disorders including PD, Schizophrenia, and Obsessive Compulsive Disorder (OCD) etc. Since handwriting, unlike reaching or walking, is a high-level motor activity, it engages large parts of cortical and subcortical regions that include SMA, PM, M1, BG, Cerebellum, Spinal cord etc. Since each of these regions contributes to handwriting output in its own unique fashion, pathology of any of these regions is manifest as characteristic features in handwriting. For example, in PD, a disorder of BG, handwriting is marked by diminutive letter size or *micrographia* (van Gemmert et al, 1999; Teulings et al, 2002) (fig.1.a). Similarly handwriting in patients with cerebellar damage is often characterized by omissions and unnecessary repetition of strokes (fig.1.b) (Silvery et al, 1999). Recognition of rich diagnostic value of handwriting had prompted a systematic study of handwriting and the extensive neuromotor organization that generates it. Computational modeling offers an integrative framework in which results of such studies – which come from several domains, like behavioral, imaging, etc – are brought together and given a concrete shape.

The present chapter starts with brief description of the pathology of Parkinson's disease and handwriting in PD. A computational model of PD handwriting is presented along with brief discussion of existing computational models.

4.2 PARKINSON'S DISEASE

PD is a progressive neurodegenerative disorder that occurs in 1% of the population over 55; the mean age at which the disease is first diagnosed (Prunier et al, 2003). PD symptoms include tremor, rigidity, postural abnormalities, micrographia and bradykinesia. The principal pathological characteristics of PD are the loss of dopaminergic neurons in SNc in BG (Singhala, 2003). PD signs appear when dopaminergic neuronal death exceeds a critical threshold. The presymptomatic period provides an opportunity for presymptomatic diagnosis and therapeutic intervention. Micrographia is an early symptom of PD. In the following paragraphs a short description of signaling in BG of normal controls and PD patients is given. This discussion draws from the excellent review presented by Vidal and Stelmach (1996).

Interaction in BG in Normal conditions

The STR serves as a major target for the inputs to BG. Striatal output projections form distinct parallel channels within the cortico-striato-pallidal pathways. These projections are termed as direct and indirect pathways due to their effect on their target nuclei, namely thalamus. The direct pathway is formed by the corticostriatal inhibitory projections from the neurons of striatal output to neurons in the GPi. Activation of striatal neurons inhibits neurons in GPi which in turns disinhibits thalamic nuclei. Conceptually, the direct pathway could be seen as a normally–closed movement gate that is opened by the corticostriatal activity that inhibits pallidal output allowing the emergence of movement. The indirect pathway is formed by corticostriatal inhibitory projections to

GPe which has an opposite effect to that of GPi neurons in the direct pathway. Cortico-Striatal activity in the indirect pathway tends to increase the activity of GPi cells, and therefore closes the "gate," via disinhibition of the subthalamic nucleus. These pathways may be involved in modulating parameters of the movement (Vidal and Stelmach 1996).

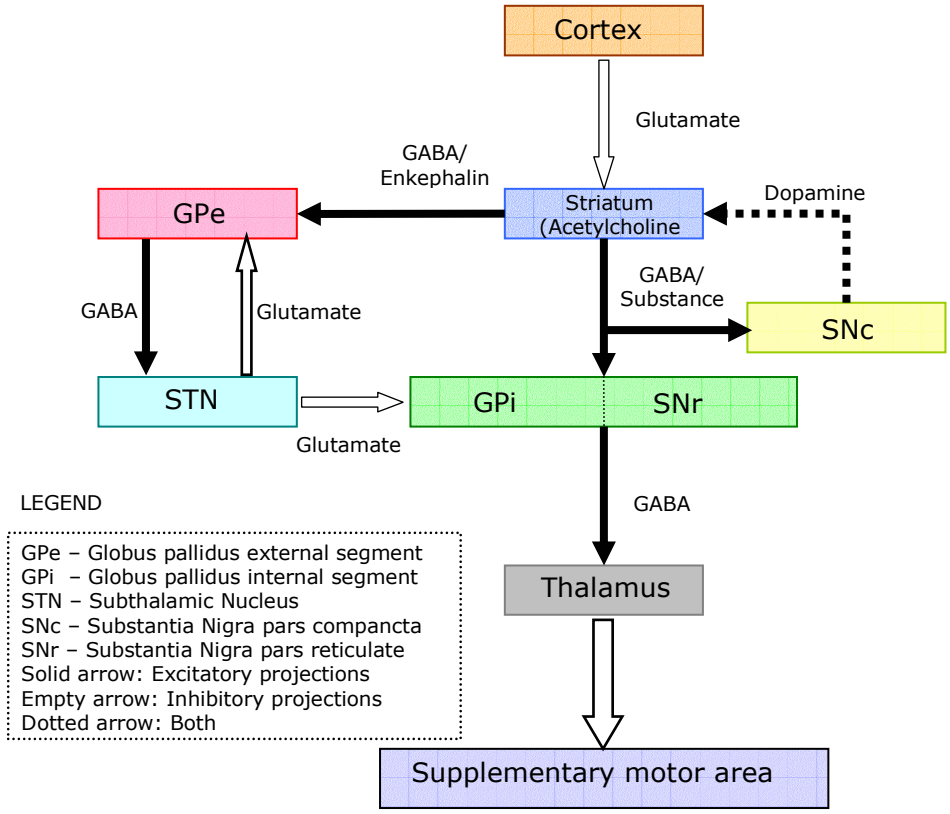

Fig.4.1. Normal functional anatomy of basal ganglia

Pathology of BG in PD

Loss of dopaminergic neurons in SNc leads to PD. It has been observed that there is a tonic increase of activity in neurons in GPi/SNr and STN, when the activity in the GPe decreases. Increased activity of the neurons from the STN resulting from a decrease in GPe output combines with the increased activity of GPi/SNr to produce a pathological degree of tonic activity in the BG output pathways. Increased-inhibition of thalamic target neurons by GPi cells leads to hypokinetic disorders (Vidal and Stelmach 1996).

Experimental and computational neurosciences suggest that in PD there is a smaller than normal activation of pallido-thalamocortical afferents, which produces reduced movement amplitudes and speeds, problems in switching between motor programs, and difficulties in executing parallel simultaneous movements (Vidal and Stelmach 1996). Lesion of GPi results in not only rigidity but also tremor and akinesia. Thus these experimental and neurophysiological data suggests that there is a functional specialization of BG neural populations that may be responsible for divergent response latency of these findings (Vidal and Stelmach 1996).

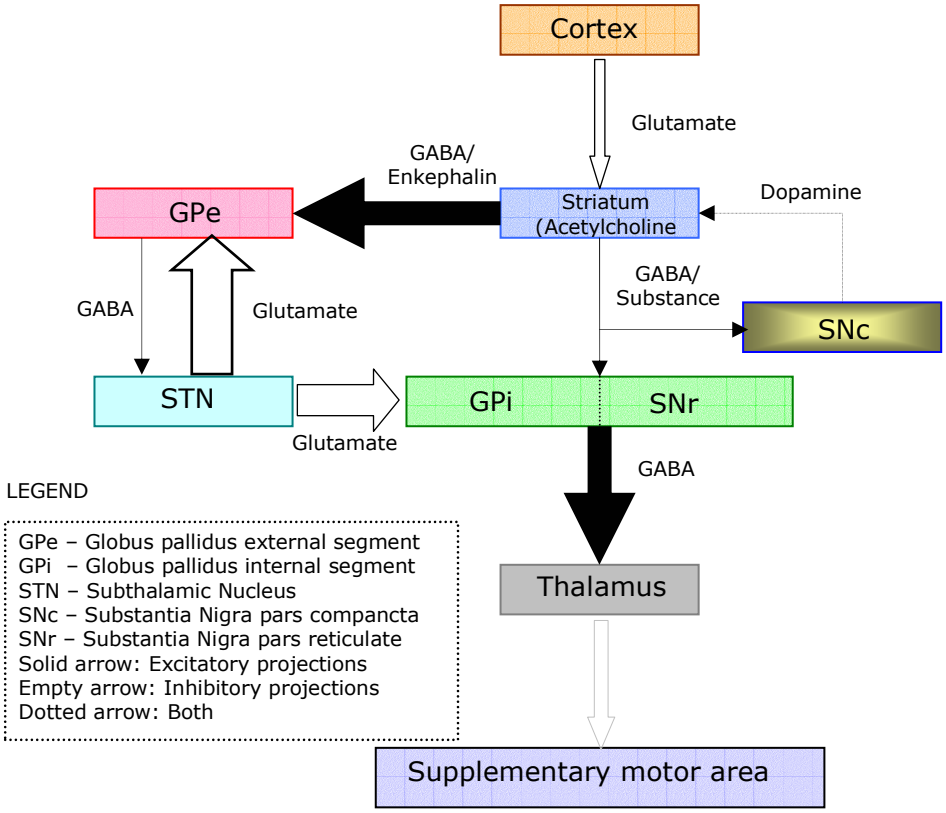

Fig.4.2 Pathology of Parkinson's disease: lesion to SNc

Voluntary movements are initiated and executed slowly in PD patients. The patients have problems in performing motor sequences. Studies by Martin et al (1994) show that there

exists instability in the movement sequence which is associated with irregular force profile, increase in peak movement velocity, and target overshoot; the overshoot became additive as the sequence was developed. It was also suggested that the tendency to slow down may be favored by complex sequences such as handwriting and speech or tapping (Vidal and Stelmach, 1996).

4.3 HANDWRITING IN PARKINSON'S DISEASE AND NEED FOR A COMPUTATIONAL MODEL

HW in PD has a characteristically distorted form known as micrographia, marked by an overall decrease in handwriting size, diminished legibility, and decreased movement speed. Handwriting acquired from PD patients has been used for early diagnosis of the PD also for the assessment of Drug-Induced PD (Guttman et al, 2003). There have been attempts to estimate the stage of maturity of PD from analysis of HW (Cubbah and Fairhrust, 2000, Stein, 2001). Such estimates have been used to control the dosage. They provide a quantitative basis to taper dose during recovery. However, most of such attempts to use HW for estimating disease stage are purely empirical, treating the brain as a black-box; they do not originate in a precise functional understanding of BG. A quantitative estimate of the stage of the disease is provided from the measured handwriting features. However, most of such studies are of empirical nature. PD handwriting is compared with that of normal subjects and the degree of difference is quantified (Cubbah and Fairhrust, 2000). It would be desirable for such studies to be backed up by a computational model that can explain why impairment in certain motor modules should result in specific handwriting changes. Such a model will require a more accurate understanding of the functional architecture of motor system.

Handwriting-based diagnostics of PD takes a "black box" approach to patients, wherein PD handwriting is compared empirically with that of normal subjects (Cubbah and Fairhrust, 2000; Stein, 2001). But unless there is a clear understanding of what aspects of handwriting are controlled by what modules of motor system, such diagnostic methods can only have limited value. There is a need to improve existing computational models of BG by an in-depth study of PD patients' handwriting performance. Such a model will be used to develop a more accurate diagnostic procedure, based on handwriting, for PD

4.4 LITERATURE REVIEW OF MODELS OF PARKINON'S DISEASE

Computational modeling can play an important role in understanding the pathophysiology of movement disorders such as Parkinson's disease. A number of groups are beginning to apply methodologies used in understanding central pattern generators and neuronal oscillations to the study of Parkinson's tremor (Terman et al, 2002; Bergman, 1998). These studies may yield insights that will eventually lead to better treatments for these disorders (Crystal and Finkel, 1996).

Borrett's model[7]

Borrett and colleagues (1993) have studied the dynamics of a 4 layer neural network where the output layer feeds back to the input layer. They propose that such a network might model the type of computation made by cortico-BG-thalamic-cortical loop that is dysfunctional in Parkinson's disease. Three types of stable states are possible from such nonlinear dynamic systems - a fixed attractor, a periodic attractor, or a chaotic attractor. Borrett showed that as the parameters of such a nonlinear system were gradually changed, the system suddenly reached a bifurcation point where output changed from a fixed attractor to a periodic attractor. In their model, they simulated the effect of

dopamine in cortico-ganglionic loops as a decrease in the threshold of excitability for units in the pre-output layer. They were able to show that as the threshold was gradually increased (simulating a decrease in dopamine levels) the output of the network first became slower and then changed from a fixed attractor state to a periodic (i.e. tremulous) state. Even though Borrett's model consists of abstract units whose output is defined by a sigmoidal function, the model makes several points that underscore the role of computational models in understanding neurological disease. First, behavior results from the dynamic interaction of multiple units from different modular systems. Second, the model suggests that some behaviors such as tremor will develop suddenly when a bifurcation threshold is reached. The decrease in dopamine in the substantia nigra of Parkinson's disease occurs gradually over several years. It is likely that there must be very significant decrease in dopamine levels (some have estimated as much as 90%) before patients become symptomatic (Crystal, and Finkel, 1996).

Contreras-Vidal and Stelmach

Vidal et al (1996) review that the wide spectrum of motor impairments observed in Parkinsonism may be due to a reduced capability of neurochemical modulation of pallio-thalamocortical activities that impairs movement implementation and execution. They suggest with a computer simulation of a network model of BG that, Parkinsonion micrographia is produced by smaller than normal pallido–thalamo–cortical activity.

van Gemmert's model

van Gemmert et al made computer simulations of network model of BG – thalamo – cortical relations which were used to provide a mechanistic account for the impairments found in PD HW. This computer simulation consists of Vidal's model (Vidal and Stelmach, 1995) of BG-thalamo cortical relations in normal and PD conditions and

Bullock's (Bullock and Grossberg, 1988) VITE model of motor cortex (SMA, PM) for central pattern generation(CPG). The VITE model accounts for the trajectory formation whereas BG model acts as a movement gating and modulation mechanism. A difference vector (DV) is computed for given target position (TPV) vector and present position vector (PPV) which contains information about desired stroke amplitude and stroke direction. This DV is modulated at thalamus by the pallido–thalamic inputs, which gate both the initiation and modulation or control the movement. Finally, the outflow command from the pallidal–gated thalamus is integrated at the PPV stage to update the trajectory. This model has been shown to reproduce many aspects of the normal and PD movement control including hypometria, bradykinesia, and akinesia, impairments in the coordination of multiple joints, micrographia, effects of levadopa on movement size and speed, and pallidotomy. The model does not include/capture the loss of complexity in STN-GPe oscillations in dopamine depletion conditions and hence does not explain tremor in handwriting.

4.5 PRESENT MODEL

The present model of PD handwriting is an integrated motor system model, consisting of enhanced BG model and neuromotor model of handwriting generation. The neuromotor model of handwriting production is the same as that of the model described in chapter 2, except that the output velocities are modulated by the BG output gating signals (Gx and Gy instead of OGP) as shown in the fig.4.1. The enhanced BG model is part of timing network in the handwriting generation model. The BG model described in chapter 3 is enhanced by adding a feedback mechanism which accounts for thalamo-cortico-striatal loop and dopamine signal from SNc. The model is described by equations as:

1) The dynamics of GPe neuron is given by,

$$\frac{dx_{ij}}{dt} = -x_{ij} + \sum_{p}\sum_{q} w_{ij,pq}^{GPe} V_{ij} + s_{ij} + I_{ij} \tag{4.1}$$

$$V_{ij}^{GPe} = \tanh(\lambda x_{ij}) \tag{4.2}$$

Where x, denotes the state of the GPe neuron, I is the external input to the GPe neuron(from striatal neurons), s is the state of STN neuron and ' V^{GPe} ' denotes output of GPe neuron and λ (>>1) controls the slope of 'tanh' function. The lateral connections $W_{ij,pq}^{GPe}$, within GPe layer are assumed to be translation invariant and are given by:

$$W_{ij,pq}^{GPe} = \varepsilon - a\exp(-r_{lat}^2 / \sigma_{lat}^2) \qquad \text{for r < R} \tag{4.3}$$

$$= 0, \text{ otherwise.}$$

where $r_{lat} = [(i-p)^2 + (j-q)^2]^{1/2}$, squared distance of the neurons; 'a' controls the depth of the Gaussian bell function and 'σ_{lat}' its width, and 'R' is the neighborhood size. Thus each unit has a negative center and a positive surround; the relative sizes of center and surround are determined by ε. Smaller ε implies, more negative lateral GPe connections, which leads to uncorrelated oscillations of STN neurons

The dynamics of STN neuron is given by

$$\frac{ds_{ij}}{dt} = -s_{ij} - V_{ij}^{GPe} \tag{4.4}$$

Where ' V_{ij}^{STN} ' ($V_{ij}^{STN} = \tanh(s_{ij})$) is the output of STN neuron. Note that while 'x' has excitatory influence on 's', 's' in turn inhibits 'x'. Such excitatory-inhibitory pair is a standard recipe for producing oscillations.

SNc neurons: A fixed dopamine signal is represented by '*DA'*.

Striatal neuron: The output of striatal neuron during modulation of movement is given by

$$y = k_1(DA) - k_2 \tag{4.6}$$

where k_1 and k_2 are constants. The input to the GPe neuron is given by

$$I_{ij} = y \quad \forall \quad (i, j) \tag{4.7}$$

GPi neurons: The output of GPi neurons is given by,

$$GPi_y = \sum_{i,j} w_{ij}^y v_{ij}^{STN} \tag{4.8}$$

$$GPi_x = \sum_{i,j} w_{ij}^x v_{ij}^{STN} \tag{4.9}$$

where w_{ij}^x and w_{ij}^y are fixed weights values connecting the STN grid to GPi_x and GP_y neurons. A dopamine signal '*DA*' is projected from SNc to STR in turn controls the numbers of active neurons in the STN layer.

The output velocity signals ($U_x(t)$and $U_y(t)$) of handwriting model are modulated by $G_x(t)$ and $G_y(t)$ signal as:

$$U_x^{M1}(t) = G_x(t)U_x(t) \tag{4.10}$$

$$U_y^{M1}(t) = G_y(t)U_y(t) \tag{4.11}$$

where the G_x and G_y are thalamic output signals similar to the pallidal signals GPi_x and GPi_y signals respectively. The signals $U_x^{M1}(t)$ *and* $U_y^{M1}(t)$ are the modulated signals at M1.

In normal conditions, the gating pulses are reasonably flat. The amplitude of these signals also controls the speed of writing. In pathological conditions in PD, due to loss of dopaminergic neurons, the dopamine (*DA*) signals decreases, which in turn reduces the overall activity if STN-GPe loop diminishing the amplitude of gating pulses. The reduced speed of writing results not only in bradykinesia but also in micrographia.

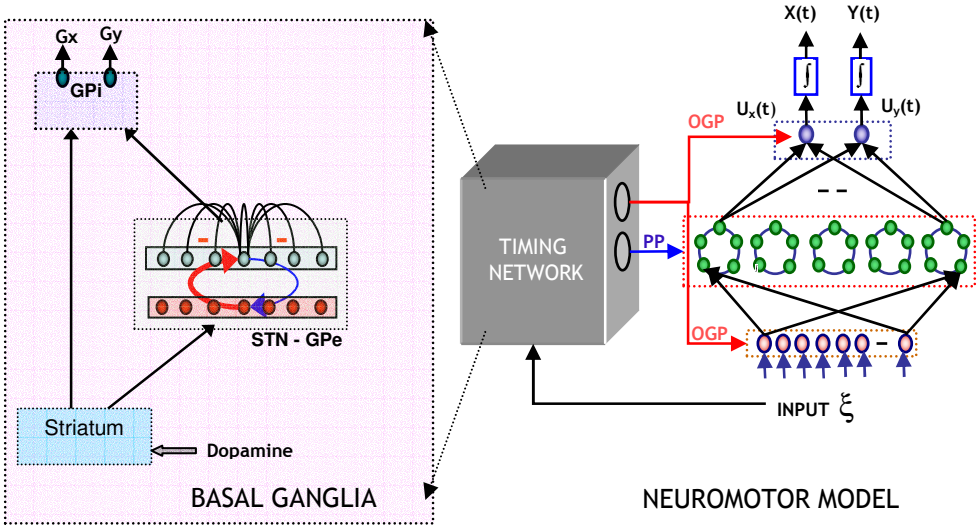

Fig.4.3: Integrated neuromotor model of handwriting generation

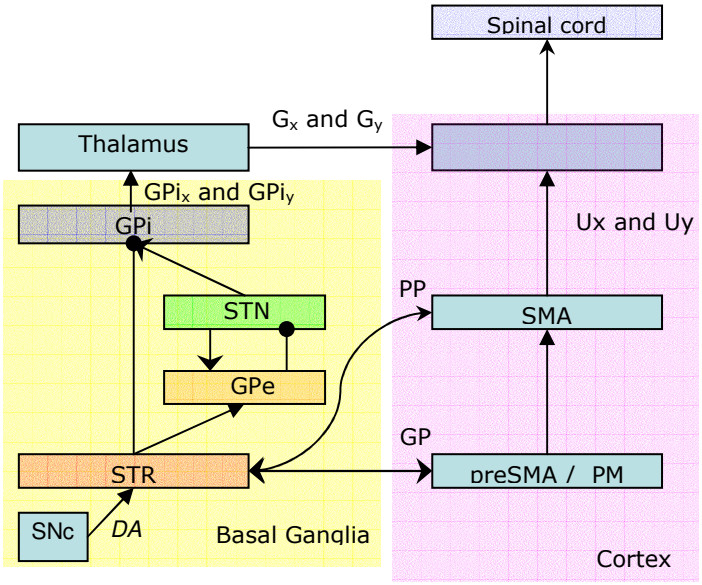

Fig. 4.4. Mapping the integrated model on to neuroanatomy

The STN – GPe neurons are connected in excitatory and inhibitory fashion: such connectivity is known to produce a range of dynamic behaviors like clustering, traveling waves and chaos (Terman, 2002) as discussed in chapter 3. It can be observed that for desired flat profile of gating signals the network needs to be in chaotic mode. Lesions can be introduced also into STN-GPe activity by disrupting the connection strengths of GPe loop. These lesions in STN-GPe loop will reduce the complexity of interaction that

results in traveling wave activity of STN producing wavy handwriting. These results are explained in detail in chapter 5.

4.6 SUMMARY

In the present chapter, the pathology of PD and handwriting in PD were discussed. Need for a computational model for understanding handwriting in PD is discussed. And a computational model of PD handwriting is presented. The results of this model are discussed in detail in chapter 5. Conclusions and predictions are discussed in chapter 6.

CHAPTER 5

RESULTS

5.1 RESULTS OF CHAPTER 2: A MODEL OF HANDWRITING GENERATION

Lower case English alphabets are collected using a stylus (electronic pen) connected to computer. Fig. 5.1 shows the handwritten strokes used in this thesis. These strokes are represented by pen tip coordinates, x(t) and y(t), along x-direction and y-direction respectively. The sampling frequency of the device is approximately 70 Hz. The collected strokes are nearly of the same length (120 samples each). The time (T) of writing for each stroke is approximately 120*(1/70) = 1.7143 seconds. These strokes are used for training the oscillator neural network model of handwriting generation.

Fig. 5.1: Handwritten stroke set

5.1.1 Experiment 1: Are Harmonics Necessary?

To find whether the oscillator network needs to have harmonics or not, the oscillatory layer is allowed to have N_s (= 10) sublayers with intrinsic frequencies of the oscillators assigned as {f, 2f, 3f, 4f, 5f, 6f, 7f, 8f, 9f and10f}, where f =1/T (~70/120 = 0.5833 Hz) and T (~120*(1/70) =1.7143ms) is the duration of the stroke (almost all of the strokes have same duration). The number of oscillators per sublayer is kept constant and is equal

to N_k (=25). The network is trained using back-propagation with momentum and batch update (discussed in chapter 2). The mean of the magnitudes of weights (after training) connecting each sublayer to output velocity nodes U_x and U_y are shown in fig. 5.2. The parameter ω_x, ω_y are means of magnitudes of weights connecting each sublayer (s^{th}) to output layer U_x and U_y (i.e. $\omega_x^s = \frac{\sum_i^{N_k} \| w_x^i \|}{N_k}$ and $\omega_y^s = \frac{\sum_i^{N_k} \| w_y^i \|}{N_k}$), where w_x^i and w_y^i are weights connecting i^{th} oscillator in s^{th} sublayer to U_x and U_y node in the output layer.

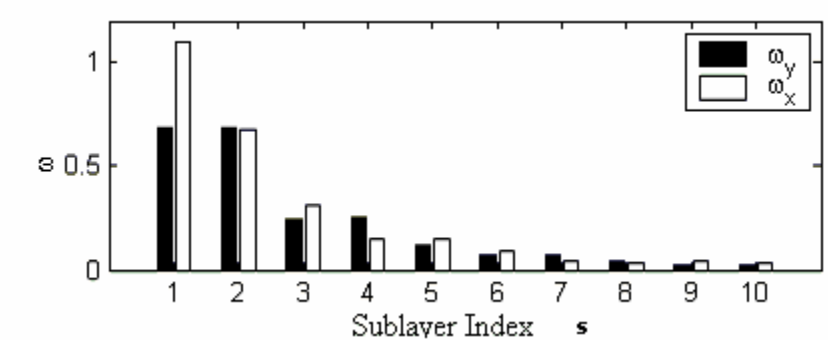

Fig. 5.2 Mean of weights of connecting each sublayer to second layer

The results on training the above network showed that the contribution of the oscillators with higher frequencies is not significant (as the corresponding weights are small); also reconstructed strokes have a "tremor-like," high-frequency distortion (see Fig.5.1.3.B). Perceiving that the cause of this problem is a very large range of oscillator frequencies, resulting in over-training, the following modification is made.

The oscillatory network is modified by limiting the number of sublayers to 5 with frequencies of each of the sublayers uniformly distributed to the band $\Delta f = [f, 3f]$. The frequency of an oscillator in the k^{th} sublayer is assigned using the formula $f^k = f + \Delta f * (k-1)/ (N_s - 1)$, where N_s is the number of sublayers in the oscillatory layer. After training with the same algorithm, the reconstructed strokes are shown in the fig.5.2(c). From the

fig.5.3 it is seen that the reconstruction is as good as, if not better, than the previous reconstruction with harmonics sublayers. This may be because there is not much high frequency content in the strokes and the network with oscillator layer with a greater range of frequencies ends up overtraining.

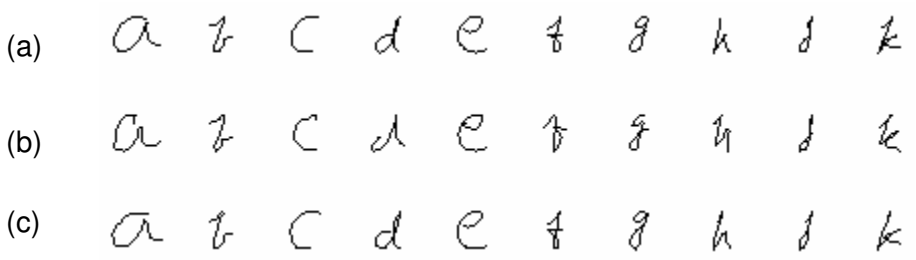

Fig. 5.3.Strokes of the experiment 1 (a) Original Strokes, (b) Reproduced with harmonics, (c) Reproduced without harmonics

5.1.2 Experiment 2: Capacity Of The Network

In this experiment the number of sublayers are varied from 6 to 1 and the number of oscillators per sublayer are kept constant (=25). The frequencies of the oscillators are limited to band Δf (as discussed in Experiment 1). The network is trained using back-propagation with momentum and batch mode update (discussed in chapter 2). As the number of sublayers increased the mean reconstruction error decreased (see fig. 5.4). The reconstructed strokes corresponding to fig.5.4 are shown in fig.5.5.

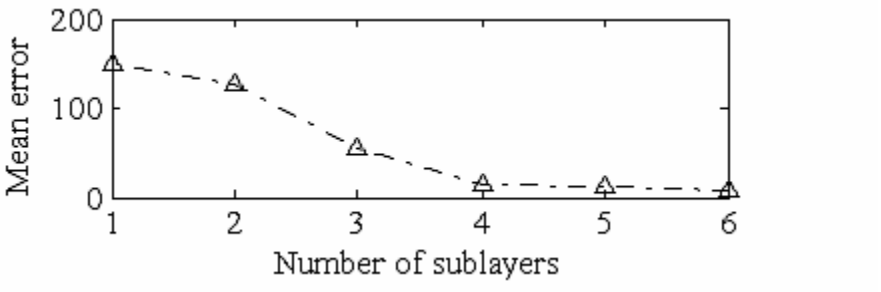

Fig.5.4 Reconstruction error vs. No. of sublayers

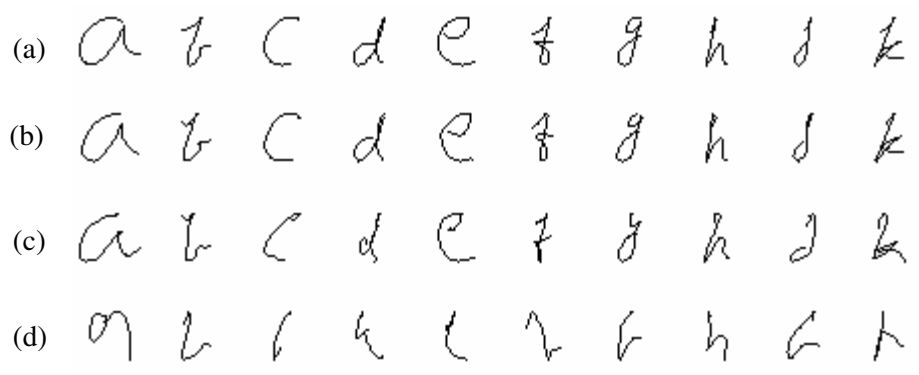

Fig.5.5. Strokes corresponding to experiment on capacity of the network (a) Original strokes, (b) 5 sublayers, (c) 3 sublayers and (d) 1 sublayer

5.1.3 Experiment 3: No. of Sublayers (N_s) Vs No. of Units Per Sublayer(N_k)

In this experiment the number of sublayers is varied from 1 to 5 in steps of 2, and the number of oscillators is varied from 5 to 25 in steps of 10. The reconstruction error is shown the Table 1. From the results shown in Table 5.1 it appears that the number of oscillators per sublayer is more crucial than number of sublayers.

Table 5.1: Mean of the reconstruction error of strokes. N_s is the number of sublayers, N_k is the number of oscillators per sublayer.

N_s \ N_k	5	15	25
1	212.6273	180.4773	110.7623
3	192.2454	94.5849	43.0385
5	168.1085	34.7874	9.6336

5.1.4 Experiment 4: Studies On Post-preparatory Delay (PPD, Δ):

After the preparatory pulse (PP) is given to the oscillatory layer, the layer is allowed to run freely for a delay period (Δ) before the onset of handwriting movement. (See fig.2.4 and fig.2.5). How does the performance of the network depend on PPD? Does the performance error decrease gradually with increasing PPD since the network gets more

time to settle in the attracting state? Simulations conducted to answer these questions show that stroke generation depends on delay in quite non-intuitive ways. The following studies illustrate the implications of delay.

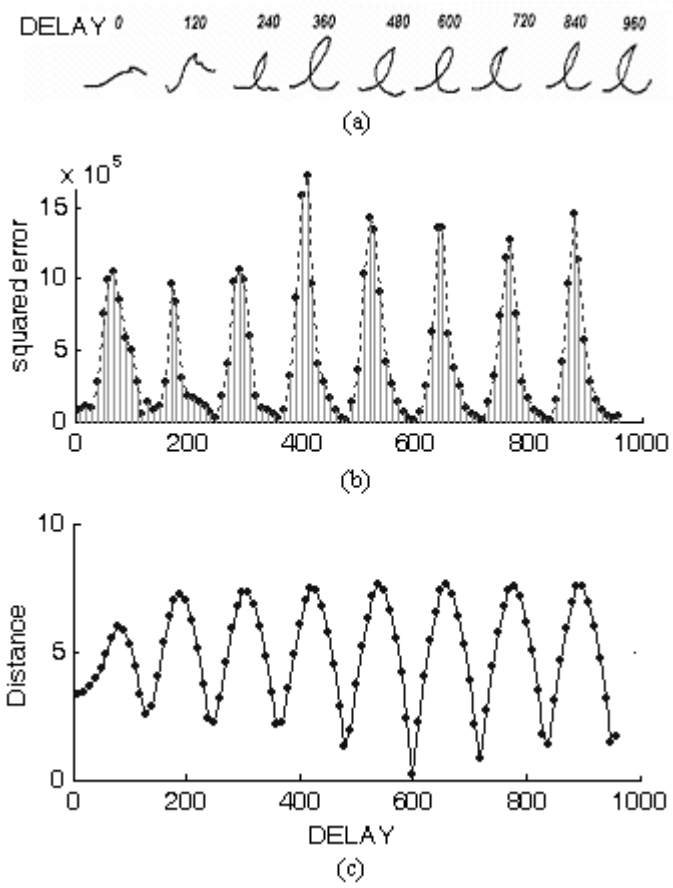

Fig.5.6. Reconstruction error and the corresponding reconstructed strokes for various PPDs. (a) Strokes reconstructed with PPDs mentioned at the top of the strokes, (b) Reconstruction error as a function of PPD. (c) The deviation from the standard state with delay. Note that the error is not a monotonic function of PPD. Error reaches small values at periodic values of delay (PPD).

The error in reproduction does not decrease monotonically with increasing PPD, but acquires minimum value at characteristic values of PPD. These valleys appear at the values of PPD for which the oscillatory layer state is closest to the "standard state" (fig. 5.6c). Also as the evolution of the state of oscillatory layer is nearly periodic, the error valleys appear almost periodically. The network is actually trained using a PPD of 600 time units (one time unit ~ 14.28 ms). The quality of reproduction of the strokes is acceptable at PPD with time units of 240, 360, 480 etc., even though 600 is the delay

during the training. Therefore, for faster reproduction the network may not really need to wait for long periods. This experiment inspires some clear predictions on human handwriting: the onset of handwriting probably always occurs at characteristic intervals after command for stroke generation is given. Handwriting movements forcibly constrained to commence at other instances might manifest larger errors.

5.1.5 Experiment 5: Origins of Motor Variability

One of the most commonly seen features in human movement is motor variability. Motor control researchers view it as a window into the central organization of the system that produces voluntary movements (Latash, 2001). One of the obvious origins of motor variability is motor redundancy. In this experiment this we argue that 'motor preparation' may also contribute to motor variability.

a) Variability due to variation delay for motor preparation

   i. Delay can be any multiples of fundamental period T (=120 time units): The onset of handwriting movement can happen at PPDs with valleys. This can contribute to variability as shown in fig.5.6.

   ii. The delay is not exactly a multiple of T (= 120 time units): We have seen that locally optimal reconstruction is obtained when PPD is a multiple of T. Variation of PPD around this local optimum introduces significant variability in stroke quality (see fig.5. 7).

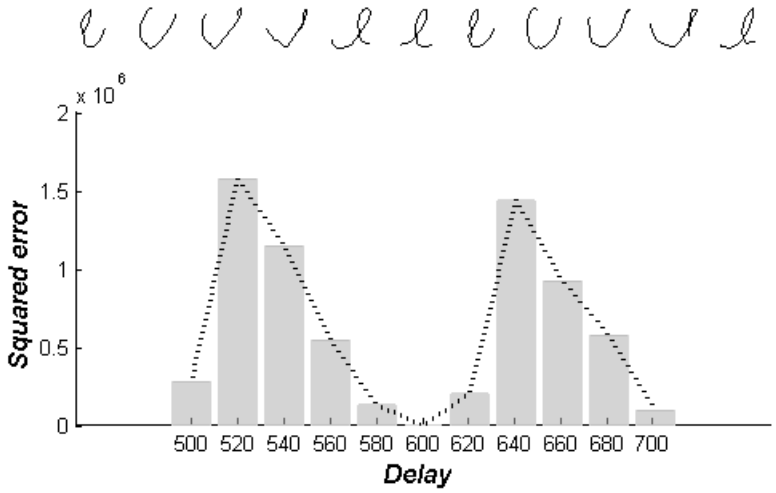

Fig.5.7 Demonstration of variability due to suboptimal gating pulse

b) Variability due to random initial state also introduces variability in the stroke produced. Though the randomness of the initial state is attenuated to some extent due to preparation, there is some residual variability (see fig.5.8).

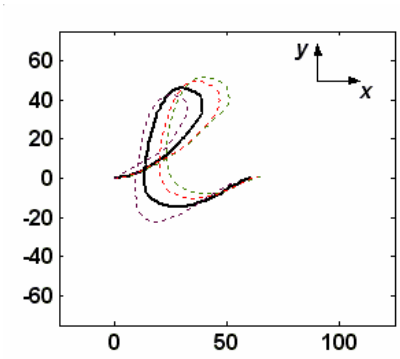

Fig. 5.8 Demonstration of variability due to random initial conditions

c) Variability due to variation in input signals: In the experiments shown hitherto, the Input Gating Pulse (IGP) is ON for the full cycle (T) of the fundamental period. Variability is seen in stroke output if IGP is less than T (fig.5.9). The IGP enables input to the oscillator layer.

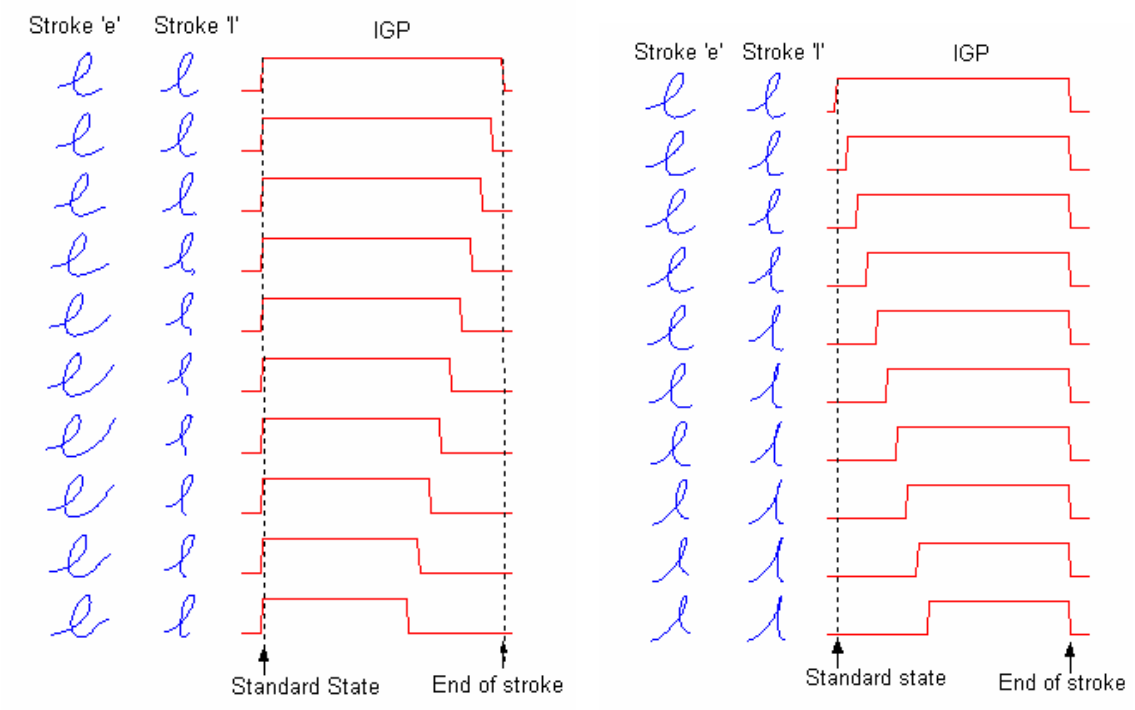

Fig. 5.9 Demonstration of motor variability with unreliable input gating signals (a) variability due to early drop in magnitude of IGP signal (b) variability due to late arrival of IGP signal. Though the duration of IGP is reduced, the OGP is ON for the full duration between "Standard State" and the "End of Stroke".

5.1.6 Experiment 6: Generating A Stroke Sequence

Natural handwriting involves a smooth, flowing execution of multiple strokes in a desired sequence. So far we have only discussed execution of single strokes. Can the model be extended to execute a stroke sequence? How are the timing events coordinated when multiple strokes are executed in a sequence? Does the network have to be prepared afresh after every stroke? Two options immediately suggest themselves: 1) to prepare the network after every stroke or 2) to generate multiple strokes with a single initial preparation before the first stroke execution. The main issues in the generation of stroke sequence are – 1) the time of execution should be small (large inter stroke delays should be decreased or avoided) and 2) the generated stroke sequence should be accurate. The following methods are evolved addressing the above issues.

a) Stroke Sequence Production with Multiple Preparations: According to the procedure described for stroke generation described in chapter 2, for every input stroke command the network has to be prepared before the execution of a stroke. The inter–stroke delay for stroke production with this strategy includes duration of preparatory pulse and post-preparatory delay (= τ_p +Δ), which is large compared to the duration of stroke production itself. Fig. 10(a) shows the stroke sequence 'elle' generated with this method. The reason for good production of the strokes is that the distance of oscillatory state from "standard state" just before stroke onset is minimized by preparation (see caption of fig. 10 b and c). Though the stroke sequence generation is legible enough, the time consumed in the execution the stroke sequence is very large.

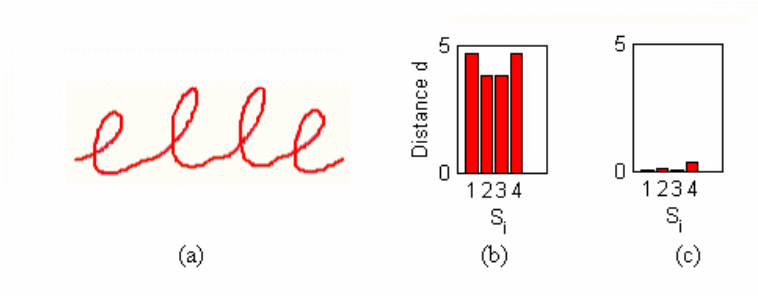

Fig.5.10. (a) The stroke sequence 'elle' generated with multiple preparations. The oscillatory layer is prepared afresh for every stroke. (b) Deviation of network state from the standard state at end of writing each stroke in sequence 'elle' (c) Deviation of Network State from the standard state after preparation. In (b) along the x – axis the stroke indices S_i are shown(S_i = 1,2,3 and 4 corresponding to 'e', 'l' , 'l' and 'e' respectively) and along y - axis the distance is shown. The deviations before preparation are 4.75, 3.75, 3.75 and 4.75.After preparation all the distances are less than 0.2.

Let $V(t_0)$ is the state of the oscillatory layer at the end of PPD – this is the "standard state," to which we expect the oscillatory layer to return before the onset of every stroke. Similarly let $V(t_1)$, $V(t_2)$, $V(t_3)$ and $V(t_4)$ be the states after strokes 1, 2, 3 and 4 respectively (at events[8] b_1, b_2, b_3, and b_4 in fig. 5.10a). The distances of these states from

[8] Notation for the events in the figures (5.11, 5.12, and 5.13):

standard state, $V(t_0)$ is shown in fig.5.10b. Note that this distance is shortened drastically by the preparation. Due to the lesser deviation of state from the standard state, the quality of the stroke sequence generation is superior. However, to allow a full preparatory delay after every stroke makes execution too long. How can the delay in inter-stroke preparation be minimized?

b) Stroke Sequence Production with Single Preparation and Full duration IGP:

In order to reduce the inordinately long time required to prepare the network after every stroke, we now allow the network to execute the entire stroke sequence as shown in fig.11c. The first two strokes 'e' and 'l' generated are legible but the subsequent strokes are illegible (see fig.11a). The reason why stroke reconstruction is poor with single preparation is that the state of oscillatory layer is disturbed after presentation of every stroke command and does not return to the standard state before the next stroke begins (see caption of fig. 11b). Poor reconstruction is only natural. One way to improve the quality of the stroke sequence generation may be to allow the network to evolve freely, without input, for sometime between strokes. Since the oscillatory layer evolves to its limit cycle attractor in free-running (no input) condition, it might approach the "standard state" sufficiently closely.

- P_1, P_2, P_3 and P_4 are start of preparatory pulses corresponding to strokes 'e', 'l', 'l' and 'e' respectively.
- a_1, a_2, a_3 and a_4 are start of input gate pulse (IGP) and start of output gate pulse (OGP) of the strokes 'e', 'l', 'l' and 'e' respectively.
- b_1, b_2, b_3 and b_4 are end of output gate pulse (OGP) of the strokes 'e', 'l', 'l' and 'e' respectively.
- c_1, c_2, c_3 and c_4 are end of input gate pulse (IGP) of the strokes 'e', 'l', 'l' and 'e' respectively.

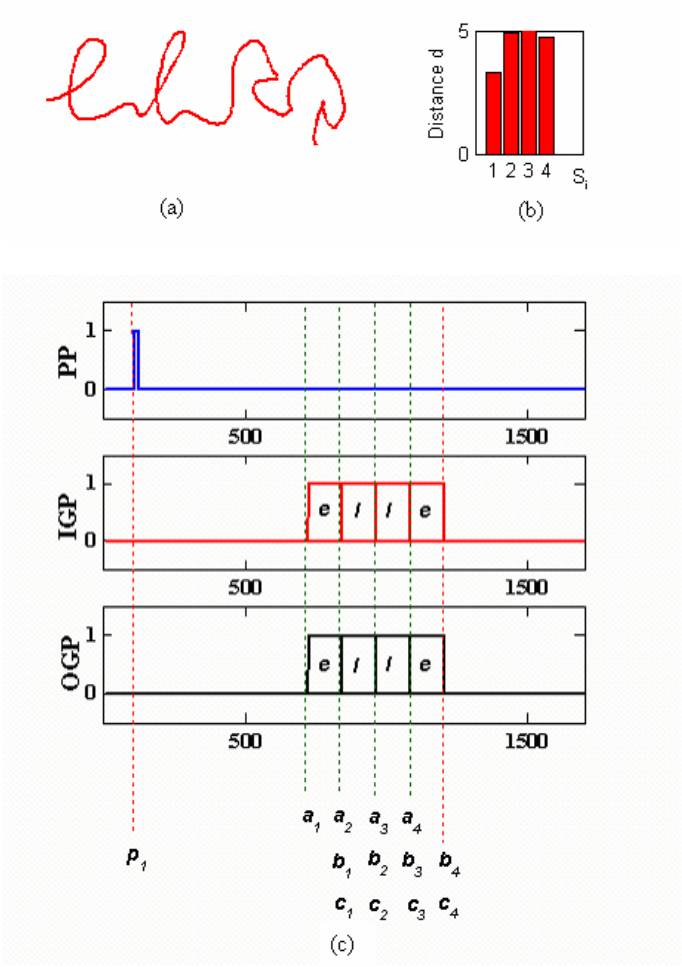

Fig.5.11. Generation of stroke sequence 'elle' with single preparation and fixed full duration input gate pulse (IGP). (a) The generated stroke sequence, (b) the distance of deviation from the networks state at the end of each stroke to the standard state. (c) Illustration of events in the production of stroke sequence 'elle' with preparatory and gating signals. The oscillator network is prepared only at the arrival of first input stroke command. There is no preparation between strokes. The strokes are executed in continuous fashion one after other without any delay. The first two strokes seem to be legible, but the later ones are not. The execution time is reduced at the cost of legibility of the stroke. The oscillatory layer state does not return to the "standard state". The distances of the states of oscillatory layer from the "standard state" just before the stroke onset are 3.3, 4.9, 5.15, and 4.75 respectively.

c) Stroke Sequence Production with Single Preparation with Partial IGP:

In the previous method, the Input Gating Pulse (IGP) to a stroke comes ON just when the IGP for the previous pulse turns OFF. That is, there is never a time when the oscillatory layer receives no input; it is never in a free-running condition. Therefore, in this method, for each input stroke, the IGP is reset to OFF state a little before (=30 time units) the

execution of the stroke finishes. That is, there is a free-running period of 30 time units between consecutive strokes. The stroke sequence generated with this method is shown in fig. 12a. Though reconstruction of strokes 3 and 4 in 'elle' is better than that of the previous method, the distortion is still unacceptable. The distances of oscillatory layer states from "standard state" is lesser than those of the previous case (see captions fig.11 and fig.12) but still unacceptably high. Is it possible to decrease them further? Reliable stroke reconstruction seems to depend crucially on the choice of the instant of stroke onset.

To fix this problem one must only look for a way of determining the exact instant when the network comes *closest* to the standard state, even if not identical. On a careful analysis of the evolution of the state of the oscillatory layer, V(t), it became clear that the frequency of the state in the "free-running" intervals between strokes is not constant. For example, in the simulation of fig.12, the period of oscillation of the first sublayer during the preparatory period is 120 time units; corresponding values in the "free-running" intervals between strokes 1 and 2, strokes 2 and 3, strokes 3 and 4 and after stroke 4 are 103 time units, 87 time units, 95 time units and 106 time units respectively[9]. The actual frequency depends in a complex way on the exact command input presented. Since there is a shift in frequency, and only a small one at that, there is no compelling reason for the state of the oscillatory layer to return precisely to the standard state, $V(t_0)$. What then is the appropriate moment to start a new stroke once a stroke is executed?

[9]These approximate values are calculated for the first period in the free running mode. However a deviation of period is observed in the later periods.

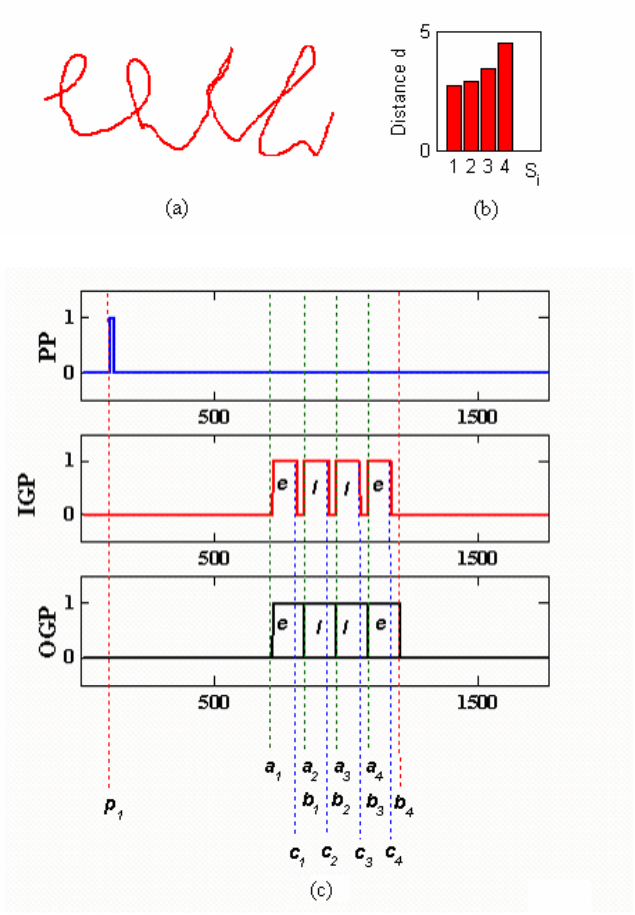

Fig. 5.12.Generation of stroke sequence 'elle' with single preparation and partial duration input gate pulse (IGP). (a) the generated stroke sequence, (b) the distance of deviation from the networks state at the end of each stroke to the standard state. (c) The events during the generation of the stroke sequence 'elle'. The oscillator network is prepared only before the first stroke. There is no preparation between strokes. But the IGP for a given stroke is not ON throughout the stroke execution period, T. For example, IGP of stroke 1 is turned OFF at 'c1' and IGP of stroke 2 is turned ON only at 'a2'. Though the strokes generated with this method are more legible that that of previous method, the legibility of the stroke generated is not appreciable. The distances of the oscillatory layer state from the "standard state" in this case are 2.7, 2.9, 3.4, and 4.5 respectively.

d) Stroke Sequence Production with Phase-triggered IGP:

The solution to the above predicament lies in the observation that accurate generation of a learnt stroke depends not necessarily on preparing the network to reach the standard *amplitude* state, $V(t_0)$), but only to a standard *phase* state, $\phi(t_0)$. Though the frequency is slightly altered in the "free-running" period between strokes, it is obvious that the phase relationships among oscillators of the oscillatory layer are still preserved and the layer

approaches a limit cycle attractor. With intact phase relationships, and altered frequency, the speed of stroke execution may vary, leaving the stroke shape unaffected. Thus our earlier restriction that the oscillator layer must return to the standard *amplitude* state, $V(t_0)$, at the beginning of each stroke is unnecessary; it suffices if the layer returns to the standard *phase* state, $\phi(t_0)$, which represents the phase relationships at the end of post-preparatory delay.

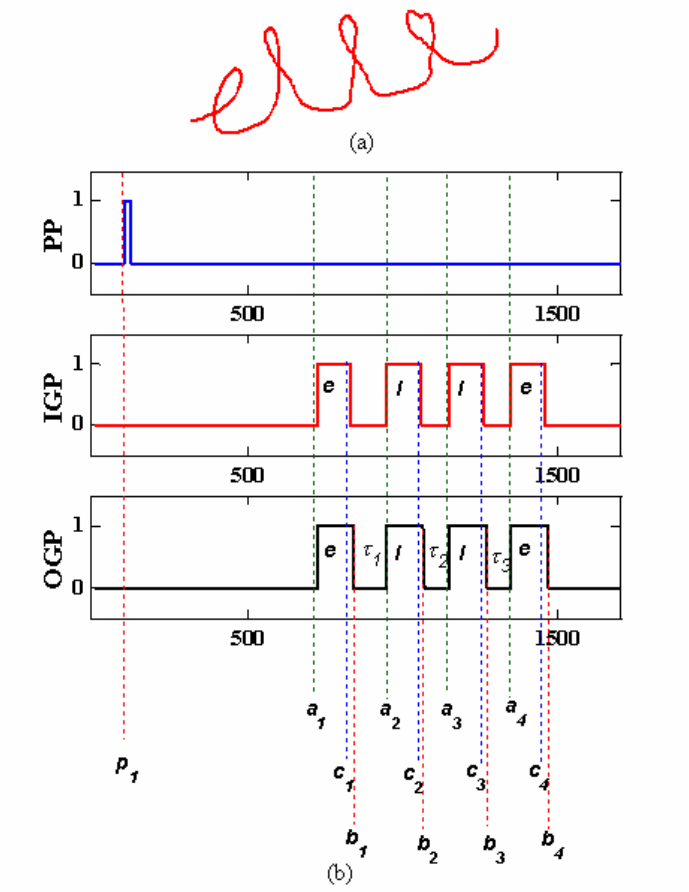

Fig. 5.13. Generation of stroke sequence 'elle' with fixed partial duration input gate pulse (IGP), and with phase-triggered gating mechanism. (a) The generated stroke sequence, (b) Illustration of the events during the generation for the stroke sequence 'elle'. The oscillator network is prepared only before the first stroke. There is inter–stroke delay during which the timing network monitors the dynamics of oscillatory layer network. Once the standard phase is reached the timing network enables input and output lines turning ON IGP and OGP. OGP is allowed to be ON during the entire duration of the stroke, T_f, but the IGP is turned OFF before that, allowing the oscillator layer a brief "free-running" period. Stroke obtained by this method are of better quality than those obtained by the two methods discussed earlier.

With this perception, we change the strategy for determination of the instant of stroke onset. In this "phase-triggered" strategy, stroke execution always begins when the oscillatory layer is at a standard phase, or when a pre-chosen neuron (say, the first neuron in the first sublayer) is at a standard phase, and the oscillatory layer has settled in a stable limit cycle. The timing pattern as per this new strategy is shown in fig. 13. The network is prepared only once - before the first stroke. The PPD is chosen not as an arbitrary constant, but as a sufficiently long duration at the end of which the oscillatory layer arrives at the standard phase. Similarly the "free-running" periods between strokes are also chosen such that the oscillatory layer arrives at the standard phase at the end of such periods. Strokes reconstructed by the new strategy are shown in fig. 13a. Notwithstanding a slight vertical drift in velocity, the shape of individual strokes is quite robust, compared to the reconstructions of figs. 11 and 12.

5.2 RESULTS OF CHAPTER 3: BASAL GANGLIA AS A SOURCE OF EXPLORATORY DRIVE

The model of basal ganglia for reaching task is trained using reinforcement learning. The model is trained to reach 'eight' points on a circle (45 degrees apart) from its centre. The training error is shown in the fig.5.14. The model reaches all the points when trained with a proper reward signal (see fig. 5.15(a)). When the training is conducted without a reward signal, the network fails to learn task; when prompted to reach a specific location the network wanders around a target making a futile attempt to reach (see fig. 5.15(b)).

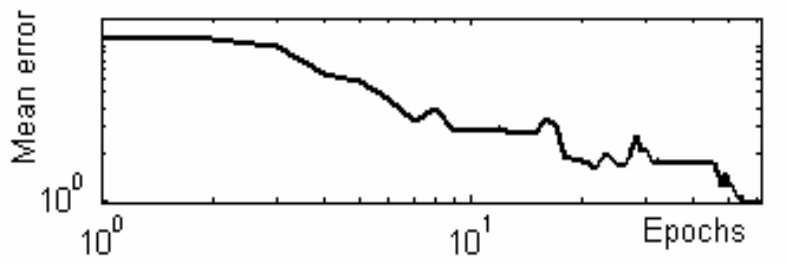

Fig.5.14. Training Error

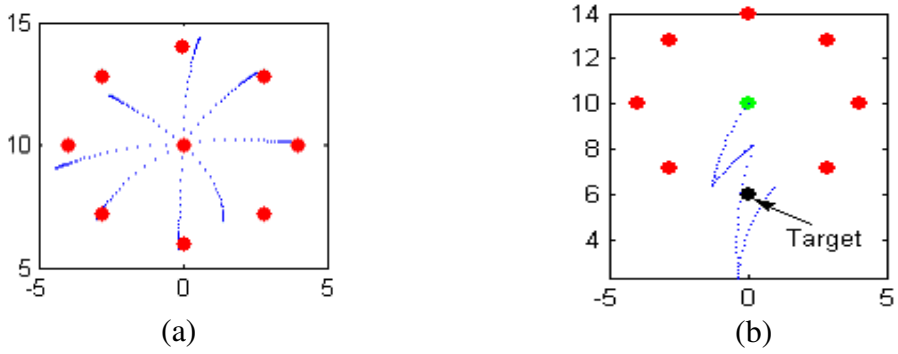

Fig. 5.15 The trajectories of the hand model corresponding to eight points around a circle.(a) Learning with strong reward, the model reaches the targets (b) Learning with weak reward, the model wanders around a target making a futile attempt to reach

5.3 RESULTS OF CHAPTER 4: A MODEL OF PARKSINSONIAN HANDWRITING

A model of Parkinsonian handwriting is developed by combining the neuromotor model of handwriting with the model of basal ganglia (see Sec.4.5, Chapter 4). Features of Parkinsonian handwriting like micrographia etc are reproduced by varying Dopamine level in the model and a parameter ε that controls the complexity of STN-GPe loop of basal ganglia.

5.3.1 Normal Handwriting

Dopamine level, DA = 50, and ε = 0 correspond to "normal" condition. The simulated handwriting samples corresponding to this normal case are shown in fig.5.16.

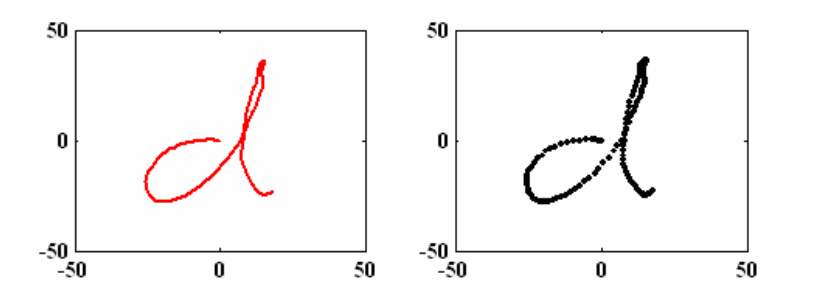

(a) (b)

Fig. 5.16 (a) The simulated handwriting with DA=50 and ε = 0.0 corresponding to normal control. (b) The dotted trajectory corresponding to (a) illustrates the speed of writing (sparse dots show fast movement whereas dense dots show the slow movement)

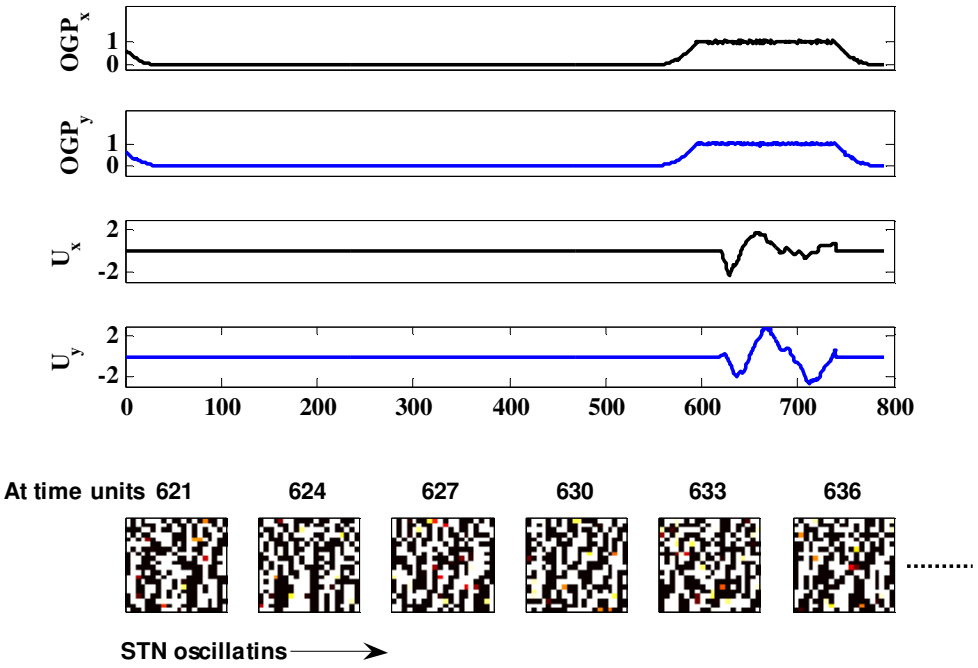

Fig: 5.17 Signals corresponding to normal handwriting. *DA* = 50 and ε = 0.0, the sub plots show OGP_x, OGP_y, U_x, U_y and snap shots of the dynamics of STN grid (each small square correspond to activity of a STN cell on the grid of 20 x 20 of which back correspond to '0' whereas white correspond to '1') respectively from top to bottom.

The signals, output gate pulse in x-direction (OGP_x), output gate pulse in y-direction (OGP_y), velocity of pen tip along x-direction (U_x) and velocity along y – direction (U_y)

and STN dynamics corresponding to execution of normal handwriting are shown in fig. 5.17. The simulated normal handwriting spans a region of [-50 to 50] in both x – direction and y – direction. It also has smooth profiles of velocities along x direction and y – direction (see fig. 5.17). The temporal profile of STN output (STN is a 20 by 20 grid of neurons; black square is shown for 'off' neuron and white square 'on' neuron) are shown for times units during execution of handwriting. The uncorrelated activity over time is responsible for smooth profile of handwriting.

5.3.2 Parkinsonian Handwriting:

a) Simulating micrographia:

A dopamine level less than 50 signifies Dopamine deficient condition that might arise due to loss of dopaminergic neurons in SNc. A sample corresponding to DA = 25 is shown in fig.5.18. Due to the reduction in the dopamine levels the overall activity of the STN-GPe loop decreases which in turn reduces the amplitude of the modulator signal OGP (Output Gate Pulse) of GPi (see fig. 5.19). Due to reduction in OGP, overall size of the stroke generated decreases, along with velocity of the pen-tip, but writing time of this sample is same as that of normal handwriting. The diminished letter size signifies micrographia whereas the slow movement of pen tip signifies bradykinesia, standard features of Parkinsonian handwriting.

b) Jagged handwriting:

The dopamine level is kept as that of normal case (=50) but the parameter ε is increased to a value 0.6. The corresponding OGP and the stroke generated are shown in fig. 5.20. The increased value of ε gives rise to synchronized oscillations in STN – GPe loop (see fig.5.21). These synchronized oscillations induce fluctuations in the output of GPi, which

is simply the Output gate pulse or OGP. Since OGP modulates both GP_x and GP_y the resulting handwriting has a jagged contour and is marked by unusual fluctuations in the velocity profile.

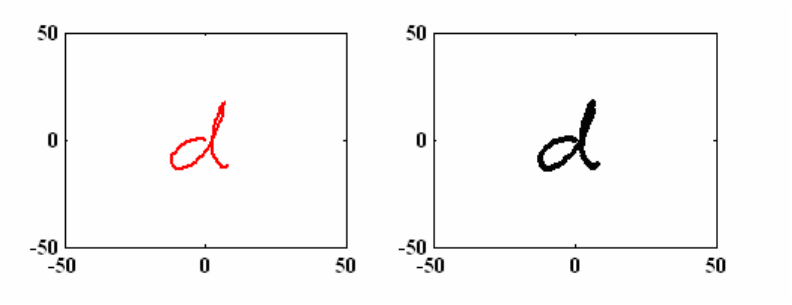

(a) (b)

Fig. 5.18 (a) The simulated handwriting with DA=25 and ε = 0.0.corresponding to PD. (b) The dotted trajectory corresponding to (a) illustrates the speed of writing (sparse dots show fast movement whereas dense dots show the slow movement).

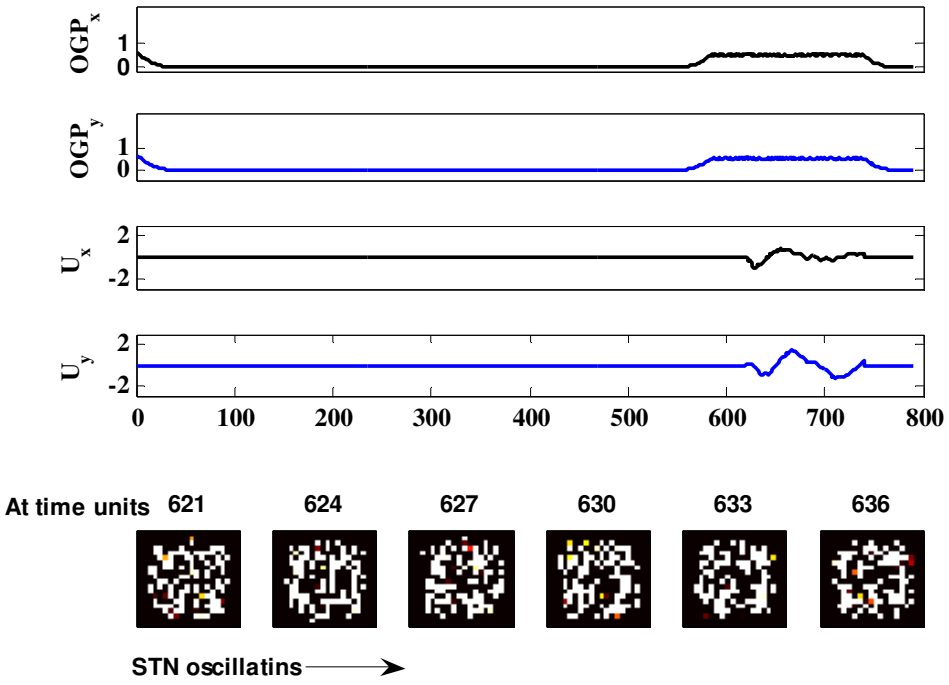

Fig: 5.19. Signals corresponding to PD handwriting with *DA* = 25 and ε = 0.0 corresponding to micrographia and bradykinesia. The sub plots show OGP_x , OGP_y , U_x , U_y and snap shots of the dynamics of STN grid(each small square correspond to activity of a STN cell on the grid of 20 x 20 of which back correspond to '0' where as white correspond to '1') respectively from top to bottom.

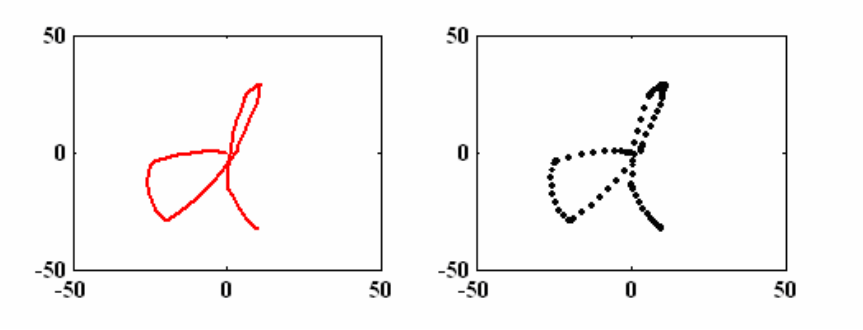

(a) (b)

Fig. 5.20 (a) The simulated handwriting with DA=50 and ε = 0.6. (b) The dotted trajectory corresponding to (a) illustrates the speed of writing (sparse dots show fast movement whereas dense dots show the slow movement).

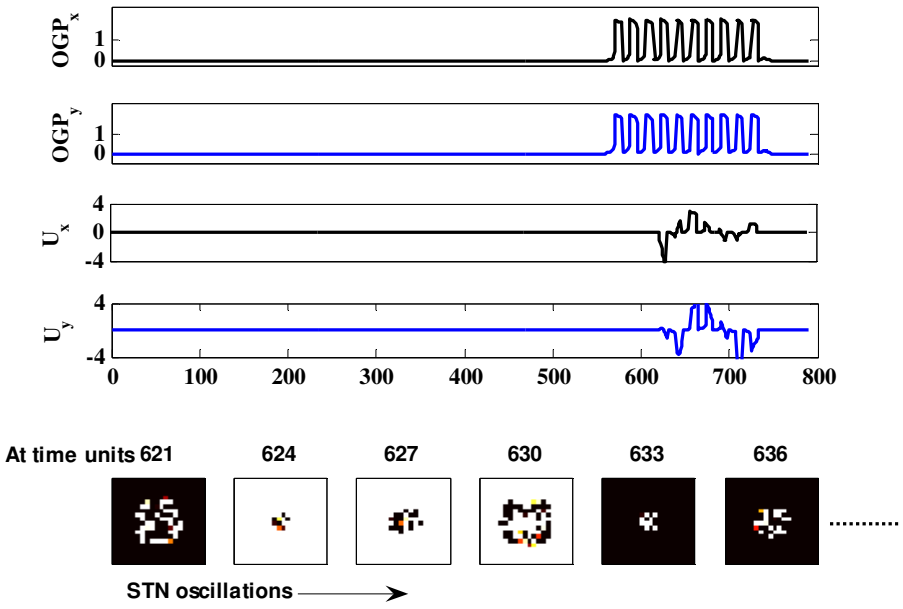

Fig: 5.21 Signals corresponding to PD handwriting with *DA* = 50 and $\varepsilon = 0.6$ corresponding to jagged/ wavy handwriting. The sub plots show OGP_x , OGP_y , U_x , U_y and snap shots of the dynamics of STN grid respectively from top to bottom.

c) PD handwriting: Both micrographia and jagged handwriting:

In PD, the loss of dopaminergic neurons leads to the correlated activity in the STN – GPe causes of which are elusive. In this section handwriting is simulated both with reduced dopamine levels and increased correlated activity. The stroke corresponding to DA = 25 and ε = 0.6 is shown in the fig.5.22. The simulated handwriting in this case is both

reduced in overall size and also has unusual stops or fluctuations in the velocity profile. The control signals corresponding to this case are shown in fig.5.23.

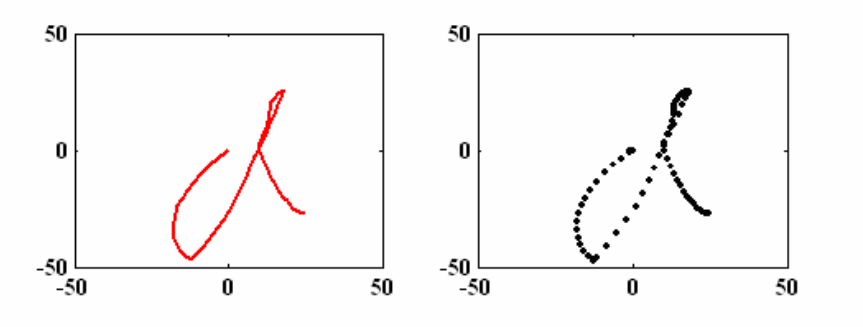

(a) (b)

Fig. 5.22 (a) The simulated handwriting with DA=25 and ε = 0.6.corresponding to PD. (b) The dotted trajectory corresponding to (a) illustrates the speed of writing (sparse dots show fast movement whereas dense dots show the slow movement).

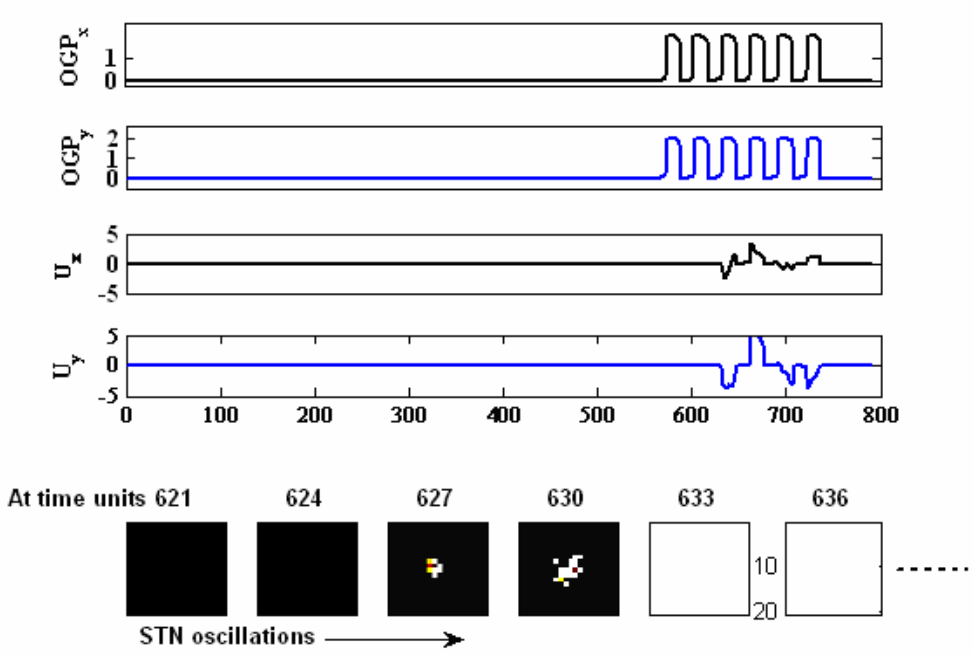

Fig: 5.23 PD handwriting with *DA* = 25 and $\varepsilon = 0.6$ corresponding both micrographia and jagged handwriting. The sub plots show OGP_x , OGP_y , U_x , U_y and snap shots of the dynamics of STN grid(each small square correspond to activity of a STN cell on the grid of 20 x 20 of which back correspond to '0' where as white correspond to '1') respectively from top to bottom.

5.3.3 Batch Results of Parkinsonian handwriting

To map the handwriting features onto the level of PD (level of Dopamine and level of damage in STN activity), the model is simulated over a dopamine level of 10 to 80 in

steps of 10 and ε from 0.0 to 0.8. The corresponding strokes are shown in fig.5.24. As the Dopamine (DA) decreased from right to left, the overall size decreases and as the ε increased from top to bottom the stroke contour becomes more and more jagged. The reduced size and jagged handwriting corresponds to micrographia in PD. The case of increased overall size of handwriting is called macrographia which can also be observed for the samples with Dopamine > 50. Such macrographia is observed in patients with Schizophrenia (Kuenstler, 1999).

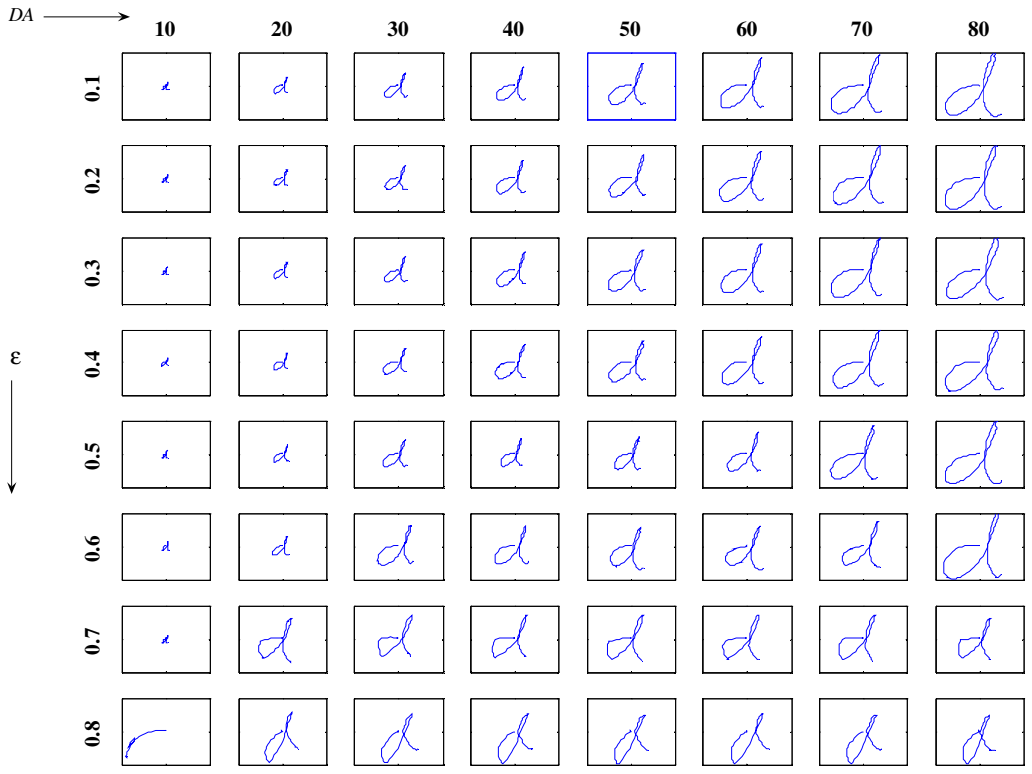

Fig.5.24 The simulated handwriting corresponding to various levels of dopamine(DA) and ε. DA decreases as along x – axis from right to left. The parameter ε increases along y axis from top to bottom. Aspects of normal handwriting and Parkinsonion handwriting (like micrographia, jagged contour etc) are captured by the model outputs.

5.4 SUMMARY

In the present chapter the results of handwriting model which aims at obtaining an optimal way of stroke generation is presented. The issues in motor preparation and multiple stroke generation are raised and solutions are attempted. The results of modeling basal ganglia as a source of exploratory drive are presented. The results of the computational model of PD handwriting, which show micrographia are discussed. The following chapter presents the conclusions of this thesis.

.

CHAPTER 6

CONCLUSIONS

Chapter 2: A Neuromotor Model of Handwriting Generation

A neural network model of handwritten stroke generation in which stroke velocities are expressed as a Fourier-style decomposition of oscillatory neural activities is presented. Though oscillatory neural models are typically used to model generation of rhythmic behavior like walking, swimming etc. (Marder, 1996), they proved to be useful in non-rhythmic motor function also (Prashanth and Chakravarthy, 2003). Since Hollerbach's insightful observation on oscillatory elements in handwriting, neural oscillators have figured in models of handwriting also. An oscillatory neural model of handwriting, to be biologically viable, has to address certain fundamental issues.

The first key issue is one of preparing the initial state of the oscillatory network. This question does not seem have received adequate attention in literature (Plamondon, 1989; Kalveram, 1996; Shcomaker, 1991; Grossberg, 2000). Primarily the network's internal state must posses a stable rhythm properly registered with respect to the time of onset of the stroke. Further there must be a mechanism to switch the network to a different, stable rhythm to produce a different stroke. Even if the network dynamics are stable enough to flow into a stable trajectory on random initialization, the temporal profile of the network may not be specific enough to produce a desired behavior. There must be some level of forgetting of initial conditions, and therefore linear oscillator models are disallowed. Networks of nonlinear oscillators, with their proneness to chaos (Chirikov, 1979), must be handled with extreme delicacy to produce stable, specific rhythms.

In the present work, we believe that a reasonable solution that addresses the above issues is provided. The oscillatory network is initialized with small random noise, but is immediately given a large PP to specific neurons. This pushes the evolution of all the sublayers in a specific direction, which, after a specific delay, Δ, fall into a nearly standard rhythm (forgetting the low-amplitude diversity in the initial conditions). A PP of inadequate amplitude or an adequate delay (Δ) after the PP will not result in the desired output. Biological significance of this "motor delay" will be discussed later in this chapter.

A coarse mapping of our network architecture onto neuroanatomy can be suggested. The timing network could possibly represent either cerebellum or basal ganglia, whose role in timing and predictive functions is well established (see fig.6.1). However, we will argue that the actions of the timing network closely match the activities of basal ganglia. The input layer could represent either the pre Supplementary Motor Area (preSMA) or Premotor (PM) area where complex motor sequences are initiated. The hidden layer could represent SMA; this region involved in preparation and initiation of movements. The output layer may be considered as a "lumped" representation including Primary Motor area (M1) and all the motor structures below it in motor hierarchy. The enabling control of the timing network on the output is analogous to the "action gating" of basal ganglia on M1 (Houk, 1995). It is well-known that striatum provides intermittent, focused inhibition within output structures which otherwise maintain inhibitory control over motor/cognitive systems throughout the brain (Harner, 1997).

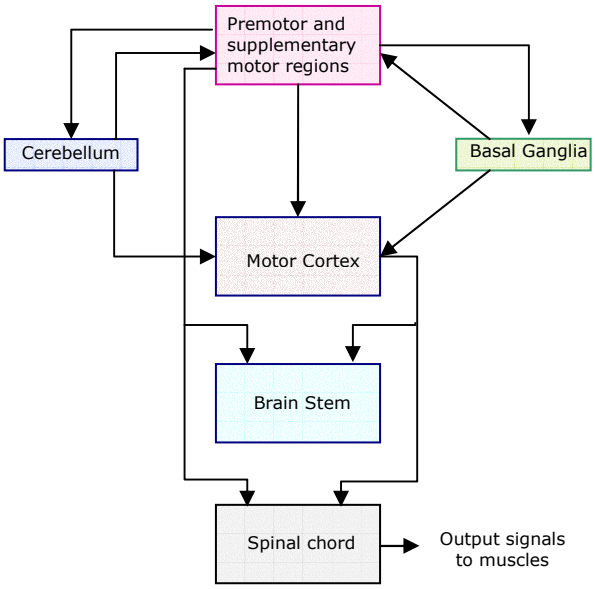

Fig. 6.1 Overview of motor system

Motor Preparation

In their classic EEG studies of voluntary motor action, Kornhuber and Deecke found slow negative shifts in cortical potential much before the initiation of movement. This potential, termed the Bereitschafts Potential (BP), is believed to signify pre-movement preparation of motor cortical areas. Careful current dipole source analysis of BP has identified SMA as a key player (Lang et al, 1991). However, preparatory activity corresponding to movement direction has been found in many other brain areas including M1 (Georgopoulos et al, 1989), premotor cortex (Kubota and Hamada, 1978), prefrontal cortex (Kubota and Funahashi, 1982), the parietal cortex (Crammond and Kalaska, 1989), and basal ganglia (Alexander, 1987). In a delayed reaching paradigm, 'delay – period' or 'preparatory activity' is observed in M1 and dorsal premotor cortex (PMd). Churchland et al argue that, for ballistic movements, successful movement generation is dependent on successful movement preparation. Movement preparation involves in settling of activity to an attractor state that is optimally suited to produce the desired movement (Churchland

et al, 2005). It would seem critical that the brain optimizes preparatory activity, so as to get the desired reward when the movement is triggered. Churchland et al show evidences for such optimization during the motor preparation (Churchland et al 2005) with the recordings from PMd of monkeys. They also suggest that the brain is capable of monitoring the state of the motor preparation, and delaying movement if further optimization is necessary. In the present model of handwriting generations, the phase triggered mechanism for the movement execution echoes well with the ideas presented in (Churchland et al, 2005).

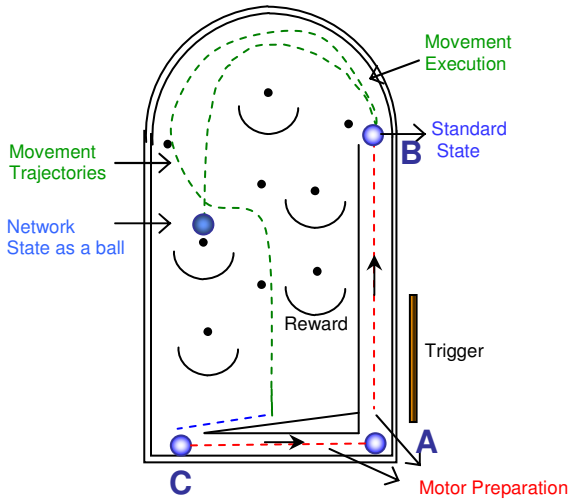

Fig. 6.2 Pin – Ball game model of motor system and movement generation

The Pin - Ball game model of Motor system:

The analogy of ideas of present model of motor system is a Pin – Ball game. The ball in the game, which represents the state of SMA, needs to be kept in position 'A'. The ball moves to position 'B' on triggering, and will be guided by the sidewalls up to the location 'B', which represents the standard state of SMA activity. This process represents Motor preparation while the time taken for the ball to reach 'B' from 'A' represents 'motor delay'. From the location 'B' the ball takes different trajectories based on the momentum

in it, representing the execution of movement (or handwritten stroke). All the trajectories may not be rewarding which represents poor skill of execution of the movement. At the end of the trial the ball reaches position 'C' which will be brought to 'A' for next trail. In the dynamical systems point of view, the position 'B' is should be a 'saddle node'. The positions from 'C' to 'A' are 'line of fixed points' in the presence of gravity (the present model does not incorporate these states, but motor system seems to have such states). The trajectory corresponding to 'C - A - B' represents the preparatory activity. This activity seems to be as optimal as possible for good movement generation (if this trajectory was curved rather than being straight, the overall momentum will be less in the Pin- Ball game). The ball at position 'B' represents the standard state, because of the fact that up to this location every ball takes the same trajectory and after which it will slide into various trajectories.

SMA and Motor Preparation

From the above account SMA seems to compete with several other motor areas as a primary source of motor preparatory signals. Single cell recordings in primates revealed more marked preparation-related changes in SMA neurons than in neurons of M1 (Tanji, 1994). The question can be resolved if it can be shown that preparatory activity in SMA neurons precedes similar activity in M1. It has been shown that SMA neurons exhibiting preparatory activity can be identified to project to M1 (Tanji et al, 1980). Contrarily, it was also established that M1 neurons that exhibit preparatory activity receive inputs from SMA and not from thalamus or parietal cortex (Aizawa and Tanji, 1994). Such studies strongly implicate a role to SMA in motor preparation. However, perhaps SMA may not be solely responsible for motor preparation. Its preparatory action might involve

interactions subcortical structures like basal ganglia, which are often implicated in motor timing functions.

SMA and Basal Ganglia in Sequence Generation

Interaction between SMA and basal ganglia is believed to play a crucial role in learnt motor sequences (Cunnington et al 1995). It has been suggested that phasic activity of basal ganglia may act as a "reset" signal to the SMA clearing the traces after one movement and preparing it for the consecutive movement (Georgiou et al 1993).

The above description of cortico-striatal interaction in event timing and sequence generation is much in line with the treatment of these temporal processing mechanisms in our model of handwriting generation. The oscillatory layer (a cortical area, most probably SMA) is stimulated by the timing network (basal ganglia) so as to induce a stable rhythm in the former. The timing network waits for a specific phase pattern in the oscillatory layer and initiates stroke execution. We have seen that other ways of determining stroke onset moment yielded suboptimal results. The two-way interaction between the timing network and the oscillatory layer is strongly analogous to the above description of the role of basal ganglia in timing and sequence generation.

Basal Ganglia and Motor Timing

Coordinating the relative timing of multiple streams of processing is crucial in both motor performance and sensory perception. Temporal processing in biological systems occurs over a range of time scales and is broadly classified into 3 categories: 1) circadian timing, which corresponds to durations of the order of days, and handled by brain structures like suprachiasmatic nuclei, 2) interval timing, which corresponds to durations in the range of seconds to minutes, and coordinated primarily by corticostriatal

interactions, and 3) millisecond timing, which obviously corresponds to millisecond durations, controlled by the cerebellum (Buhusi and Meck, 2005).

The role of basal ganglia in 'interval timing' appears to emerge from the dynamics of thalamo-cortico-striatal loops. In a model – the Striatal Beat Frequency (SBF) model – that highlights the timing function of basal ganglia, the cortical oscillators are assumed to increase synchrony just before movement onset and maintain the rhythm throughout the performance (Buhusi and Meck, 2005). The dopaminergic burst at trial onset could trigger the synchronization of cortical oscillators according to SBF model. And the striatal neurons are tuned to respond to specific patterns of cortical oscillations (Buhusi and Meck, 2005).

Isochrony in Handwriting

The isochrony principle shows that duration of handwriting movement tends, within certain limits, to be relatively independent of the length of the trajectory. The perception of human movement is influenced by the implicit knowledge of motor rules (Viviani 1983; Thomassen and Teulings 1985). This feature is an intrinsic behavior of the current model of handwriting generation. As the model is trained to generate all strokes in one cycle of hidden layer oscillation, it takes almost equal time for the generation of each stroke.

Motor variability

One of the most commonly seen features in human movement is motor variability. Motor control researchers view it as a window into the central organization of the system that produces voluntary movements (Latash, 2001). One of the obvious origins of motor

variability is motor redundancy. Variability in movement generation is a problem where accuracy is needed and is an asset for adjusting the movement during learning. The motor variability needs to be controlled depending on the context. For example in learning archery one needs variability in force production and directional tuning for the release of arrow onto the target. But after learning, for skilled archery, the learner needs to suppress the variability.

The motor system, which is a large complex dynamical system, has all the ingredients to generate innate variability. In the present work it is also argued that apart from the noise in the initial conditions in the network and properties of dynamics systems, the 'motor preparation' may contribute to motor variability. The preparation of the network may not precisely land the network state exactly onto the standard state, but it confines the network state to a narrow region around the standard state (the standard state is the state of the network in its state space, from which the onset of a movement lead to an accurate movement). These states in this subset act as the initial noise in the network, which may lead to variability in the movement generation.

We are aware that our model has several simplifying assumptions. The input layer in our model which represents inputs from source areas of handwriting information (probably language areas in parietal cortex) and the model's output layer which represents all motor areas in motor hierarchy below SMA are obviously given a summary treatment. This is because one of the key motivations of the work is to highlight the role of SMA and basal ganglia in sequential behavior, specifically handwriting. The timing network, which represents basal ganglia, is at the moment defined in terms of its inputs and outputs and not defined as a neural network model. Further, the most important element of basal

ganglia is perhaps the dopamine signal which is thought to contain reward information. These necessities provide direction to future extensions of the present work.

Chapter 3: The Model of Basal Ganglia

In spite of availability of extensive experimental and clinical data, the essential function of basal ganglia (BG) continues to elude computational modelers (Harner, 197; Berns and Sejnowsky, 1998; Houk, 1995; Montague e al 1996), as evidenced in the diversity of existing views on the subject. Dominant thought considers BG as an Action gate that releases and places motor resources at the disposal of commands originating from higher motor cortical areas. BG have also been afforded roles in sequence generation and working memory. An idea that had gained significant concurrence is that BG is involved in motor learning by reinforcement with Dopamine as a reward signal (Montague et al, 1996; Barto, 1999). Any realization of reinforcement learning requires, in addition to a reward signal, a noise source that can exhaustively explore the output (or action) space. In this thesis it is proposed that the complex activity of the STN-GPe loop implements this noise signal which accounts for the exploratory drive. It has been observed that there is a loss of complexity (greater regularity) in the STN-GPe loop activity in dopamine depleted conditions (Terman et al, 2002; Beyan et al, 2003; Berman et al, 1994; Nini et al, 1995, Raz et al, 2000; Brown et al, 2001). We had suggested a possible functional consequence of this loss of complexity and presented a view of BG as a source of exploratory drive for reinforcement based motor learning with an enhanced model of BG involved in reaching. When there is a reliable dopamine-based reward signal the model successfully learns to reach, and when the signal is absent the arm wanders around the target failing to reach.

Basal Ganglia as a Source of Exploratory Drive: Consolidation Exploration

The proposed model is a neural network architecture consisting of two parallel pathways. We rename these pathways, traditionally called "direct" and "indirect" pathways, as "consolidation" and "exploration" pathways. The consolidation pathway from striatum to GPi consists of learnable connections that represent the sensory-motor map involved in reaching task. The exploratory pathway consisting of the STN-GPe loop is a network of oscillatory neurons; internal connections among the oscillators are designed such that the STN-GPe loop produces chaotic activity (similar to the model of STN-GPe in Terman et al 2002). Output of the loop to GPi provides the "noisy" or exploratory signal necessary for reward-based learning. Reward signal, representing dopamine, from Substantia Nigra compacta (SNc) is projected onto striatum which selects between the consolidation pathway and the exploratory pathway depending on the reward level. When the reward is low, the exploratory pathway is selected. Complex activity of STN-GPe loop, then, explores the output space, resulting in exploratory movement of the arm. When the exploring arm chances upon the target, the system receives a strong reward signal, the consolidation pathway is selected (the exploratory drive is suppressed) and the connections between striatum and GPi are reinforced in a Hebb-like fashion.

Chaotic Oscillations in STN – GPe Activity and Reinforcement Learning:

The presence of chaotic (uncorrelated activity) in BG in normal rats and correlated activity in Rat models of PD are reported by Terman et al (2002). What is the functional significance of chaos in basal ganglia? How chaos helps in healthy controls in daily living? What is the role of chaos in BG in learning? What function could natural, ubiquitous chaos serve?

BG has known to have role in Reinforcement learning. Any realization of reinforcement requires a reward signal along with a controllable noise signal. We argue that this noise signal comes from the indirect pathway in terms of STN-GPe chaotic oscillations. These oscillations are controllable by dopamine levels which codes reward signal in an indirect way (Dopamine is projected on to striatal neurons, some of the striatal synapses end in GPe).

The work of Freeman and colleagues with olfactory bulb revealed the functional significance of chaotic neural activity in sensory pattern recognition, where a chaotic response of the bulb represents stimulus novelty (Freeman, 1987)[10]. Chris King, who has written extensively on the subject of brain chaos and its implications, says of olfactory response to stimuli (King, 2003)[11],

…On inhalation a transition occurs from low level chaos ... to a trajectory which in the case of a familiar odor will settle into one of several periodic orbits, but in the case of a new odor will avoid existing periodic attractors hunting chaotically until a new periodic attractor is established over time, forming a both a new familiarized response and a new symbol…

In a model of a simulated "Morris water maze" experiment, Sridharan et al(2005) discovered that the SNT-GPe loop in the model exhibits chaotic activity when the virtual rat is turned away from the submerged platform and engaged in exploration; loop activity suddenly switches to a regular rhythm when the rat orients towards the platform (Sridharan et al, 2005). Just as in sensory processing, chaos may be found to play a deep and significant role in motor learning.

[10]W.J. Freeman theorized four possible functions for ubiquitous chaotic activity as – 1) A rapid method of memory access, 2) A novel stimuli flag, 3) Neuronal exercise and 4) A drive for new nerve cell connectivity.

[11] Chris King's list on the functional role of chaos in the brain is – 1) Chaotic access 2) Symbol, 3) Self – organizing stability structures, 4) Local minima escaping 5) Data compression, and 6) Indeterminism.

Chapter 4: A Model of Pd Handwriting

Recognition of rich diagnostic value of handwriting had prompted a systematic study of handwriting and the extensive neuromotor organization that generates it. Handwriting can be used a source of diagnostic information in neurological disorders like in Obsessive Compulsive disorder (Marvogiorgou et al, 2001), Schizophrenia (Gallucci et al, 1997), cortical dysfunction in old age (Erricson et al, 1991), Dysgraphia and Dyslexia (Rosenblum, 2003) and Parkinson's disease (Teulings et al, 1991and Philip et al, 1991) .

Handwriting in Parkinson's disease

Parkinsonian handwriting is typically characterized by micrographia, jagged line contour, and unusual fluctuations in the velocity of pen tip. Attempts have been made to use quantitative parameters of Parkinsonian handwriting to determine appropriate drug dosage. However most such attempts treat the motor system as a "black box" and are based on an empirical relationship between the handwriting parameters and the stage of maturity of the disease. However, since impairment of basal ganglia function underlies Parkinson's disease, an insight into the understanding of basal ganglia function and the precise role of these nuclei in handwriting generation is indispensable to produce an accurate computational model.

The current model of Parkinsonian handwriting generation maps the handwriting features like stroke size onto the dopamine levels empirically. Jagged line contour in handwriting are claimed to be due to the synchronized oscillations of STN – GPe dynamics. Apart from the above features, the model captures few other PD symptoms like,

1) *Micrographia:* The depletion of dopamine in the model shows handwriting with micrographia features. The overall size of the stroke becomes smaller as one decreases the dopamine. Van Gemmert et al with experimental studies on PD patients show evidence for the significantly smaller strokes than normal controls (Van Gemmert et al, 2005). They also report that the decreased mean acceleration and diminished peak velocity in PD patients.
2) *Bradykinesia:* As isochrony is the model's intrinsic property, the model generates all the strokes in more or less same time. In dopamine depletion conditions the model takes same time as that of normal time. So the overall movement is slower. Van Gemmert et al with experiment studies found that the average stroke duration of the patients with PD was no longer than the average stroke duration of normal controls(Van Gemmert et al, 2005)
3) Tremor in handwriting (Waverly handwriting): Tremor in handwriting can be observed by decrease of complex activity of the STN-GPe loop. Low frequency synchronous burst activity in STN – GPe loop may be propagated down the motor system which contributes to jagged handwriting.

The conclusions from the above model shows some applications could to be useful in assisting Clinicians and surgeons and computational modelers by answering the following questions,

1) Is it possible to map the handwriting features onto the severity of PD and the nuclei that is dysfunctioning? Solutions to this question might be useful in finding target nuclei for Deep Brain Stimulation (DBS) for Parkinson's disease.

2) Can we use the handwriting for monitoring the effect of drugs on PD patient? Stein suggests that changes in handwriting can be used to help monitor drug dose in various disorders (Stein, 2001). Computer analysis of handwriting dynamics during Dopamimetic tests in Parkinson's disease by Cobbah and Faihrust (2000) shows that there are positive responses to drugs. Studies of dynamic descript-characteristics of PD handwriting have clearly shown potential in identifying various stages of PD (Cubbah and Fairhrust, 2000).
3) How does motor system use extensive noise in the indirect pathway of BG for leaning handwriting? Will this noise helps in learning proper movement synergies for handwriting sequence execution?

Handwriting as a Source of Diagnostic Information

The developments in data collection technology now permit the examination of set of handwriting outcome measures. With the aid of a digitizing tablet and instrumented pen a subject's handwriting can be monitored in real time with kinetic and kinematic analysis (Rosenblum, 2001and Rosenblum, 2003). Subtle changes in person's handwriting might reveal neurological and psychiatric conditions years before other symptoms (of a neurological or psychiatric disease) become obvious (Persuad, 2002). Multiple sclerosis, dementia, Parkinson's disease, Huntington's chorea, Schizophrenia and obsessive compulsive disorder are just some of the conditions that affect handwriting in specific ways[12](Persuad, 2002). Rosenblum et al proposed the temporal measures of poor and

[12] **A written diagnosis** (Persuad, 2002):
PARKINSON'S DISEASE: patients write smaller and more slowly than healthy controls. Acceleration phases are significantly lower.
HUNTINGTON'S CHOREA: lower and less consistent writing speed and a tendency for less consistent strokes length.
SCHIZOPHRENIA: in consistent repetitive hand movements. Mean stroke duration and time spent in acceleration and are significantly longer.

proficient handwrites (children) as: i) total time to complete each task, ii) 'in air' time, and iii) mean writing speed. These measures found useful for dyslexic and Dysgraphic and ADHD (Attention Deficit Hyperactive Disorders). The temporal features of handwriting observed in OCD are i) lower peak velocity (Bradykinesia), ii) Micrographia, iii) shortened acceleration phase per stroke, and iv) repetition of strokes (Marvogiorgou et al, 2001). Similarly patients with cerebellar damage show typical features of Dysgraphia, manifested as omission and repetition of stroke and letters.

Simple geometric shape drawing tasks are commonly used to diagnose and monitor patient performance for a range of clinical and neuropsychological conditions (Guest et al, 2000). Errícson et al (1991) uses graphic skills as an instrument for detecting higher cortical dysfunctions in old age. The skills suggested are like, (i) copying tasks (3D cube, a circle, two rectangles, a rhombus and two pentagons), (ii) handwriting ability (writing a spontaneous sentence and writing from dictation), and (iii) free-hand figurative drawing (a dressed man or woman from the front). Gallucci et al (1997) suggest stroke characteristics (duration and length), stroke consistency (duration and length), stroke trajectory (efficiency and skew) and preservation for diseases related BG dysfunction like Parkinson's disease, Huntington's disease also for Schizophrenia (Galucci, 1997). Philips et al suggested stroke length, duration, peak velocity and a skew ness coefficient (a value of 0.5 indicates equal periods of time spent in accelerative and decelerative phase of movement) for Huntington's disease (Philips et al, 1995).

DEMENTIA OF ALZEHEMERLS TYPE: patients write less efficiently, with more cycles of acceleration and deceleration per writing stroke.
MULTIPLE SCELEROSIS: writing speed is reduced and stroke duration is increased. The profile of pen speeds associated with a single stroke is irregular and multi peaked, but stroke size is in normal range.

Handwriting features like, stroke size, peak acceleration, and stroke duration can be used for diagnosis of Parkinson's disease (Teulings et al 1991, van Gemmert et al, 2003). Philip et al suggested measures of the quality of handwriting for the analysis of PD: (i) The ratio between mean and standard deviation of stroke length or duration; (ii) The average number of zero crossings in acceleration relative to velocity functions; (iii) The average number of zero crossings in jerk relative to velocity functions; and (iv) The velocity frequency spectra.

There is no standardized measure or test battery for Parkinson's disease. The test battery for neurological disorders based on handwriting needs to be unified with the extensive understanding of spatial and temporal features of handwriting and the visuo-motor systems which generates and modulates it.

REFERENCES

1. **Aizawa, H. and J. Tanji** (1994) Cortico-cortical and thalamo-cortical responses of neurons in the monkey primary motor cortex and their relation to a trained motor task, *J Neurophysiol*, **71**, 550–560.
2. **Alexander, G. E.** (1987) Selective neuronal discharge in monkey putamen reflects intended direction of planned limb movements. *Exp. Brain Res.*, **67**, 623-634, 1987.
3. **Alexander, G. E.** *Basal ganglia* pp. 139-144. *In The Handbook of Brain Theory and Neural Networks*, **Arbib., M.A**.(ed.) MIT Press, Cambridge,1995.
4. **Barto, A.G. and P. Anandan** (1985) Pattern recognizing stochastic learning automata. *IEEE Transactions on Systems, Man and Cybernetics*, **15**, 360-374.
5. **Barto, AG.** (1999) *Reinforcement Learning. In The Handbook of Brain Theory and Neural Networks* ***Arbib, M.A.*** (ed.) Cambridge, MA: MIT Press.
6. **Bergman, H., A. Feingold, A. Nini, A. Raz, H. Slovin, M. Abeles and E. Vaadia** (1998) Physiological aspects of information processing in the basal ganglia of normal and parkinsonian primates. Trends in Neuroscience, **21**, 32-38, 1998.
7. **Bergman, H., T. Whichman, B. Karmon, M.R. DeLaong** (1994) The primate subthalamic nucleus. II. Neural activity in MPTP model of Parkinsonism. *J Neurophysiol,* **72**, 507-520.
8. **Berns, G.S., T.J. Sejnowski** (1998) A computational model of how the Basal Ganglia produce sequences. *Journal of Cognitive Neuroscience*, **10**(1), 108-121.
9. **Bevan, M.D., P.J. Magill, D. Terman, J.P. Bolam and C.J. Wilson** (2003) Move To The Rhythm: Oscillations In The Subthalamic Nucleus-External Globus Pallidus Network. *Trends in Neuroscience (in press)*
10. **Bhuhusi, C.V. and W.H. Meck** (2005) What makes us tick? Functional and neural mechanisms of interval timing *Nature reviews neuroscience*, **6**, 755.
11. **Bilney, B., M.E. Morris and D. Sonia** (2003) Physiotherapy for people with movement disorders arising from basal ganglia dysfunction. *NZ journal of Physiotherapy*, **31**, 2.
12. **Bjorne, P. and C. Balkenius** (2005) A model of attentional impairments in autism: First steps toward a computational theory. *Cognitive Systems Research*, **6**(3), 193-204.
13. **Borrett, D.S., T.H. Yeap and H.C. Kwan** (1993) *Candian Journal of Neurological Sciences* **20**,107.
14. **Bressloff, P.C., S. Coombes, and B. Souza** (2002) Dynamics of a Ring of Pulse-Coupled Oscillators: Group Theoretic Approach. *Phys Rev E Stat Nonlin. Soft. Matter. Phys.* **66**.
15. **Brown, P., A. Olivero, P. Mazzone, A. Insola, P. Tonali, V.D. Lazzaro** (2001) Dopamine dependency of oscillations in between subthalamic neucleus and pallidum in Parkinson's disease. *J Neurosci*, **21**, 1033-1038.
16. **Buhusi, C.V., W.H. Meck** (2005) What makes us tick? Functional and neural mechanisms of interval timing. *Nat. Rev. Neurosci.* **6** (10):755-6
17. **Bullock, D. and S. Grossberg** (1988) The VITE: a neural command circuit for generating arm and articulator trajectories. *In dynamic patterns in complex systems,* **Kelso, *A. and*** **Shlesinger, M.M.** (eds), Singapore: world Scientific. (1988).
18. **Bullock, D., R.M. Bongers, M. Lankhorst P.J. Beek** (1999) A vector-integration-to-endpoint model for performance of viapoint movements. *Neural Netw*.**12** (1), 1-29.
19. **Chirikov, B.** (1979) A universal instability of many – dimensional oscillator systems, *Phy.Rev.,* **52**, 263-379.

20. **Churchland, M.M., M.Y. Byron and I.R. Stephen, G. Santhanam, A. Afshar, V.S. Krishna** (2005) *Neural variability in premotor cortex provides a signature of motor preparation*. In the proceedings of COSYNE , March.
21. **Churchland, P. and T.J. Sejnowski** The Computational Brain MIT Press, Cambridge, Massachusetts, 1992
22. **Cobbah, W.G.K. and M.C. Fairhurst** (2000) Computer analysis of handwriting dynamics during dopamimetic tests in Parkinson's disease. *EUROMICRO*. 2414-2418.
23. **Crammond, D. J., and J. F. Kalaska** (1989) Neuronal activity in primate parietal cortex area 5varies with intended movement direction during an instructed – delay period. *Exp. Brain Res.* **76**, 458- 462.
24. **Crystal, H., L.H. Finkel** *Computational approaches to neurological disease*. *In* Reggia, J.A., E. Ruppin, R.S. and Berndt (eds.) *Neural Modeling of Brain and Cognitive Disorders*. Singapore: World Scientific, 1996.
25. **Cunnington, R., R. Iansek, J. A. Bradshaw and J.G. Phillips** (1995) Movement-related potentials in Parkinson's disease: Presence and predictability of temporal and spatial cues, *Brain,* **118**, 935-950.
26. **Dayan, P and L.F. Abbot** Theoretical Neuroscience: Computational and Mathematical modeling of neural systems, MIT press , Cambridge, Massachusetts, 2001.
27. **Dominey, P., M. Arbib, and J.P. Joseph** (1995)A model of cortico striatal Plasticity for learning oculomotor associations and sequences. *Journal of Cognitive Neuroscience,* **7** (3), 311-336.
28. **Ellis, A.W.** *Modeling the writing process. In Perspectives in cognitive neuropsychology*, **Denes, G, C. Semenza, P. Bisiacchi and E. Andreewsky**(eds.) London: Erlbaum, 1986.
29. **Ericsson, K., L. Forssell, K. Amberla, K. Holmén, M. Viitanen and B. Winblad** (1991) Graphic skills used as an instrument for detecting higher cortical dysfunctions in old age, *Human Movement Science* , **10**(2-3), 335-349.
30. **Fiala, J., S. Grossberg, D. Bullock** (1996) Metabotropic glutamate receptor activation in cerebellar Purkinje cells as substrate for adaptive timing of the classically conditioned eye-blink response. *The Journal of Neuroscience*, **16**, 3760-3774.
31. **Gallucci, R.M., J.G. Phillips, J.L. Bradshaw, K.S. Vaddadi and C. Pantelis** (1997) Kinematic analysis of handwriting movements in schizophrenic patients. *Biol. Psychiatry.* **41** (7)**,** 830-833.
32. **Georgiou, N., R. Iansek , J.L. Bradshaw, J.G. Phillips, J.B. Mattingley and J. A. Bradshaw** (1993) An evaluation of the role of internal cues in the pathogenesis of parkinsonian hypokinesia. *Brain*, **116**, 1575-1587.
33. **Georgopoulos, A.P., J.T. Lurito, M. Petrides, A.B. Schwartz, and J.T. Massey** (1989) Mental rotation of the neuronal population vector. *Science,* **243**, 234-236.
34. **Grossberg, S. and R.W. Paine** (2000) A neural model of corticocerebellar interactions during attentive imitation and predictive learning of sequential handwriting movements, *Neural Networks*, **13**, 999-1046.
35. **Grossberg, S. and D. Seidman** (2006) Neural dynamics of autistic behaviors: Cognitive, emotional, and timing substrates. *Psychological Review*, in press.
36. **Grossberg, S.** *Neural models of normal and abnormal behavior: what do schizophrenia, parkinsonism, attention deficit disorder, and depression have in common?* pp. 375-406. *In* **Reggia, J.A., E. Ruppin, D.L. Glanzman** (eds.) *Disorders of Brain, Behavior, and Cognition: The Neurocomputational Perspective* New York: Elsevier, 1999.
37. **Guest, R.M., M.C. Fairhurst and J.M. Potter** (2000) Automated Extraction of Image Segments from Clinically Diagnostic Hand-Drawn Geometric Shapes, *euromicro*, Proceedings of The 26th EUROMICRO Conference **2**, 2440,

38. **Gurney, K., T. J. Prescott and P. Redgrave** (2001) A computational model of action selection in the basal ganglia I. A new functional anatomy. *Biological Cybernetics,* **84**, 401-410.
39. **Guttman, M., J.K. Stephen and Y. Furukawa** (2003) *Current concepts in the diagnosis and management of Parkinson's disease CMAJ,* **168** (3).
40. **Harm, M.W. and M.S. Seidenberg** (1999) Phonology, Reading Acquisition, and Dyslexia: Insights from Connectionist Models. *Psychological Review*, **106** (3), 491-528.
41. **Harner, A.M.** (1997) An Introduction to Basal Ganglia Function. Boston University, Boston, Massachusetts
42. **Haykin. S.** *Neural Networks: A Comprehensive Foundation*, Prentice Hall PTR, July 1998,
43. **Hertz, J., A. Krogh, and R.G. Palmer** *Introduction to the Theory of Neurocomputing*, Addison-Wesley, Reading, MA, 1991.
44. **Hollerbach, J.M.** (1981) An oscillation theory of handwriting. *Biological Cybernetics*, **(156)**39, 139.
45. **Horn, D. and E. Ruppin** (1995). Compensatory mechanisms in an attractor neural network model of schizophrenia. *Neural Computation*, **7**, 182-205.
46. **Houk, J. C., J. L. Davis, and D. G. Beiser** (1995). *Models of Information Processing in the Basal Ganglia*. Cambridge, MA, MIT Press
47. **Jennings, C and S. Aamodt** (2000) Computational approaches to brain function. *Nature Neuroscience*, **3**, 1160.
48. **Kalveram, K. Th.** (1996) A neural oscillator model learning given trajectories, or how an allo-imitation algorithm can be implemented into a motor controller. *In Motor control and human skill: A multi-disciplinary perspective*, **J. Piek (Hrsg.)** eds. Champaign: Human Kinetics. 1996
49. **Klopf, A.H.,** *The Hedonistic Neuron: A Theory of Memory*, *Learning, and Intelligence*. Hemisphere, Washington, D.C., 1982.
50. **Kornhuber, H.H. and L. Deecke** (1990) Readiness for movement – The Bereitschafts potential-Story *Current Contents Life Sciences*, **33**, 22.
51. **Kubota, K. and I. Hamada** (1978) Visual tracking and neuron activity in the post – arcurate area in monkeys. *J. Phyiol. Paris*. **74**, 297-312.
52. **Kubota, K. and S. Funahashi** (1982) Neuron activities of monkey prefrontal cortex during the learning of visual discriminations tasks with Go/No-Go performances. *Neurosci. Res.*, **3**,106-129.
53. **Kuenstler, U., U. Juhnhold, W. H. Knapp, and H.J. Gertz** (1999) Positive correlation between reduction of handwriting area and D2 dopamine receptor occupancy during treatment with neuroleptic drugs. *Psychiatry Research: Neuroimaging*, **90** (1), 31-39.
54. **Lang, W., R. Cheyne, R. Kristeva, R. Beistener, G. Lindinger and L. Deeke** (1991) Three dimensional localization of SMA activity preceding voluntary movement: a study of electric and magnetic fields in a patient with inflation of the right supplementary motor area. *Exp. Brain Res.*, **87**,688-695.
55. **Latash, M.L., J.F. Scholz, F. Danion, and G. Schöner** (2001) Structure of motor variability in marginally redundant multi-finger force production tasks. *Exp. Brain Res.***141**, 53–165.
56. **Marder, E., and R. L. Calabrese** (1996) Principles of rhythmic motor pattern production *Physiological Reviews*, **76**,687–717.
57. **Martin, K.E., J.G. Phillips, R. Iansek, J.L. Bradshaw**(1994) Inaccuracy and instability of sequential movements in Parkinson's disease**.** *Exp. Brain. Res.* **102,** 131–40.
58. **Mavrogiorgou, P., R. Mergl, P. Tigges, J.E. Husseini, A. Schröter, G. Juckel, M. Zaudig, U. Hegerl** (2001) Kinematic analysis of handwriting movements in patients with obsessive-compulsive disorder. *J Neurol Neurosurg Psychiatry***70**, 605-612.

59. **Mink, J.W.** (1996) The basal ganglia: Focused selection and inhibition of competing motor programs. *Progress in Neurobiology*, **50** (4), 1009-1023.
60. **Montague, P.R., P. Dayan and T.K. Sejnowski,** (1996) A framework for mesencephalic dopamine systems based on predictive Hebbian learning. *Journal of Neuroscience,* **16**, 1936-1947.
61. **Montague, R., P. Dayan, and T.J. Sejnowski** (1996). A Framework for Mesencephalic Dopamine Systems Based on Predictive Hebbian Learning, *The Journal of Neuroscience*, **16** (5):1936-1947.
62. **Nini. A., A. Feingold, H. Slovin and H. Bergman** (1995) Neurons in the Globus pallidus do not show correlated activity in the normal monkey, but phase locked oscillations appear in the MPTP model of parkinsonism. *J. Neurophysiol,* **74,** 1800-1905.
63. **Persuad, R.** (2002) New Scientist.**9**, 40-42.
64. **Phillips, J. G., G. E. Stelmach and N. Teasdale** (1991) What can indices of handwriting quality tell us about Parkinsonian handwriting? *Human Movement Science*, **10** (2-3), 301-314.
65. **Plamondon, R.** (1989) An evaluation of motor models of handwriting. *IEEE Transactions on Systems, Man and Cybernetics.***9** (5), 1060-1072.
66. **Plamondon, R. and W. Guefali** (1998) The generation of handwriting with delta lognormal synergies, *Biological Cybernetics*, **78**, 119-132.
67. **Prashanth, P.S., and V.S. Chakravarthy** (2006) An oscillator theory of motor unit recruitment in skeletal muscle. To appear in *Biological Cybernetics.*
68. **Prescott, T. J., K. Gurney, and Redgrave, P.** (2002). *Basal ganglia*. In M. A. Arbib (ed.) *The Handbook of Brain Theory and Neural Networks (2nd Edition)*. Cambridge, MA: MIT Press.
69. **Prunier, C., E. Bezard, J. Montharu, M. Mantzarides, J.C. Besnard, J.L. Baulieu, C. Gross, D. Guilloteau and S. Chalon** (2003) Presymptomatic diagnosis of experimental Parkinsonism with I-PE2I SPECT. *NeuroImage*, **19**, 810–816.
70. **Raz, A., Vaadia, E. and H. Bergman** (2000) Firing patterns of spontaneous discharge of pallidal neurons in the model of Parkinsonism. *J Neurosci*, **20**, 8559-8571.
71. **Redgrave, P., T.J. Prescott and K. Gurney** (1999) The basal ganglia: a vertebrate solution to the selection problem? *Neuroscience*, **89**, 1009-1023.
72. **Reggia, J, E., Ruppin and R. Berndt** Neural Modeling of Brain and Cognitive Disorders. World Scientific. 1996.
73. **Rescorla, R. A., and A.R. Wagner** (1972) *A theory of Pavlovian conditioning: Variations in the effectiveness of reinforcement and nonreinforcement*. pp. 64-99. *In Classical conditioning II: Current research and theory* **Black, A. H., and W. F. Prokasy** (eds), New York: Appleton-Century-Crofts.
74. **Reynolds, J. N., B.I. Hyland, and Wickens, J. R.** (2001) A cellular mechanism of reward-related learning. *Nature* **413**, 67-70.
75. **Riederer, P., Wuketich, S.** (1976) Time course of nigrostriatal degeneration in Parkinson's disease. *J. Neural Transm.* **38**, 277–301.
76. **Rosenblum, S., S. Parush and P.L. Weiss** (2001) Temporal measures of poor and proficient handwriters, In **Meulenbroek., R.G.J. and B. Steenbergen** (eds), Proceedings of Tenth biennial conference of the IGS, University of Nijmegen The Nether Lands, 119-125.
77. **Rosenblum, S., S. Parush, L. Epsztein, and P.L Weiss** (2003) Process Versus Product Evaluation of Poor Handwriting among Children with Developmental Dysgraphia and ADHD, In **Teulings, H.L., and A.W.H Van Gemmert**, Proceedings of 11th conference of the IGS, USA; Scottsdate Arizona. 169-173.

78. **Ruppin, E., D. Horn, N. Levy, and J. Reggia** Computational Studies of Synaptic Alterations in Alzheimer's Disease. *In* **Reggia, J., E. Ruppin, & R. Berndt** (eds.), *Neural Modeling of Brain and Cognitive Disorders*, World Scientific. (1996)
79. **Ruppin. E., J.A. Reggia and D. Glanzmann** (1999) Understanding brain and cognitive disorders: the computational perspective, *Prog. Brain. Res.,* **121**, ix-xv**.**
80. **Schomaker, L.R.B.** (1991) Simulation and recognition of handwriting movements: a vertical approach to modeling human motor behavior, PhD thesis, Nijmegen University, Netherlands,
81. **Silva, L. F. H. and J.P. Pijn** *Epilepsy: Network models of generation* pp. 367-369. *In* **Arbib.. M.** (ed.) *The handbook of brain theory and neural networks*. Cambridge, MA: MIT Press. 1995.
82. **Silveri, M.C., S. Misciagna, M.G. Leggio and M. Molinari** (1999) Cerebellar spatial dysgraphia: further evidence. *J Neurol.* **246** (4)**,** 312-3.
83. **Singhala, B., J. Lalkakaa and C. Sankhlab** (2003) Epidemiology and treatment of Parkinson's disease in India, *Parkinsonism and Related Disorders* **9**, 105–109.
84. **Skarda, C. A., and W. J. Freeman** (1987). How brain makes chaos in order to make sense of the world. *Behavioral and Brain Sciences*, **10**,161-195.
85. **Sridharan, D., P.S. Prashanth and V.S. Chakravarthy** (2005) On the Exploratory Role of complex oscillations in a model of Basal Ganglia based on Reinforcement Learning. To appear in *Journal of Neural Engineering*.
86. **Stein, D.J.** (2001) Handwriting and obsessive-compulsive disorder. *Lancet.* **18**, **358**(9281):524-5.
87. **Sutton. R.S. and A.G. Barto** *Reinforcement Learning: An Introduction*. MIT Press, 1999.
88. **Tanji, J.** (1994) The supplementary motor area in the cerebral cortex. *Neurosci Res.***19** (3), 251–268.
89. **Tanji, J., K. Taniguchi, and T. Saga** (1980) Supplementary motor area: neuronal response to motor instructions. *J. Neurophysio.*, **43**, 60–68.
90. **Terman, D., J.E. Rubin, A.C. Yew and C.J. Wilson** (2002) Activity Patterns in a Model for the Subthalamopallidal Network of the Basal Ganglia. *J Neurosci,* **22** (7), 2963-2976.
91. *Tesauro, G.* (1992) Practical issues in temporal difference learning. *Machine Learning*, **8**, 257--277.
92. **Teulings HL, C.J.L. Vidal, G.E. Stelmach and C.H. Adler** (2002) Handwriting size adaptation under distorted visual feedback in Parkinson's disease patients, elderly controls and young controls, *Journal of Neurology, Neurosurgery, and Psychiatry*, **72**(3):315-324.
93. **Teulings, H.L. and G.E. Stelmach** (1991) Control of stroke size, peak acceleration, and stroke duration in Parkinsonian handwriting. *Human Movement Science* **10**, (2-3), 315-334.
94. **Teulings, H.L., A.J.W.M. Thomassen, L.R.B. Schomaker, and P. Morasso** (1986) Experimental protocol for cursive script acquisition: The use of motor information for the automatic recognition of cursive script. *In Report 3.1.2*., *ESPRIT project,* 419.
95. **Thomassen, A., H. Teulings** Time, size, and shape in handwriting: exploring spatio-temporal relationships at different levels *In*: Michon, J., and Jackson, J. (eds.), *Time, Mind, and Behavior*, Springer-Verlag, 1985.
96. **Thorndike, E.L** (1911), Animal Intelligence, Macmillan press.
97. **van Galen, G. and J. Weber** (1998**)** On-line size control in handwriting demonstrates the continuous nature of motor programs, *Acta Psychologica*, **100**,195-216.

98. **Van Gemmert, A. W. A., C.H. Adler, and G.E. Stelmach** (2003) Parkinson's disease patients undershoot target size in handwriting and similar tasks. *Journal of Neurology, Neurosurgery, and Psychiatry,* **74***,* 1502-1508.

99. **Van Gemmert, A.W.A., H.L., Teulings, J.L Contreras –Vidal and G.E. Stelmach** (1999) Parkinson's disease and the control of size and speed in handwriting', *Neuropsychologica* **37**, 685-694.

100. **Vidal, C.J., H. Teulings and G. Stelmach** *a Neural Network Model of Movement Production in Parkinson's disease and Huntington's disease. In* **Reggia, J.A, E. Ruppin, and R. Berndt** (eds.), *Neural Modeling of Brain and Cognitive Disorders*, World Scientific, 1996.

101. **Vidal, J.L and G.E. Stelmach** (1995) A neural model of basal ganglia-thalamocortical relations in normal and Parkinsonian movement. *Biological Cybernetics*, **73**, 467-476.

102. **Vidal, J.L. and G.E. Stelmach** (1996) Effects of Parkinsonism on motor control. *Life Sciences*, **58**, 165-176.

103. **Viviani, P. and G. McCollum** (1983) The relation between linear extent and velocity in drawing movements. *Neuroscience.* **10** (1), 211-8.

104. **Watkins, C. J. C. H.** *Learning with Delayed Rewards*, Ph.D. thesis, Cambridge University, Psychology Department, 1989.

105. **Widrow, B., N. K. Gupta, and S. Maitra** (1973) Punish /reward: Learning with a critic in adaptive threshold systems. *IEEE Transactions on Systems, Man, and Cybernetics* **5**, 455-465.

APPENDIX A

I. The proof for the system governed by the equations (i), (ii) and (iii) has a "*limit cycle*".

$$\frac{dx}{dt} = -x + v - s + I \qquad \text{(i)}$$

$$v = tahn(\lambda x) \qquad \text{(ii)}$$

$$\frac{ds}{dt} = -s + v \qquad \text{(iii)}$$

We can use Lienard's theorem for existence of limit cycle. Follow the steps given below to convert (i), (ii) and (iii) to Lienard's equation.

Differentiating (i)

$$\ddot{x} = -\dot{x} + \lambda \sec h^2(\lambda x)\dot{x} - \dot{s} \qquad \text{(iv)}$$

Substituting (ii) and (iii) in (iv)

$$\ddot{x} = -\dot{x} + \lambda \sec h^2(\lambda x)\dot{x} - (-s + \tanh(\lambda x)) \qquad \text{(v)}$$

Using (i) and (v)

$$\ddot{x} = -\dot{x} + \lambda \sec h^2(\lambda x)\dot{x} - (-(-\dot{x} - x + \tanh(\lambda x) + I) + \tanh(\lambda x))$$

On rearranging

$$\ddot{x} + \dot{x}(2 - \lambda \sec h^2(\lambda x)) + (x - I) = 0 \qquad \text{(vi)}$$

Eq. (vi) is similar to Lienard's equation $\ddot{x} + \dot{x}f(x) + g(x) = 0$ where $f(x) = 2 - \lambda \sec h^2(\lambda x)$ and $g(x) = x - I$.

Checking for the Lienard's conditions: Let us assume I = 0.

Both $f(x)$ and $g(x)$ are continuously differentiable for all x;

$g(-x) = -g(x)$ for all x (i.e., $g(x)$ is an odd function);

$g(x) > 0 \; for \; x > 0$;

$f(-x) = f(x)$ for all x (i.e., $f(x)$ is an even function);

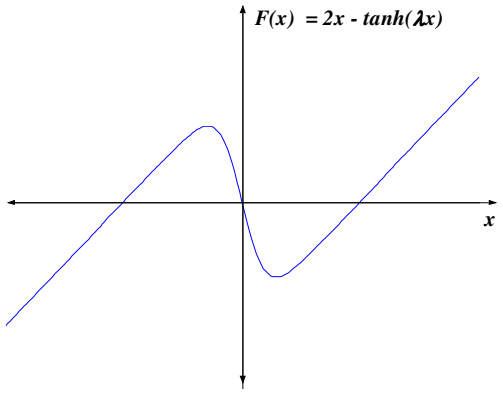

Fig. A.1 The state variable, 'x' Vs the odd function, '*F(x)*'

The odd function $F(x) = \int_0^x f(u)du = 2x - \tanh(\lambda x)$ has exactly one positive zero at $x = x_o$, is negative for $0 < x < x_o$, is positive and non decreasing for $x > x_o$, and $F(x) \to \infty$ as $x \to \infty$.(one can estimate x_o from graph(fig. A.1) of $F(x)$).

So the system has a unique stable limit cycle surrounding the origin in the phase plane

CURRICILUM VITAE

1. NAME **:** Garipelli Gangadhar
email: *ganges.g@gmail.com*

2. DATE OF BIRTH **:** 04 January 1980

3. EDUCATIONAL QUALIFICATIONS

2003 Bachelor of Technology (B. Tech.)

Institution	: Kamala Institute of Technology and Science (Singapur), Affiliated to Jawaharlal Nehru Institute of Technology, Hyderabad.
Specialization	: Electronics and Communications Engineering.

Master of Science (M. S)

Institution	: Indian Institute of Technology – Madras.
Specialization	: Computational Neuroscience (From Electrical Engineering Dept.).
Registration Date	: 05 January 2004

PUBLICATIONS:

Journals:

1. **Mohan. V, Y.V. Joshi, A. Itagi, and G. Gangadhar**(2005) studies on an Electronic Analog of a Recurrent Neural Network with Retrieval Phase Weight Adaptations, *Journal of Advanced Computational Intelligence and Intelligent Informatics*, **9**(2), 127-133.
2. **Gangadhar.G and V.S. Chakravarthy**, A neuromotor model of handwriting generation: highlighting the role of basal ganglia, submitted to *IEEE Systems Man and Cybernetics.*

Conferences:

1. **Gangadhar.G and V.S Chakravarthy**, An Oscillatory Neural Network Model for Handwriting Generation, in proceedings of *12th Conference of the International Graphonomics Society,* 2005.
2. **Gangadhar.G, S. Jasthi, and V.S.Chakravarthy,** A Neural Model of Visuo-motor coordination in Copying: Implications to understanding Dysgraphia, in proceedings of *International conference on biomedical engineering,* 2005, Singapore.
3. **Gangadhar.G, D. Karthikeyan, S. Devarajan and V.S.Chakravarthy***,* Basal Ganglia as a source of exploratory drive: A model for reaching, communicated to *Advances in computational motor control*-2005, Washington.
4. **Gangadhar.G, D. Karthikeyan, and V.S.Chakravarthy,** Understanding parkinsonian handwriting through a computational model of Basal Ganglia, presented at *International Symposium on Advances in Research on Neurodegenerative diseases* 2005, India.
5. **Gangadhar.G, and V.S.Chakravarthy**, A neuromotor model of handwriting generation – highlighting the role of basal ganglia, Presented at *Annual courses in clinical neuroscience,* 2006, India.